Clim. Past Discuss., 10, 2163–2291, 2014
www.clim-past-discuss.net/10/2163/2014/
doi:10.5194/cpd-10-2163-2014

Climate of the Past
Discussions
Open Access

The Global Monsoon across Time Scales: is there coherent variability of regional monsoons?

P. X. Wang[1], B. Wang[2], H. Cheng[3,4], J. Fasullo[5], Z. T. Guo[6], T. Kiefer[7], and Z. Y. Liu[8,9]

[1]State Key Laboratory of Marine Geology, Tongji University, Shanghai 200092, China
[2]Department of Meteorology, University of Hawaii at Manoa, Honolulu, HI 96825, USA
[3]Institute of Global Environmental Change, Xi'an Jiaotong University, Xi'an 710049, China
[4]Department of Earth Sciences, University of Minnesota, Minneapolis, MN 55455, USA
[5]CAS/NCAR, National Center for Atmospheric Research, 3090 Center Green Dr., Boulder, CO 80301, USA
[6]Key Laboratory of Cenozoic Geology and Environment, Institute of Geology and Geophysics, Chinese Academy of Sciences, P.O. Box 9825, Beijing 100029, China
[7]PAGES International Project Office, Zähringerstrasse 25,3012 Bern, Switzerland
[8]Laboratory Climate, Ocean and Atmospheric Studies, School of Physics, Peking University, Beijing 100871, China
[9]Center for Climatic Research, University of WisconsineMadison, Madison, WI 53706, USA

Received: 21 April 2014 – Accepted: 8 May 2014 – Published: 15 May 2014

Correspondence to: P. X. Wang (pxwang@tongji.edu.cn) and B. Wang (wangbin@hawaii.edu)

Published by Copernicus Publications on behalf of the European Geosciences Union.

Abstract

Monsoon has earned increasing attention from the climate community since the last century, yet only recently regional monsoons have been recognized as a global system. It remains a debated issue, however, as to what extent and at which time scales the global monsoon can be viewed as a major mode of climate variability. For this purpose a PAGES Working Group (WG) was set up to investigate the concept of the global monsoon and its future research directions. The WG's synthesis is presented here. On the basis of observation and proxy data, the WG found that the regional monsoons can vary coherently, although not perfectly, at various time scales, ranging from interannual, interdecadal, centennial and millennial, up to orbital and tectonics time scales, conforming the global monsoon concept across time scales. Within the global monsoon system each subsystem has its own features depending on its geographic and topographic conditions. Discrimination of global and regional components in the monsoon system is a key to reveal the driving factors of monsoon variations, hence the global monsoon concept helps to enhance our understanding and to improve future projection of the regional monsoons. This paper starts with a historical review of the global monsoon concept in both modern and paleo-climatology, and an assessment of monsoon proxies used in regional and global scales. The main body of the paper is devoted to a summary of observation data at various time scales, providing evidence for the coherent global monsoon system. The paper concludes with a projection of future monsoon shifts into a warming world. The synthesis will be followed by a companying paper to discuss driving mechanisms and outstanding issues in the global monsoon studies.

1 Introduction

Scientific interest in the monsoons can be traced back nearly 350 years. However, only recently have the regional monsoons been viewed and analyzed as being part of a

CPD
10, 2163–2291, 2014

global system. Traditionally, the variability of the monsoon has been studied almost exclusively on regional scales, in both the modern and paleo-monsoon communities. With the application of remote sensing and other new techniques, the concept of the "Global Monsoon" (GM) has been introduced as a global-scale seasonal reversal of the three-dimensional monsoon circulation associated with migration of the rainfall in monsoon trough and intertropical convergence zone. The GM thus represents the dominant mode of annual low-latitude variation of the climate system and is a defining feature of Earth's climate. However, the extent to which the GM concept can provide meaningful insights for variability across a broad range of temporal and spatial scales remains an open question.

In an effort to better understand the dynamics of monsoon variability, the PAGES Working Group "Global Monsoon and Low-Latitude Processes: Evolution and Variability" was established in 2007. The Working Group conducted two symposia in 2008 and 2010 successively in Shanghai (P. Wang et al., 2009, 2012a). The symposia brought together paleo- and modern climatologists as well as data producers and modelers to compare monsoon studies from all regional monsoon systems and identify their similarities and differences across an exceptionally broad range of timescales from interannual to tectonic, and to unravel the mechanisms causing variations in the GM system and regional deviations from the global trend.

In 2012, a collection of 13 contributions to the symposia were published as a GM special issue in "Climate Dynamics", trying to put regional monsoons into the context of the global system and to analyze their variations across a range of timescales (P. Wang et al., 2012b). In December 2012 a writing workshop was held in Shanghai to prepare the final synthesis of the Working Group. After repeated discussions and revisions of the manuscript, here is the final product of years' endeavor, the scientific synthesis of the Global Monsoon Working Group.

The paper starts with a historical review of the GM concept in both modern and paleo-climatology, and an assessment of monsoon proxies used at regional and global scales. The main body of the present paper is devoted to a summary of observations

CPD
10, 2163–2291, 2014

at various time scales, from inter-annual, inter-decadal, centennial, millennial, orbital, and tectonic time scales, providing evidence for the existence of a coherent GM system. The synthesis concludes with a discussion of the potential future of the GM and some issues and recommendations for the further study. In addition to the material herein, an accompanying manuscript, currently in preparation, will address fundamental mechanisms of GM variability and outstanding issues in GM science as a key component of the Working Group synthesis.

2 Concept of the global monsoon

2.1 Concept of monsoon in retrospect

The modern monsoon study has received ardent attention over the nearly 350 years since the pioneering works of Halley (1686) and Hadley (1735). Monsoon, in a general sense, means seasonality: the word "Monsoon" originates from Arabian word "Mausam" which means season (Ramage, 1971). The Indian Monsoon represents the most typical monsoon climate, as it is characterized by (a) a robust annual reversal of the prevailing surface winds (summer southwesterlies and winter northeasterlies) and (b) a sharp contrast between rainy summer and arid winter, with 70–80 % of the total annual precipitation falling in June-July-August-September (Webster, 1987; Wang and LinHo, 2002). Monsoon climate is characterized by both the annual reversal of surface winds and the contrast between rainy summer and dry winter.

Quantitative delineation of the monsoon extent has been an ongoing effort since the early 20th century. The classical monsoon definition was based solely on surface wind reversal. In an attempt to delineate monsoon domains, Hann (1908) defined a "monsoon index" using the maximum difference between the mid-winter and mid-summer. This index was subsequently modified by Schick (1953), Khromov (1957), Ramage (1971), and recently by Li and Zeng (2003). Of note is that the domains defined based on annual wind reversal alone included many isolated areas over the midlatitudes,

CPD
10, 2163–2291, 2014
The Global Monsoon across Time Scales
P. X. Wang et al.

which are affected by the annual march of the extratropical westerlies. It was vigorously debated in 1950s and 1960s as to whether these regions were monsoonal or not (e.g., Alisov, 1954; Shapaev, 1960; Kao, 1961; Bluthgen, 1966; Ramage, 1971), as some have a dry summer and wet winter climate, thus more closely representing Mediterranean, rather than monsoonal, climates. Others are dominated by transient cyclones/anticyclones, so unlike typical monsoons, their prevailing winds during the solstice seasons are unsteady. To exclude these regions, Ramage (1971) added strength and steadiness criterions to define monsoon extent, thus confining the monsoons to South and East Asia, Australia, and northern Africa, all in the eastern Hemisphere.

Ramage's domain delineated the most typical or strongest monsoon wind variations over the planet; but it does not take into account rainfall characteristics, because it was thought that "no simple correlation exists between surface pressure gradient and rainfall" (Ramage, 1971). In fact, there exists a robust and dynamically consistent relationship between rainfall, surface pressure, and winds known as the "Gill pattern" (Webster, 1972; Gill, 1980). Figure 1 shows the idealized low-level wind response (vectors) to tropical heating (contours). Monsoonal precipitation drives heating located north of the equator, inducing a low-level cyclonic circulation to its western and poleward sides, due to its excitation of westward propagating Rossby waves. Thus, the southwesterly monsoon flow is located to the westward and equatorward boundaries of the Northern Hemisphere (NH) monsoon precipitation, which is also associated with cross-equatorial flow from the Southern Hemisphere (SH). This schematic illustrates how the NH summer southwest monsoon flows are dynamically connected to monsoon precipitation and associated heating, which in nature is also augmented by cloud radiative effects. When the precipitation migrates to the SH during NH winter the corresponding monsoon flows reverse direction accordingly. For detailed monsoon rainfall-circulation relationships for the regional monsoons, readers are referred to Yim et al. (2013) .

The monsoon definition based solely on winds is grossly inadequate for characterizing the socio-economic and scientific importance of rainfall. Monsoon precipitation, which accounts for 31 % of the global total rainfall (Wang and Ding, 2008) , exists

CPD
10, 2163–2291, 2014

as the life-blood of about two-thirds of the world's population and its spatial-temporal variation has much more important socio-economic value than monsoon winds. Precipitation also plays an essential role in determining the atmospheric general circulation and hydrological cycle, and in linking external radiative forcing and the atmospheric circulation. Therefore, delineating the monsoon domain based on the character of precipitation is imperative. Given the robust precipitation-circulation relationship that exists (e.g. Fig. 1), such regions are also likely to reflect the reversal of surface winds, as discussed further below.

Satellite observations of the monsoons began in the mid-1970s, making it possible for the first time to estimate rainfall over the open oceans, where major components of the monsoons exist. Initially, retrievals of outgoing longwave radiation (OLR) provided a good indication of deep convection and, indirectly, precipitation in the tropics. Using OLR data, B. Wang (1994) first attempted to delineate monsoon domains based on synthesis of the local seasonal distribution of OLR, the peak phase and duration of the rainy season, and the range of the annual cycle. The domains defined in terms of rainfall cover not only South and East Asia, West Africa, Australia, but also span portions of Southern Africa, and North and South America, thereby covering all continents except Antarctica, and both the eastern and western hemispheres and both land and ocean.

2.2 Concept of global monsoon

2.2.1 Delineation of global monsoon precipitation domain

It is necessary to delineate the GM precipitation domain objectively, in part in order to study its variability. Such a quantitative definition facilitates not only the interpretation of observations and evaluation of model simulations, but also assessment of its projected shifts in a changing climate.

The GM precipitation regime can be defined by regions where (a) the local summer-minus-winter precipitation rate exceeds 2 mm day^{-1} and (b) the local summer precipitation exceeds 55 % of the annual total (Wang and Ding, 2008). Here the local summer

CPD
10, 2163–2291, 2014

denotes May through September for the NH and November through March for the SH. The first criterion distinguishes the monsoon climate from arid and semi-arid and Mediterranean climate regimes. The second criterion warrants concentration of precipitation during local summer, so that it distinguishes the monsoon climate from equatorial perennial rainfall regimes where the annual range is small compared to its annual mean.

The GM precipitation domain defined by the above two criteria (Fig. 2) include all major monsoon regions: Asia, Australia, Northern Africa, Southern Africa, North America, and South America. The Asian monsoon has three sub-monsoon systems: South Asia, Western North Pacific (WNP), and East Asia (B. Wang et al., 2003). They are separated approximately at 105° E and 20° N. The East Asian monsoon is located to the east of the Tibetan Plateau and is a unique subtropical monsoon (all other regional monsoons are tropical). The South Asian monsoon, also known as Indian monsoon, and WNP monsoon are tropical monsoons but the latter is largely oceanic. It should be noted that the monsoon precipitation domain does not depend critically on the specific values of the two rainfall criteria. For instance, an alternative criterion was used by Wang and Ding (2006) (the local summer precipitation is greater than 35 % of the annual total) and by Liu et al. (2009) (the local summer (MJJAS or NDJFM) precipitation exceeds 55 % of annual rainfall). The resultant domains were in an excellent agreement with those in Fig. 2.

Note that the monsoons entail substantial oceanic regions, including the marginal seas in South and East Asia, and the tropical WNP, southwest Indian, and tropical eastern North Pacific Oceans. The monsoonal oceans are extensions of the corresponding continental monsoons and are integral parts of the GM system. These oceanic monsoon regions are similar to the continental monsoon regions in that they are controlled by summer monsoon troughs, moisture convergence, and deep convection. They differ from the trade wind regions where divergence and sinking motion prevail during summer. While the variations in the ratio between oceanic and continental monsoons may

CPD
10, 2163–2291, 2014

potentially leave an isotopic imprint in paleo-records, the role of oceanic precipitation has yet to be broadly considered in paleo-monsoon studies (e.g., Oppo et al., 2007).

In the central subtropical South Pacific, there is also an isolated oceanic region that has a similar seasonal distribution as monsoon regimes. But, due to lack of the land-ocean thermal contrast, this pure oceanic region is considered atypical. It is however suggestive that even in an aqua-planet, monsoon regimes may exist due to annual variation of the solar forcing, even in the absence of a land-ocean thermal contrast (Chao and Chen, 2001).

Note as well that dry regions are generally located to the west and poleward side of the monsoons (Fig. 2), due to the descent resulting from the interaction between westward propagating Rossby waves and the mean westerly flow on their poleward side (Hoskins, 1996; Rodwell and Hoskins, 1996). The resultant coupled monsoon - desert interactions govern a large portion of the tropics and subtropics (Fig. 2).

The monsoon domains defined by precipitation are different from, but dynamically consistent with, those defined by low-level winds. The tropical monsoon domains as depicted by the annual reversal of zonal wind can be define by the following criterion: The local summer westerly minus winter easterly at 850 hPa exceeds 50 % of the annual mean zonal wind speed (Wang and Ding, 2008). Such defined monsoon wind domains are shown in Fig. 3 (bold black contours) and they agree closely with previous definitions made by Ramage (1971) using three wind criteria. Unlike Ramage (1971) however, the North and South American monsoons are discernible, albeit relatively weak. Of note is that the monsoon westerly and precipitation domains do not coincide precisely but are dynamically consistent. The westerly monsoon domains are situated to the equatorward and westward sides of the precipitation domains generally (Fig. 3), as expected from the Rossby wave response to the precipitation heat sources, discussed in Fig. 2.1. The East Asian monsoon is a subtropical-extratropical monsoon and is characterized by annual reversal of the meridional winds (Guo, 1983), thus it can be described by using monsoon southerlies in a similar manner as westerly winds are used to define tropical monsoons (Wang and Ding, 2008).

CPD
10, 2163–2291, 2014

2.2.2 Evolution of the global monsoon concept

Regional monsoons are bonded by the global divergent circulation. Trenberth et al. (2000) depicted the global monsoon as the global-scale seasonally varying overturning circulation throughout the tropics. Considering that the physical principle of conservation of mass, moisture, and energy applies to the global atmosphere and its exchange of energy with the underlying surfaces, the analysis of broader monsoon variability from a global perspective is imperative and advantageous for understanding fundamental monsoon controls and dynamics.

The GM can be quantitatively defined as the dominant mode of the annual variation of precipitation and circulation in the global tropics and subtropics (Wang and Ding, 2008). The first empirical orthogonal function mode of the annual variation of global precipitation and low-level (850 hPa) winds (Fig. 4) accounts for 71 % of the total annual variance, has a prominent annual peak, and features an inter-hemispheric contrast in precipitation (Fig. 4a). This mode can be simply characterized by the difference in mean precipitation and circulation between the two extended solstitial seasons, June-July-August-September (JJAS) and December-January- February-March (DJFM) (Fig. 4b). This solstitial mode depicts seasonal changes in the GM precipitation and associated low-level monsoon circulation and reflects the fact that the GM is a forced response to the variation of solar insolation, with a phase delay of a few months that reflects the oceans' considerable thermal inertia. The regional monsoons (Fig. 2) are thus mutually synchronized by this forcing. Due to their existence in a seasonally variable, deep convective environment, their variability is also governed in part by this common forcing and shared feedback processes. Therefore, a broader understanding of the regional monsoons can be gained from this global perspective.

It is clear that the GM includes both the so-called summer and winter monsoons. As inferred from Fig. 4b, during NH summer, the NH monsoons experience a summer rainy season and southwesterly winds, while the SH experiences a local winter monsoon with below-normal rainfall and an equatorward and westward displaced "winter monsoon", whereby moisture is transported from the winter to summer hemisphere. During NH winter, precipitation anomalies (deviation from the annual mean) reverse sign and surface winds reverse direction. The "winter" monsoon over East Asia is particularly strong due to the cold Eurasian land mass and the relatively warm North Pacific Ocean. During winter, the powerful Siberian High and Aleutian Low set up a strong cold and dry northerly circulation over East Asia, whereas during summer, the strong Asian low and WNP Subtropical High reverse the zonal pressure gradient and drive a strong and moist southerly low-level flow. In this sense, the East Asian monsoon has the strongest annual reversal of surface winds of any monsoon, and contrasting seasonal rainfall, which forms a unique subtropical-extratropical monsoon region.

In summary, the GM exists on a planetary scale, with a seasonal reversal of the three-dimensional monsoon circulation that is accompanied by migration of the monsoon rainfall zones. The GM is thus a defining feature of Earth's climate.

2.2.3 Global monsoon and ITCZ

The GM has intimate relationship with annual migration of the inter-tropical convergence zone (ITCZ) (Gadgil et al., 1988) but is also distinct. The ITCZ typically refers to the surface wind convergence zone in the tropics and also indicates the location of maximum persistent rainfall. The climatological location of the ITCZ in February and August based on the maximum rainfall rate (Fig. 2) shifts in response to changes in solar forcing. The northern (southern) ITCZ extreme occurs in August (February) and thus lags the peak solar forcing hemisphere by a few months.

The largest annual displacement of ITCZ is seen in the Indian Ocean and western Pacific warm pool (Asian-Australian) and over the African and South American land regions (Fig. 2). These regions also coincide with the GM. On the other hand, over the eastern Pacific and Atlantic Oceans, where the equatorial cold tongues exist, the ITCZ persists in the NH throughout the year, and thus the ITCZ displacement is small. The existence of the equatorial cold tongues is essentially a consequence of the equatorial atmosphere-ocean interaction induced by the north-south asymmetric land-ocean

CPD
10, 2163–2291, 2014

distribution (Philander et al., 1996; Wang and Wang, 1999) with a potential influence from global energy constraints (Frierson et al., 2013).

The ITCZ may itself be categorized by two types: monsoon trough and trade wind convergence zones (B. Wang, 1994). From Africa to Australia, the ITCZ moves from 10–15° S in February to 10–25° N in August (Fig. 3a). The northern fringe in boreal summer occurs over India and is due to strong warming of the Eurasian landmass and the Tibetan Plateau heating effect (Yanai and Wu, 2006). The southern extreme in austral summer occurrs near Madagascar and is related to the impact of the strong southward cross equatorial flow originating from NH winter monsoon and associated Iranian High (Fig. 3b). Due to the large meridional scale of the flow (greater than 20 degrees of latitudes), geostrophic effects divert the cross-equatorial flow eastward on the equatorward side of the summer hemisphere ITCZ; and the winds in between the northernmost and southern most locations of the ITCZ reverse direction annually (Fig. 3). This portion of the summer ITCZ is often associated with a low-pressure monsoon trough. For this reason, the oceanic convergence zones over the Southern Indian (40–100° E), WNP (110–150° E), Southwest Pacific (150–180° E), far eastern North Pacific (70–110° W), and eastern Atlantic Oceans can be regarded as *marine monsoon troughs* that are characterized by a uni-modal annual variation of rainfall, with a significant peak in summer and development of monsoon westerlies on their equatorward side. Conversely, in the central Pacific Ocean, where the ITCZ annual displacement is less than 5 degrees of latitude, the zonal wind (trade winds) between the ITCZ do not change direction between summer and winter, and therefore a monsoon is absent. This portion of the ITCZ can be referred to as "trade wind convergence zone" (B. Wang, 1994). This *trade wind convergence zone* has a persistent rainy season throughout the year and a bi-modal seasonal distribution of rainfall with maxima in the equinoctial seasons.

In summary, the ITCZs between the dateline and 110° W in the Pacific and between 30 and 60° W in Atlantic have minimal seasonal meridional migration and a bi-modal seasonal rainfall distribution, and are thus viewed as trade wind convergence zones. The bulk (about three quarters) of the ITCZ is embedded within the monsoon regions and exhibits prominent seasonal migration (Fig. 2). The ITCZ's meridional migrations are governed largely by the GM and both are direct consequences of the annual variation in solar forcing. GM variability represents, to a large extent, changes in ITCZ and the associated Hadley circulation. Over East Asia, the subtropical monsoon rain band is not a part of tropical monsoon trough over the WNP, but rather is located to the northwest edge of the WNP Subtropical High. The WNP monsoon tough and WNP Subtropical High are thus a dynamically coupled system (Tao and Chen, 1987), and changes in the tropical WNP monsoon can indirectly influence the EA subtropical monsoon through changing the WNP Subtropical High. In this sense, the EA summer monsoon is best viewed as part of the GM system.

2.3 Modern monsoon observation

Monitoring the GM entails observing winds, temperature, rainfall, clouds, and humidity, among other fields, on a planetary scale across a broad range of temporal scales from hourly to interdecadal. The challenges involved are therefore considerable. The era of coordinated planetary scale tropospheric observations adequate for this task commenced with the establishment of the northern hemisphere upper air network in the 1940's (e.g. Kalnay et al., 1996). Early monsoon studies used data from this network, primarily in a piecemeal fashion addressing phenomenology of regional monsoons. Building upon these data, atmospheric "reanalysis" enabled diagnosis of the monsoons on a global scale, with a more coordinated and holistic approach. Reanalyses provided an unchanging data assimilation scheme and modeling framework in an effort to remove sources of spurious variability from operational analyses. Nonetheless, due to their variable input data streams, reanalyses do suffer from spurious temporal variability and a lack of sufficient observations results in reanalysis fields that are strongly model influenced and therefore of questionable realism. Still, given their detailed nature and global scope, reanalysis products are among the mostly widely used data sources for diagnosing the GM and have proven to be instrumental in understanding it, when interpreted with appropriate care. Improvement in reanalyses also offers the prospect for

CPD
10, 2163–2291, 2014

enhanced realism and diagnostic capabilities over time, as products have evolved from 1st generation (e.g. Kalnay et al., 1996; Kistler et al., 2001), to 2nd generation (e.g. ERA-40, Uppala et al., 2005, JRA-25, Onogi et al., 2007), and 3rd generation products (ERA Interim, Dee et al., 2011, MERRA, Rienecker et al., 2011), incorporating more sophisticated data assimilation approaches (e.g. analysis increments and 4D-Var) and models.

Satellite retrievals are also a fundamental source of data for understanding the GM, providing a multi-decadal record of rainfall, clouds, water vapor, temperature, and surface winds. The satellite record is particularly valuable given that the majority of monsoon domains lie over data-scarce ocean regions. As with reanalyses, satellite retrievals are also being improved over time and new instruments offer new capabilities and potential for understanding the monsoons. For example, the recently launched Global Precipitation Measurement (GPM) instrument, has greater sensitivities to a range of precipitation intensities and greater spatial coverage than did its predecessor satellites. Combined with improvements in reanalyses, these sources of data offer considerable promise for continued progress in understanding the GM. Counter-examples to these advances also exist, as other aspects of the observing system have degraded over time. For example, the density of surface rain gauges has decreased considerably in recent years (e.g. Becker et al., 2013) and observations of river discharge have been in decline for decades (e.g. Bjerklie et al., 2003). These deficiencies present a considerable challenge.

3 Paleo-Monsoon and proxies

3.1 Paleo-monsoon research in retrospect

Quantitative studies of the paleo-monsoons first began in the early 1980s and focused on variability in the African monsoon, based on terrestrial records of lake level fluctuations in North Africa (Kutzbach, 1980, 1981), marine records of eolian dust from

CPD
10, 2163–2291, 2014

the Atlantic (Sarnthein et al., 1981), and of sapropels in the Mediterranean (Rossignol-Strick et al., 1982; Rossignol-Strick, 1983). At the same time, paleo-records of the Indian monsoon were discovered in the Arabian Sea on the basis of upwelling variations (Prell, 1984). All these studies focused on the latest Quaternary with a temporal resolution of about 1 kyr, using two groups of proxies: those related to wind, using deep-sea eolian dust, upwelling-induced marine productivity, and those related to rainfall, such as lake level and flood-induced sapropels. Given the short duration of the analyzed sections and relatively coarse time resolution, there was a good correlation between the two groups of proxies, with both indicating a key role for orbital forcing at the precessional band.

The 1990s witnessed a boom in the development of paleo-monsoon research over several regions. The Ocean Drilling Program (ODP) Leg 117 in the western Arabian Sea in 1987 was the first drilling cruise specifically designed for retrieving proxies of the evolution and variability of the Indian monsoon, extending the monsoon history back to the late Pliocene and significantly improving our understanding of the driving mechanism of monsoon variability (e.g., Clemens et al., 1991, 1996). Another long-term sequence of paleo-monsoon records was obtained from the Loess Plateau of China, where thick eolian deposits were successfully cross validated with deep-sea sediments, yielding a history of the East Asian monsoon over the last 7-8Ma (e.g., An et al., 2001). For the African monsoon, the ODP Leg 108 in 1986 to the Equatorial Atlantic recovered a Plio-Pleistocene sequence of Sahara dust that documented the period of hominids evolution in conjunction with variability in the African monsoon (deMenocal, 1995).

While the above-discussed monsoon sequences were primarily based on wind-related proxies (eolian dust, upwelling-induced productivity), others have been established using precipitation-related proxies, including several from the Mediterranean and South China Seas. The ODP Leg 160 to the Eastern Mediterranean in 1995 (Emeis et al., 1996) and Leg 184 to the South China Sea in 1999 (P. Wang et al., 2000) recovered monsoon records back to the Neogene based on the rain-related proxies of chemical

CPD
10, 2163–2291, 2014

weathering rate, sapropel occurrence, and types of land vegetation. With the application of new techniques like X-ray fluorescence core-scanning, the time resolution of these reconstructions approach 2–3 hundreds years for the last 5 Ma (e.g., Tian et al., 2011).

Monsoon archives with much higher resolution have been recovered from marine or lacustrine cores with lamination or ultra-high sedimentation rates for the late Quaternary. For example, reconstructions of monsoon sequences with decadal resolution were provided from the South China Sea (L. Wang et al., 1999; Higginson et al., 2003) and the Arabian Sea (Agnihotri et al., 2002; Gupta et al., 2003). Even very high resolution records (4–5 years) have been made available from the Cariaco Basin for the North American monsoon (Haug et al., 2001) and elsewhere. However, sediment archives have their limitations in resolving absolute age, and paleoclimate records with annual or even seasonal resolution can be retrieved from other sorts of material such as tree rings, coral reefs, ice cores and stalagmites. Of particular significance are the latter two archives: ice cores and stalagmites.

Although ice core drilling began as early as in the 1960s, monsoon variations recorded in ice-core air-bubble have become available only since in the 1990s. Of particular importance are two parameters: methane concentration (Chappellaz et al., 1990; Blunier et al., 1995) and atmospheric oxygen isotope fraction (Bender et al., 1994). Since 2000, speleothem records have become available in several monsoon regions and have become the focus of recent paleo-monsoon work. Given the annual banding and highly precise dating technique of thorium-230, speleothem's paleoclimate sequence can be resolved at annual resolution, improving upon many previous monsoon reconstructions. Over the last decade, numerous speleothem oxygen isotope sequences have been published, including those from South China (e.g., Y. Wang et al., 2001, 2005; Yuan et al., 2004), now extending back to over 380 ka (Cheng et al., 2009a), and to South America (X. Wang et al., 2004; Cruz et al., 2005). These speleothem records clearly demonstrate predominance of precession forcing of the

CPD
10, 2163–2291, 2014

Asian monsoon in orbital scale and its correlation with high-latitude variations at millennial scales.

The new findings resulting from speleothem records have attracted broad interest but have also raised new debates in the paleo-climate community. As in ice-core records, speleothem-derived monsoon sequences are dominated by a 23 ka precessional periodicity. This finding is in sharp contrast to the monsoon records from the Arabian Sea in which the obliquity forcing exceeds that of precession (Clemens and Prell, 2003). The two diverging views on monsoon variations differ in orbital-scale periodicity and phasing: with the former assuming a direct response to boreal summer insolation, while the latter infers an 8-ka delay in responding to precession, due to latent heat transfer from the Southern Hemisphere (Ruddiman, 2006).

This divergence in opinion has evoked a hot debate as to which proxies are representative of the Asian monsoon: the marine records from the Arabian Sea or the speleothem records from the Asian land (e.g., Clemens and Prell, 2007; Clemens et al., 2010; Ziegler et al., 2010; Weber and Tuenter, 2011) which will be discussed in in our follow on work. Here our goal is to note that the divergence of opinion is, at least partly, related to the different nature of the proxies used: with upwelling records based on wind being physically distinct from the speleothem records based on rain. Looking back at the evolution of paleo-monsoon research, it was initiated with both wind- and rain-based proxies, and the two kinds of sequences correlated fairly well at that stage. Controversies appeared however with the introduction of new proxies over the last decade, in particular $\delta^{18}O$ from the speleothem calcite and atmospheric oxygen. Both are proxies related to hydrological processes and the resultant monsoon sequences show small lags of 2–3 ka in response to insolation, in contrast to considerably longer lags of 5–8 ka of the sequences in the Arabian Sea. A small lag has been supported by some recent experiments with numerical modeling (Kutzbach et al., 2008; Weber and Tuenter, 2011), yet the debate remains largely unresolved.

Nonetheless, given this increased availability of proxies, paleo-monsoon proxy data spans all continents and now allows for a global synthesis. Over recent years a number

CPD
10, 2163–2291, 2014

of publications have reviewed the Asian monsoon system as whole (e.g., P. Wang et al., 2005; Clemens, 2006), but it remains a new endeavor to comprehensively examine the GM from a paleo perspective (P. Wang, 2009).

3.2 Proxies for local and regional monsoons

Modern GM variations are primarily studied on the basis of instrumental records while assessing monsoon variations beyond instrumental records relies on the use of proxies, i.e. indirect measures of past climate features preserved in natural archives. Concerning the GM, two questions are to be addressed here: firstly, which proxies can be used for quantitative assessment of regional monsoons for a global synthesis and, secondly, can we find proxies to measure GM variations?

3.2.1 Monsoon proxies

In general, monsoon proxies can be divided into two groups according to the primary aspects of the monsoon that they address: proxies related to monsoon winds (direction, strength and persistence), and those associated with monsoon precipitation. Attached is a simplified table of frequently used proxies to indicate monsoon variations in geological records (Table 1). For more detail the reader is referred to the SCOR/PAGES review of the Asian monsoon evolution and variability (Table 1 in P. Wang et al., 2005).

3.2.2 Wind-based proxies

As seen from Sect. 3.2.1 and Table 1, eolian dust and coastal upwelling are the most frequently used of the wind-based monsoon proxies. Eolian dust has been used for estimating monsoon variations in various oceans (e.g., Sarnthein et al., 1981; Sirocko et al., 1993), as well as in loess-type deposits, particularly in China. In the 1990s, the Plio-Pleistocene history of the East Asian monsoon was diagnosed from the Loess Plateau in China, using the grain size of loess particles to indicate winter monsoon and magnetic susceptibility of the loess-paleosol sequences for summer monsoon (e.g., An

CPD
10, 2163–2291, 2014

et al., 1991; Porter and An, 1995). However, confusion has also arisen from a simplistic approach to interpreting monsoon proxies in the Loess Plateau by ascribing the monsoon alteration indiscriminately to the glacial cycle. Paleo-monsoon reconstructions in the Loess Plateau have also raised questions concerned the validity of various proxies. Does the grain size of eolian dust really depend on monsoon intensity, or on the approximation of the source area (Ding et al., 2005)? Is winter monsoon or westerly wind primarily responsible for the dust transport (Sun, 2004)?

Regarding marine sediments, initial proxies come from micropaleontology, with the most popular monsoon-index species of *Globigerina bulloides*. According to modern observations, different phases of upwelling in the Indian Ocean can be monitored using different species (Kroon and Ganssen, 1989), and in upwelling regions of the South and East China Seas where *G. bulloides* is rare, *Neogloboquadrina dutertrei* has been applied as an upwelling indicator (Jian et al., 2001). Unfortunately, the occurrence of microfossils is sensitive to many environmental factors and often influenced by processes unrelated to the monsoons. Therefore, a multi-proxy approach is employed. Hence the summer monsoon factor for the northern Arabian Sea was proposed on the basis of factor analyses of five proxies: lithogenic grain size, Ba accumulation rate, δ^{15}N, abundance of *G. bulloides* and opal mass accumulation rate (Clemens and Prell, 2003). Since all of the five proxies are indicative of primary productivity, even the use of multi-proxy approach is challenged. In the geological records, the enhanced productivity can be induced by processes other than the summer monsoon, “such as the strength of winter monsoon winds blowing offshore, or changes related to ice-volume cycles, including changes in ocean nutrients and in offshore transport of particulate and nutrient material from the continental shelf ” (Ruddiman, 2006).

3.2.3 Rain-based proxies

As mentioned earlier, a quantitative approach to paleo-monsoon assessment began with numerical modeling of the African monsoon, validated with lake levels fluctuations, a rain-based proxy (Kutzbach, 1980, 1981). The newest high-resolution paleo-monsoon proxies, such as stalagmites and ice-cores, are also rain-based. Since the modern monsoon is most often studied in the context of hydrological cycle, rain-based proxies offers the opportunity for an analogous assessment of the GM across time scales.

Over recent years there has thus been an increase in the number of paleo-monsoon publications based on rain-based proxies. For example, high-resolution records of chemical weathering rate in marine sediment ascribed to monsoon precipitation have been used extensively. With introduction of the new techniques of nondestructive analyses such as X-ray fluorescence, some element ratios such as Ti / Al and K / Si have been used to explore variability in monsoon precipitation with much higher time resolution than previously available chemical analyses (e.g., Tian et al., 2011). River runoff is another index used in paleo-monsoon assessment, with the best example perhaps being the sapropel layers deposited in the Mediterranean produced by the extreme Nile flooding in response to the intensified African summer monsoon (e.g., Ziegler et al., 2010). A number of weathering-related chemical proxies have also been applied to monsoon analysis at tectonic time scale (Clift et al., 2014). Table 1 shows a wide range of proxies indicative of humidity changes in marine and terrestrial records, including the loess sequences. While the pioneering works on paleo-monsoons in the Loess Plateau of China mostly used wind-induced proxies, newer studies have emphasized the proxies resulting from pedogenesis (e.g., Guo et al., 2000).

It is remarkable that almost all new, high-resolution archives of paleo-monsoon variability are associated with hydrological rather than wind processes. This includes proxies derived from tree rings, ice-cores and speleothemes, which each hold the potential for achieving annual resolution. Nonetheless, there are also caveats for using these rain-based proxies, including uncertainties arising from the use of tree-ring δD (Feng et al., 1999, 2002; Zhou, 2002). Among the most remarkable progress since 2000 are the exciting paleo-monsoon records of the late Quaternary yielded by speleotheme analyses from East Asia and South America (e.g., Y. Wang et al., 2001; Cheng et al.,

CPD
10, 2163–2291, 2014

The Global Monsoon across Time Scales

P. X. Wang et al.

2009a), although, at mentioned above, the extent to which speleotheme $\delta^{18}O$ acts as a strongly constrained indicator of summer monsoon intensity remains unclear.

3.3 Exploring proxies for global monsoon

The recognition of the GM as a global system poses a question: how can we collectively measure the GM intensity variations in the past? Since seasonality is an inherent feature of the GM, its intensity can be measured explicitly, for example, as globally averaged seasonal range of monsoon precipitation (summer-minus-winter precipitation) (Wang and Ding, 2006), or merely from the global averaged local summer rainfall, which dominates the seasonal range (B. Wang et al., 2012). The local summer rainfall in the monsoon region dominates the annual total rainfall amount, hence the annual total rainfall, to a large degree, can be used as an approximate indication of overall monsoon strength. In this sense, proxies with annual resolution are sufficient. Because the monsoon signals from various regions are being mixed and intergrated by atmospehic and oceans circulations, the air-bubble and marine records are more promising for assessment of GM intensity than the terrestrial reocrds which mostly reflect the effects of the prevailing regional monsoon. Accordingly, the following discussions will be focused on ice-core air bubbles and on marine records.

3.3.1 Ice-core air bubble

Ice cores provide an invaluable record of climate changes with “fossil air” captured in their bubbles. Of the various proxies available from air bubbles, two have been suggested as being indicative of GM variability: atmospheric methane concentration and oxygen isotope fractionation.

Atmospheric CH_4

An outstanding feature of CH_4 concentration sequences in ice-cores is the strong presence of a precession signal at 23 ka (Fig. 5c; Chappellaz et al., 1990; Loulergue et al., 2008). Since atmospheric CH_4 originates mainly from the inter-tropical wetland in the NH, with secondary input from boreal sources, the changes in CH_4 concentration are thought to be influenced primarily by insolation forcing of monsoonal wetlands (Ruddiman and Raymo, 2003). If true, this implies the potential for CH_4 concentration to be used as a proxy for the GM at orbital timescales.

Meanwhile, CH_4 timeseries of the past 800 ka show strong 100 and 40 ka periodicities (Loulergue et al., 2008), which are characteristic of glacial cycles (Lisiecki and Raymo, 2005). As boreal wetlands are also a main methane source, their extent is closely linked with the climate and ice conditions at the northern high- latitudes (Landais et al., 2010). As shown by a recent study, atmospheric CH_4 records integrate all wetland processes, including the important effects of changes in monsoonal circulations of both hemispheres and the non-monsoonal contributions mainly from boreal wetlands. Approximately, it contains ~60 % of the signals from the past changes of GM, and ~40 % from the boreal wetlands (Guo et al., 2012). Therefore, the use of CH_4 as a GM proxy is likely to be limited by the major influence of boreal wetlands on the overall methane budget.

Atmospheric $\delta^{18}O$ and Dole Effect

Another parameter available from ice cores clearly related to monsoon variability is atmospheric $\delta^{18}O$ in air bubbles. A strong similarity exists between the $\delta^{18}O_{atm}$ and 65° N summer insolation on orbital time scale (Fig. 5b; Petit et al., 1999; Landais et al., 2010) with a shared precession signal suggestive of monsoon influences. Because the atmospheric oxygen originates from sea water in which $\delta^{18}O$ is governed primarily by ice volume variations, $\delta^{18}O_{atm}$ can be decomposed into two constituent parts

CPD
10, 2163–2291, 2014

relating to ice volume and monsoon-related orbital variations respectively (Shackleton, 2000). Consequently, the $\delta^{18}O_{atm}$ record, like that of CH_4, is a somewhat convoluted but potentially useful proxy of the GM.

A more viable basis for a GM proxy may be the Dole effect, i.e. the difference between the $\delta^{18}O$ of atmospheric O_2 in air and the $\delta^{18}O$ of contemporaneous seawater (Fig. 5a; Bender et al., 1994; Landais et al., 2010). $\delta^{18}O$ of atmospheric O_2 over glacial cycles responds to changes in the $\delta^{18}O$ of seawater, and the Dole effect represents oxygen isotope fractionation during photosynthesis, respiration, and hydrologic processes (evaporation, precipitation, and evapotranspiration); all of these are processes related to the GM. The influence of low-latitude processes on isotopic fractionation governing the Dole effect is highlighted by the similar magnitude of its LGM and present values despite vast environmental differences between the two periods (Bender et al., 1994). According to Luz and Barkan (2011), the Dole effect is not primarily sensitive to past changes in the ratio of land-to-sea photosynthetic rates, but rather to changes in low-latitude hydrology. Therefore, the strong correlation between variability in the Dole effect, Northern Hemisphere insolation, and monsoon records are unsurprising (Severinghaus et al., 2009).

In general, the use of the Dole effect as a proxy of GM is supported by both theoretical analyses and observations. However, the current method of calculating the Dole effect (the difference between $\delta^{18}O_{atm}$ and $\delta^{18}O_{sw}$) is likely simplistic, because of the complex process of isotopic fractionation in the hydrological cycle. At least three issues should therefore be considered when calculating the Dole effect: (1) the absence of a common timescale for marine and ice core records (Landais et al., 2010); (2) difficulties in obtaining pure values of $\delta^{18}O_{sw}$ (Rohling and Bigg, 1998; Waelbroeck et al., 2002); and (3) the non-climate factors in $\delta^{18}O_{atm}$ changes, such as biotic and topographic changes.

CPD
10, 2163–2291, 2014

3.3.2 Deep-sea sediments

Another potential archive of GM variability is deep-sea sediment. In addition to marine $\delta^{18}O$, which is used for Dole effect calculation, marine $\delta^{13}C$ is a useful proxy at time scales longer than glacial cycles. Because of the long residence time of carbon in the oceanic reservoir beyond 100 ka, the carbon isotope record exhibits 400 ka eccentricity cycles over the last 5 Ma, with maximum values ($\delta^{13}C_{max}$) occurring at eccentricity minima (Fig. 6). The 400 ka periodicity is observed in both benthic and planktic $\delta^{13}C$ records, as well as in carbonate preservation records, implying rhythmic fluctuations in the oceanic carbon reservoir (P. Wang et al., 2010). In high-resolution deep sea records, the 400 ka long eccentricity cycles can be traced back through the entire Cenozoic (see below Sect. "Eccentricity modulation").

However, it is still premature to use long-term records of marine $\delta^{13}C$ as a GM proxy over this long eccentricity band. The main problem is that the long-eccentricity cycles in the oceanic carbon reservoir can be disturbed by changes in the oceanic circulation. The 400 ka periodicity so clearly visible in the Pliocene $\delta^{13}C$ records is obscured in the Pleistocene after ~1.6 Ma, and since then, the $\delta^{13}C_{max}$ no longer correspond to eccentricity minima (P. Wang et al., 2004). A similar effect also happened in the middle Miocene beginning ~13.9 Ma (Holbourn et al., 2005, 2007; Tian et al., 2009). The 1.6 and 13.9 Ma breakdown of the 400 ka cycles in oceanic $\delta^{13}C$ records probably derived from reorganization of the ocean circulation, as both cases correspond to times of significant expansion of the polar ice-sheets accompanied by the establishment of new deep ocean circulations. It is suggested that ice-sheet growth may have disturbed the normal 400 kyr periodicity of the Earth's climate system (P. Wang et al., 2010, 2014).

Meanwhile there are observations indicating the presence of long eccentricity cycles in monsoon records after 1.6 Ma. For instance, the $\delta^{13}C_{max}$ remained present at 1.2 and 0.8 Ma in the Mediterranean (Fig. 6b), and dust flux minima at 0.4 Ma due to a weaker monsoon have been found in the equatorial Atlantic (Tiedemann et al., 1994). In the equatorial Indian Ocean, the 400 ka cycles are observed in primary productivity records (Beaufort et al., 1997) whereas the $\delta^{13}C$ and carbonate records from the same site display 500 ka cycles (Bassinot et al., 1994). It is likely that the influence of the 400 kyr cycle persisted in low-latitude processes in the climate system such as monsoons, but was dampened in the oceanic carbon reservoir (Wang et al., 2010). Thus, it remains unclear as to how the GM signal enters marine inorganic $\delta^{13}C$ records. We also do not know how the observed 500 ka "super-cycles" are related to GM variations.

Nevertheless, the above discussion narrows the choice of GM proxies to two ideal candidates: the Dole effect at the precession frequency band represented by the $\delta^{18}O_{atm}$ record in ice-cores with ice-volume signals removed, and the marine inorganic $\delta^{13}C$ at the long- eccentricity band. The two parameters are mutually connected by the monsoon-driven low-latitude hydrological cycle. Although the Dole effect and marine $\delta^{13}C$ are proposed as GM proxies, there is a long way to go before confidence in them is high, and a number of important questions have yet to be answered before the physical meaning of these and related parameters can be revealed. The Dole effect will also evolve in its definition and method of calculation, and the marine $\delta^{13}C$ record, with its long eccentricity period, needs to be further explored during periods of high ice-volume and especially during the Pleistocene.

4 Global Monsoon in Instrumental Records

4.1 Interannual variation

Quantification and understanding of present-day monsoon variability are crucial for interpreting its past and predicting its future. Interannual variations can best be studied using the modern observed record and have been widely studied on regional rather than global scales due to their indigenous characteristics associated with specific land-ocean configuration and differing feedback processes. The principal regional domains include South Asia (e.g., Webster et al., 1998), East Asia (e.g., Tao and Chen, 1987), Australia (e.g., McBride, 1987), Africa (e.g., Nicholson and Kim, 1997), North America (e.g., Higgins et al., 2003), and South America (e.g., Zhou and Lau, 1998). To what extent can the interannual variations of GM precipitation (GMP) be driven by internal feedback processes in the climate system?

Interannal variability is commonly studied using the calendar year to delineate successive time periods. However, for the analysis of GMP, doing so is inadequate, because, seasonal distribution of GMP has two peaks, one in July-August (due to NHSM) and one in January-February (due to SHSM), with a minimum in April. In order to depict GMP interannual variation, we therefore use the "global monsoon year", which begins on 1 May and extends through the following 30 April, which includes the NHSM from May to October followed by the SHSM from November to April next year. The monsoon year concept is also suitable for depicting ENSO evolution, because ENSO events normally start in late boreal spring or early summer, mature toward the end of the calendar year, and decay in the following spring.

Analysis of global observations over the past three decades reveals a coherent interannual variation across regional monsoons from one monsoon year to the next (B.Wang et al., 2012). The spatial pattern of the interannual monsoon precipitation variability (Fig. 7a) is characterized by a coherent rainfall signature across a majority of monsoon regions except the southwestern Indian Ocean and the southern part of the South American monsoon. Notably, this coherence exists over nearly all *continental* monsoon regions. An overall drying pattern is associated with the warm phase of El Niño-Southern Oscillation (ENSO) (Fig. 7b), while enhanced precipitation characterizes La Niña conditions. Thus, from one monsoon year (May to the next April) to the next, most monsoon regions, despite being separated by vast areas of arid trade winds and deserts, vary in a coherent manner, connected by ENSO and associated atmospheric teleconnections.

Despite the generally uniform pattern of the leading GMP mode (Fig. 7a), ENSO exerts a tighter control on the NHSM than on the SHSM. ENSO also tends to more strongly influence continental monsoon rainfall than the oceanic monsoons. Thus the

CPD
10, 2163–2291, 2014

total amount of the NHSM land rainfall is highly related to ENSO with correlation coefficient $r = 0.73$ for 1979–2008.

In many respects, this ENSO influence can be thought of a governing influence on the competition between rainfall over land and ocean on a global scale, which influences the global-integrated storage of water over land and contributes significantly to interannual variability of sea level (e.g. Boening et al., 2011). In regions where the atmospheric response to ENSO tends to produce a regional dipole pattern, such as over East Asia, southern Africa, and South America, regional characteristics of variability should be emphasized. In addition, the dominant spectral peaks in monsoon precipitation associated with ENSO vary by region as variations are 3–7 years over West Africa, North America and Australia but only 2–3 years over South and East Asia and southern Africa (Zhou et al., 2008a).

4.2 Interdecadal variation

On interdecadal timescales, numerous studies have investigated the linkage between regional monsoons and other major modes of climate variability. For instance, Indian summer monsoon precipitation has been shown to exhibit a correlation with the North Atlantic Oscillation (Goswami et al., 2006), Northern China's rainfall iscorrelated with the Pacific Decadal Oscillation (Cheng and Zhou, 2013), and west African and North American monsoon variability is related to the Atlantic Multidecadal Oscillation (AMO) (Zhang and Delworth, 2006). A variety of decadal and interdecadal variations of regional monsoons has been identified, with differing periodicity and phase change points (Yim et al., 2013). However, the underlying causes of GM interdecadal variability has yet to be widely studied.

Studies of the GM change on interdecadal timescales requires long-term well-calibrated observations. The scarcity of extended duration oceanic rainfall observations makes it difficult to examine interdecadal variations of GMP while land monsoon areas have longer records due to the presence of the rain gauge network. The total amount of global *land* monsoon rainfall during 1948–2003 does exhibit considerable

Discussion Paper | Discussion Paper | Discussion Paper | Discussion Paper |

CPD

10, 2163–2291, 2014

The Global Monsoon across Time Scales

P. X. Wang et al.

interdecadal variability, with a decreasing trend mainly due to weakening of the West African and South Asian monsoons from 1950s to 1970s. However, since 1980 the global land monsoon rainfall has no significant trend, while global oceanic monsoon precipitation shows an increase (Wang and Ding, 2006; Zhou et al., 2008a; Fasullo, 2012). This long-term reduction in global land monsoon precipitation can be reasonably well captured by atmospheric general circulation models forced by the observed sea surface temperature (SST) anomalies (Zhou et al., 2008b). It is notable however, that major observational uncertainties also exist as the gauge network has major spatial gaps and quality control issues and global land monsoon rainfall records from other sources (e.g. reanalyses) show significant discrepancies. Across reanalyses, mutual discrepancies arise from changes in the assimilated data streams, both prior to and during the satellite era, suggesting that trends that in other studies have been taken as real are likely be spurious (Fasullo, 2012).

With the most updated GPCP data (Huffman et al., 2009), B. Wang et al. (2012) show that during the recent global warming of about 0.4 °C since the late 1970s the GMP has intensified over the past three decades mainly due to the significant upward trend in NHSM while the SHSM has exhibited no significant trend. A recent intensification of the NHSM originates primarily from an enhanced east-west thermal contrast in the Pacific Ocean, coupled to intensification of the subtropical high in the eastern Pacific and decreasing pressure over the Indo-Pacific warm pool. This enhanced Pacific zonal thermal contrast is largely a result of natural variability (e.g. Merrifield, 2012) and tends to amplify both the NHSM and SHSM. On the other hand, the hemispherical thermal contrast may be enhanced due to anthropogenic forcing. The stronger (weaker) warming trend in the NH (SH) creates a hemispheric thermal contrast, which favors intensification of the NHSM but in turn weakens the SHSM. The combined effects of the two factors may help explain why the NHSM has intensified over recent decades while the SHSM has exhibited little trend.

The aforementioned studies of monsoonal trends in the modern record have yet to be able to definitively conclude whether these trends are attributable to anthropogenic

CPD
10, 2163–2291, 2014

forcing or arise from internal variability. Using a circulation index for the NHSM, it is possible to investigate the interdecadal variability of the GM as reanalysis data has become available for the past century (e.g., monthly circulation data taken from 20th Century Reanalysis for 1871–2010, Compo et al., 2011). B.Wang et al. (2013) used the NHSM circulation index defined by the vertical shear of zonal winds between 850 and 200 hPa averaged in (0°–20° N, 120° W–120° E) (Fig. 8a). While NHSM circulation index is highly correlated with the NHSM rainfall intensity over the modern record ($r = 0.85$ for 1979–2011), this approach has the drawback of potentially being insensitive to changes in rainfall since it is based on dynamics alone. Nonetheless, a major finding of the work has been to demonstrate that the NHSM circulation has experienced large amplitude interdecadal fluctuations since 1871, which is primarily associated with what has been termed "Mega-ENSO", the SST difference between the western Pacific K-shape area and eastern Pacific triangle (Fig. 8b). The mega-ENSO has larger spatial scale then ENSO and a longer decadal-to-multidecadal time scale. The mega-ENSO index is an integrated measure of ENSO, the Pacific Decadal Oscillation (PDO, Mantua and Hare, 2002), and Interdecadal Pacific Oscillation (IPO, Power et al., 1999), and is defined by using the total anomaly field, rather than an EOF decomposition. On the decadal time scale, as measured by the 3 year running mean time series, the long-term variation of the NHSM circulation index has been shown to be strongly correlated to the Mega-ENSO index ($r = 0.77$, for 1958–2010) using ERA-40 reanalysis data (Uppala et al., 2005). This significant correlation is confirmed for the period 1871–2010 ($r = 0.62$) by using the 20th century reanalysis dataset (Fig. 8c). Physically, the eastern Pacific cooling and the western Pacific warming are consistent with a strengthening of the Pacific subtropical Highs in both the North and South Pacific and their associated trade winds, causing moisture to converge into the Asian and African monsoon regions and contribute to the intensification of NHSM rainfall.

In addition, Zhao et al. (2012) show that an amplified land–ocean thermal contrast between the Eurasian landmass and its adjacent oceans can be described by a positive phase of the Asian-Pacific Oscillation (APO), whose positive phase corresponds to a

CPD
10, 2163–2291, 2014

stronger than normal NH summer monsoon and strengthened southerly or southwesterly monsoon winds over tropical Africa, South Asia, and East Asia. These circulation anomalies induce enhanced summer monsoon rainfall over all major NH land monsoon regions.

Monsoon interdecadal variability includes not only interdecadal variations of the mean monsoon but also variations of interannual variability itself (second moment), which also has considerable impacts. It is well known that the monsoon-ENSO relationship is non-stationary and it changes over the multi-decadal time scale (Webster et al., 1998). For instance, the ISM-ENSO relationship has weakened since late 1970's (Kumar et al., 1999), while the relationships between ENSO and the East Asia-western North Pacific, and Indonesian monsoons have strengthened (B. Wang et al., 2008). As such, both the year-to-year variability and interconnectedness of the monsoons often exhibits strong interdecadal variability, which can be attributed in part to changes in ENSO characteristics (amplitude, frequency, and onset characteristics). What drives such variability in ENSO remains an open science question.

There has been little study of the changes in the interannual variability of the global or hemispheric monsoons on the interdecadal time scales. As for interannual variability, decadal shifts in the GM are linked to changes in rainfall over land globally and are mirrored in the changing rates of sea level rise (Fig. 8). These shifts have the potential to extend an understanding of monsoon variability back in time through scrutiny of the sea level gauge record.

4.3 Summary

As discussed in Sect. 4.2, ENSO has dominant influence on the interannual variation of the GM while interdecadal variations of the NHSM are likely driven by Mega-ENSO or Interdecadal Pacific Oscillation (IPO) influences (e.g. Power et al., 1999; Parker et al., 2007). In addition, NHSM interdecadal variations are shown to be significantly associated with the Atlantic Multi-decadal Oscillation (B. Wang et al., 2013) and APO (Zhao et al., 2012). Thus, regional monsoons can be coordinated not only by changes

CPD
10, 2163–2291, 2014

in orbital forcing (Kutzbach and Otto-Bliesner, 1982; Liu et al., 2004) and variations on centennial-millennial time scales (Liu et al., 2009), but also by internal feedback processes on interannual and multidecadal time scale. These are likely to act dynamically, through global atmospheric teleconnections and related atmosphere-ocean interactions on a planetary scale.

It is likely therefore that the NH and SH summer monsoons are not only governed by a common set of processes, such as the enhanced east-west thermal contrast in the Indo-Pacific, but also by inter-hemispheric thermal asymmetries associated with their contrasting land extents that have potentially opposing effects on the NH and SH monsoons (B. Wang et al., 2012). Study of such interdecadal variation of GM is still in an early stage, however there are strong indications that the causes of the interdecadal variability of the SHSM and the GSM warrant further study. An improved understanding of the physical processes that control the GM and its interdecadal variability is therefore a top priority.

5 Global monsoon at sub-orbital time scale

Climate variations on sub-orbital timescales in low- to middle latitude monsoon regions have been identified in high-resolution proxy records provided by ice-core, coral, tree ring, lacustrine, loess, marine deposit, and historical records (e.g., Thompson et al., 1986; Cobb et al., 2003; Ge et al., 2003; Cook et al., 2010; Bird et al., 2011; Sun et al., 2012; Bard et al., 2013; Ziegler et al., 2013; Deplazes et al., 2013). Over recent decades, however, speleothems have attracted primary scientific attention and offered a new perspective on paleo-climate reconstructions (Henderson, 2006). This archive is particularly suitable for characterizing GM variability on sub-orbital timescales, because of the distinct advantage of its considerable spatial coverage in all major regional monsoon domains, and its high temporal resolution and precise chronology. Today, a considerable fraction of our current knowledge of sub-orbital monsoon variations and

CPD
10, 2163–2291, 2014

related coherent variability across the regional monsoons is due to the speleothem records.

5.1 Millennial scale variability

Millennial-scale climate oscillations or events were large in amplitude and well documented over the past few glacial periods, contrasting to the much smaller counterparts during interglacial periods, for example the Holocene. In the 1970s, Greenland ice core records revealed a series of millennial events, which demonstrated that temperatures over Greenland have oscillated on millennial-scale during the last glacial time abruptly and significantly between two modes, extremely cold (stadials) and relatively mild (interstadials) intervals (e.g., Broecker et al., 1985). Such millennial oscillations are referred to as Dansgaard–Oeschger (D/O) oscillations with an apparently dominant pacing of ca. 1500 years (Dansgaard et al., 1993; Grootes et al., 1993) (Fig. 9a). In the 1980s, North Atlantic marine sediment records revealed several episodes of usually abundant ice rafted debris (i.e., Heinrich 1988; Bond and Lotti, 1995), referred as Heinrich events (H events) (Fig. 9). In addition, it was also found that colder temperatures over Greenland correlate with lower ocean temperatures inferred from larger percentages of the polar foraminifera species in marine sediment records from the North Atlantic Ocean (e.g., Bond et al., 1993). In contrast however, millennial events revealed from Antarctic ice cores have much smaller amplitudes. On the basis of CH_4 correlations (Blunier and Brook, 2001), a gradual Antarctic warming was found to coincide with Greenland cold events. This pattern of opposing temperature changes in the North Atlantic and Antarctica was termed the "bipolar seesaw" (e.g., Stocker et al., 1992; Broecker, 1998; Stocker and Johnsen, 2003), a hypothesis that attributes changes in the Atlantic meridional overturning circulation in the Atlantic Ocean as a trigger and/or propagator of global millennial oscillations (e.g., Broecker and Denton, 1989; Broecker, 2003).

Similar millennial-scale climate oscillations have also been clearly documented in low to middle latitude regions, particularly in monsoonal regions, including the East Asian

CPD
10, 2163–2291, 2014

monsoon region (e.g., Y. Wang et al., 2001, 2008; Cheng et al., 2006), the Indian monsoon region (e.g., Burns et al., 2003; Deplazes et al., 2013; Bard et al., 2013), North American and Mesoamerican monsoon regions (e.g., the tropical North Atlantic Ocean, Rühlemann et al., 1999; Cariaco basin, Peterson et al., 2000; Santa Barbara basin, Hendy and Kennett, 2000; southwestern America, Asmerom et al., 2010; Wagner et al., 2010; and Mesoamerica, Lachniet et al., 2013), the South American monsoon region (e.g., X. Wang et al., 2004; Cruz et al., 2005; Kanner et al., 2012; Mosblech et al., 2012; Cheng et al., 2013), the Indo-Australia monsoon region (e.g., Lewis et al., 2011; Ayliffe et al., 2013), and the North-South African monsoon regions (e.g., Weldeab et al., 2007, 2012; Garcin et al., 2007; Mulitza et al., 2008; Ziegler et al., 2013). These monsoonal variations correlate strongly with those revealed in the Greenland and Antarctic ice cores, including the Younger Drys (YD), D/O and H events. In fact, a new nomenclature, the Chinese interstadials (CIS), was introduced to describe not only the millennial Asian monsoon events that can be individually correlated to the Greenland interstadials (GIS) during the last glacial time (Cheng et al., 2006), but also the similar events during the penultimate glacial period, which Greenland ice core records fail to sample due to their limited temporal span (Cheng et al., 2006; Y. Wang et al., 2008).

On the basis of this considerable body of proxy records, a comprehensive pattern of GM millennial variability has merged (e.g., Cheng et al., 2012a). While the NH summer monsoons (i.e., the North African, Asian including both Indian and East Asian, and North American-Mesoamerican summer monsoons) weakened abruptly during millennial-scale cold events (such as the YD event, Greenland stadials or Chinese stadials), the Indo-Austrian, South American and South African monsoons intensified in SH during same episodes, and *vice versa*. This contrasting interhemispheric behavior is now evident across a wealth of proxy data (Fig. 9). In addition, records from southwestern America in the North American monsoon domain also show a series of millennial events during the last glacial period (Asmerom et al., 2010; Wagner et al., 2010). However, when cold events occur in the North Atlantic region, the polar jet stream shifts southward, modulating the position of the winter storm tracks and, in turn, winter precipitation increases (Asmerom et al., 2010). As a result, the millennial-scale events in this region are apparently anti-phased, in terms of precipitation $\delta^{18}O$ and possibly amount, with their counterparts in Cariaco basin/the tropical North Atlantic Ocean, Mesoamerican, and the Asian-North African monsoons (Fig. 9). To first order, anti-phased millennial monsoon events in both hemispheres are broadly similar in terms of their amplitude and abruptness as inferred from proxy records. They also appear to be more comparable with Greenland than with Antarctic events.

5.2 Abrupt vs. gradual changes: the Holocene history

The Holocene (the past 11.5 ka) climate in monsoon regions is generally stable in comparison to during the last glacial period. It generally exhibits a long-term trend broadly tracking the summer insolation. A warm and wet period in NH monsoon regions occurred approximately between 9–5 ka BP during the so-called the Holocene Climatic Optimum. In contrast, monsoon variations in the SH during the Holocene, such as for example in South America, relate strongly to austral summer insolation and thus are approximately anti-phased with the NH monsoons (see next section for details). In addition to gradual changes in insolation, non-linear response/feedback mechanisms may result in a series of abrupt monsoonal variations. For example, Morrill et al. (2003) emphasized two major abrupt climate events, likely occurred synchronously in the Asian monsoon domain at ~11.5 ka and 5.0–4.5 ka BP, respectively. The first abrupt intensification of the Asian monsoon occurred at ~11.5 ka BP and corresponds to the onset of the Holocene. This monsoon jump also marks the end of the YD event, which is extremely abrupt with a major shift that occurred over ~30 years (Alley et al., 1993; Ma et al., 2012). The onset of the Holocene at 11.5 ka BP is a very dramatic event with global effects, including intensification of the North African (deMenocal et al., 2000), Asian (Cheng et al., 2009a), and North American and Mesoamerican (Lachnieta et al., 2013; Asmerom et al., 2010) monsoons, and weakening of the South American (X. Wang et al., 2006, 2007b) and possibly South African (Garcin et al., 2007) monsoons.

CPD
10, 2163–2291, 2014

While it is clear that the onset of the Holocene was extremely abrupt and exhibited global influence, another abrupt change in the Asian monsoon domain between 5.0–4.5 ka BP as described by Morrill et al. (2003) is still unclear in terms of its spatiotemporal scope and mechanism. The event occurred at a time between Bond events 3 and 4 (see the following section), when the Asian monsoon was waning along a summer insolation decrease trend at the precession band. Actually, we can see similar abrupt changes often occurred under the same insolation condition when looking deep into the Asian monsoon history as documented in sepleothem records. For example, at the end of MIS 5e is an exceedingly rapid shift (e.g., Yuan et al., 2004; Kelly et al., 2006; Y. Wang et al., 2008). However, new high-resolution and absolute-dated speleothem (e.g., Y. Wang et al., 2005; Cai et al., 2010b) and synthesized lake (Zhang et al., 2011) records do not corroborate this event. One possibility in explaining this disagreement is that the climate events in the Asian monsoon domain around this time are not representative of a single synchronous event. For instance, a recent new high-resolution record of the Indian monsoon from NE India reveals an abrupt event ca. 4.0 ka BP and, in contrast, there are no abrupt events observed between 5.0–4.5 ka BP in the same record (Berkelhammer et al., 2012). Given the fact that Asian summer monsoon weakened progressively, and its fringe likely retreated southwards, during the transition from middle to late Holocene, it is unclear whether climate variations in the region are really well characterized as a single coherent event across the monsoons' geographical extent.

In Africa, it has become clear that summer insolation provides an overarching control on the North African monsoon on orbital timescales, including for example during the Holocene (e.g., Kutzbach and Street-Perrott, 1985; deMenocal and Rind, 1993; Kutzbach et al., 1996). During the early and mid-Holocene epoch ($\sim$ 11.5–5 ka BP), paleohydrological data suggest that both North and East Africa experienced wetter conditions relative to today (e.g., Gasse, 2000). In North Africa, this Holocene pluvial period is often referred to as the "African Humid Period" (deMenocal et al., 2000), and during the period, the Sahara became green with lakes and a rich vertebrate fauna in a region that is now desert. Pollen evidence indicates that the Saharan desert at this time was transformed into an open grass savannah, dotted with shrub and tree species that today grow hundreds of kilometers to the South (e.g., Ritchie et al., 1985; Adams 1997; Jolly et al., 1998; Kröpelin et al., 2008) (Fig. 10). Nevertheless, the suddenness of the end of the African Humid Period nearby 5 ka BP is still a matter of debate (deMenocal et al., 2000; Adkins et al., 2006; Renssen et al., 2006; Liu et al., 2006, 2007; Kröpelin et al., 2008; Brovkin and Claussen 2008; McGee et al., 2013).

The marine sediment record (Hole 658C) off northwestern Africa provides a classic record that documents an abrupt increase in terrigenous (eolian) concentration at ~5.5 ka BP (deMenocal et al., 2000). This event has been corroborated recently by additional marine records along the northwest African margin with a revised age of 4.9 ka BP (McGee et al., 2013). Together, these records suggest that the end of the African Humid Period was rather abrupt and potentially linked to the collapse of the Saharan savannah (Claussen et al., 1999; deMenocal et al., 2000), although it remains unclear whether the suddenness was simply a direct response to an abrupt event in the monsoon precipitation or a nonlinear response to a regional vegetation threshold which ultimately was reached due to the gradual waning of the monsoon.

The precipitation record from the marine sediment core in the Gulf of Guinea (MD03-270), an indicator of relative changes in the outflow of the Niger and Sanaga rivers, shows only a minor event at about 5 ka BP (Weldeab et al., 2007). The results from examination of North Atlantic marine sediments also indicate a gradual change in the coastal upwelling and accompanying SST around the time (Adkins et al., 2006). There is currently no clear evidence of an abrupt collapse in large-scale North African monsoon precipitation around 5 ka BP, suggesting an ecosystem threshold mechanism: a sudden transition from grassland to desert despite a relatively gradual change in rainfall. Furthermore, on the basis of paleo-environmental reconstructions from Lake Yoa in northern Chad, Kröpelin et al. (2008) argue that the end of the African Humid Period is a gradual shift, rather than an abrupt termination, which is contradictory to the abrupt dust flux increase documented in marine records along the northwest African margin.

CPD
10, 2163–2291, 2014

It thus appears that at least one of proxy records, the Atlantic marine sediment core or the Yoa record, may not be representative of the hydrological history throughout broader North Africa.

Notwithstanding this ambiguity, it is likely that the summer monsoon northern fringes in North African and Asia retreated southward hundreds of kilometers from the mid-early to late Holocene (Winkler and Wang 1993; Adams 1997; Jiang and Liu et al., 2007) (Fig. 10). In other words, a substantial part of the land in the region that is currently arid or semi-arid was once "greener" during the early to mid-Holocene and these previously monsoonal fringe belts experienced a transition from relatively wet conditions to today's arid state. Still, it remains unclear if this transition is characterized by a gradual progressive shift or by an abrupt jump, and what the associated impacts may have been in regions where the modern summer monsoon prevails. A recent cave record, likely from the northern fringe region where the Asian monsoon withdrew, is the Kesang record from western China, which remarkably reveals a Holocene hydroclimate pattern very similar to records established from the modern Asian monsoon domain (Fig. 10) and might potentially provide new insights into the transition history from the middle to late Holocene (Cheng et al., 2012b). However, additional high-resolution and absolutely-dated paleohydrological records are critically needed to expand their spatiotemporal coverage in order to definitively establish the monsoon zonal migration transition time in broader Holocene.

5.3 Centennial scale variations during the Holocene

Despite the Holocene's climate stability, which is generally devoid of millennial-scale climatic oscillations with amplitude comparable to those observed during the glacial periods, there clearly exist many distinct climatic events on centennial-decadal scales. For example, a series of cold/dry events did occur in many monsoon realms in the NH, such as events centered approximately at 11.4, 10.2, 9.2, 8.2, 6.6, 5.6, 4.2, 2.7, 1.4 ka BP, the Little Ice Age (LIA, ~ AD 1400–1850), and warm/wet events, the Medieval Climate Anomaly (MCA, ~ AD 950–1250) and the Roman Warm Period (RWP,

CPD
10, 2163–2291, 2014

~ 250 BC–AD 400), and possible counterpart events in Southern Hemisphere (e.g., Talbot and Delibrias, 1977; Bond et al., 1997; Verschuren et al., 2000; Haug et al., 2001; Dykoski et al., 2005; Hodell et al., 2005; Russell and Johnson, 2005; Newton et al., 2006; Fleitmann et al., 2007; Zhang et al., 2008; Cheng et al., 2009b; Sachs et al., 2009; Wanner et al., 2011; Tan et al., 2011; Sinha et al. 2011; Novello et al., 2012; Vuille et al., 2012; Liu et al., 2013; Sletten et al., 2013; Rodysill, et al., 2013). Most of these events likely coincided with Bond events, primarily identified from fluctuations in ice rafted debris in the North Atlantic Ocean (Bond et al., 1997) (Fig. 11). Increasingly, evidence now suggests that at least some of these events are of larger spatial extent than previously recognized.

In monsoon regions, the most prominent and widespread climate event during the Holocene is perhaps the 8.2 ka event (e.g., Cheng et al., 2009b; Liu et al., 2013). The timing and structure of the event has been well documented in Asian (i.e., Hoti and Qunf records, Oman and Heshang-Dongge records, China) and South American monsoon records (i.e., Paixão, Padre Lapa Grande records) (X. Wang et al., 2006; Cheng et al., 2009b; Stríkis et al., 2011) (Fig. 11). Similar to the millennial-scale events during the last glacial period, the 8.2 ka event manifests as a weak Asian monsoon and strong South American monsoon event. Many other events, such as for example the Bond events, are likely to have had spatial extents larger than previously believed in the monsoon regions (e.g., Gupta et al., 2003; Y. Wang et al., 2005; Stríkis et al., 2011; Cheng et al., 2012a). However, the amplitudes of the events are most likely smaller than the 8.2 ka event and, thus, potential noise associated with climatic proxies may be relatively high in comparison with the climate signals from the events themself. As such, additional high-resolution, accurately dated climate proxy records are required to characterize and understand such events. For instance, a high-resolution stalagmite record from central-eastern Brazil recently revealed the out of phase relationship between Holocene Bond events in Asian and South American monsoon domains (Stríkis et al., 2011; Cheng et al., 2012a) (Fig. 11). In addition, the Bond events are estimated to reoccur approximately every 1500 ± 500 years (e.g., Denton and Karlen, 1973; O'Brien

CPD
10, 2163–2291, 2014

P. X. Wang et al.

et al., 1995; Bianchi and McCave, 1999; Bond et al., 1997, 2001; Wanner and Bütikofer, 2008; Wanner et al., 2008, 2011). This periodicity is similar to the observed millennial oscillation during the last glacial period (Rahmstorf, 2003). However, the mechanisms underlying this periodic change at an interval of about 1500 years remain unclear.

Although the spatial patterns of the centennial monsoon variability are likely to be complex, a number of events during the past two millennia appear to have exhibited an apparent anti-phased relationship across hemispheres. For example, the LIA has been shown to be drier in the Asian monsoon region and wetter in the South American and southern Asian-Australian monsoon regions (e.g., Newton et al., 2006; Zhang et al., 2008; Reuter et al., 2009; Vuille et al., 2012; Cheng et al., 2012a). As noticed in Cheng and Edwards (2012), some of these events may have had considerable socio-economic consequences (Fig. 12). For example, in the late 9th Century, the Mayans and Tang Chinese societies both faced more arid conditions (Yancheva et al., 2007). The Vikings settled Greenland in the 980's, during the Europe's MCA, while the Northern Song Chinese prospered, with expanded rice cultivation and a large growth in population. Also, at this time, the newly established Guge Kingdom thrived. Meanwhile, in contrast, the Tiwanaku, of tropical South America faced drought (Ortloff and Kolata, 1993), consistent with the hemispheric contrast in rainfall suggested by data. If one aspect of this climatic phenomenon is a meridional shifts in the low latitude (to mid-latitude in the case of the Asian monsoon) rainbelt, as has been inferred for other times (Cheng et al., 2009b; Reuter et al, 2009), then dry conditions faced by the Tiwanaku may well be part of the same phenomenon that brought abundant rainfall to the Guge Kingdom and the Northern Song Chinese: a broad northward shift of the ITCZ, with additional rain at the northern fringes of the belt, but with less rainfall on its southern fringes. Another example of this mechanism comes from the 4.2 ka event, when an arid event occurred in the NH. This event is believed to be one of the most severe Holocene droughts in terms of instigating cultural upheavals. The event is likely to have initiated the southeastward habitat tracking of the Indus Valley Civilization as the Indian monsoon was waning during the event (Giosan et al., 2012). At the same time, the drought associated with the event associated with a weakened monsoon may have caused the collapse of Neolithic Cultures around central China (Wu and Liu, 2004). It is likely that the event had considerable reach across the Asian monsoon domain (Berkelhammer et al., 2012), and there is also an indication that the Southern Hemisphere experienced wet conditions during the event (Fig. 11). However, additional data and analysis will likely be needed to further confirm the link between climate events, human cultural shifts, and the meridional shifts of monsoonal rainfall on centennial to decadal timescales.

In summary, the largest amplitude and most abrupt millennial oscillations appear to have been centered near Greenland and the North Atlantic Ocean. In contrast, small, gradual, and approximately out of phase variability is apparent in Antarctic records. In the context of available data, it appears likely that low-latitude monsoon variability on a millennial timescale is manifested primarily by a broad anti-phased relationship between the hemispheres. It does not appear impossible that centennial-multidecadal monsoon variations, at least some of major events, concurred during the Holocene with anti-phased relation between two Hemispheres as well. These observations clearly demonstrate that the dominant variability of regional monsoons on sub-orbital timescales is coherent on a planetary scale.

6 Global monsoon at orbital time scale

6.1 Orbital forcing and insolation

Orbital forcing exerts a major influence on the GM. The monsoon itself is a consequence of the Earth's orbit and tilt, and as Earth's orbit has varied throughout geological history low frequency changes in the GM have occurred. Indeed orbital variability was the primary motivating factor behind many of earliest paleo- monsoon studies (e.g. Kutzbach, 1981).

The solar insolation received at the Earth's surface is determined by three orbital parameters with different periodicities: precession (20 000 years), obliquity (40 000 years)

CPD
10, 2163–2291, 2014

and eccentricity (100 000 and 400 000 years). According to geological records and numerical modeling, low-latitude monsoon variations are mainly caused by changes in precession (Molfino and McIntyre, 1990; McIntyre and Molfino, 1996; Short et al., 1991), but tropical solar insolation varies not only on the 20 ka cycle of precession, but also strongly on the 100 and 400 ka eccentricity and 10 ka semi-precession cycles (Berger and Loutre, 1997; Berger et al., 2006). The precessional cycle does not change insolation's annual total, but rather influences its seasonality and, in turn, the GMs, significantly. Since seasonal variations are out of phase between hemispheres, the insolation changes associated with precession are also out of phase, resulting in hemispheric contrasts in paleomonsoon records at the precessional time scale.

Increasingly, proxy evidence has revealed that orbital cycles have influenced the GM throughout the Phanerozoic. Orbital cycles in monsoon proxy records have been widely reported from the Paleozoic and Mesozoic deposits (e.g., Armstrong et al., 2009; Wilde et al., 1991; De Vleeschouwer et al., 2012; Vollmer et al., 2008; Floegel et al., 2005). Although a global assessment of the Pre-Quaternary paleomonsoon is hampered by a scarcity of data, the orbital forcing in monsoon variability is global in nature. Of particular significance is the cyclic occurrence of African monsoon induced sapropel layers in the Mediterranean Sea. The precession-paced sapropel and carbonate cycles have been used to construct astronomical time scale for the Neogene period in the global geochronology (Lourens et al., 2004). Apparently the most significant advances in the past two decades have been in understanding the GM during the Quaternary. Thanks to extensive works on loess-soil sequences (Guo et al., 1996, 2000), stalagmites (Cheng et al., 2009a; Cheng et al., 2012b; Y. Wang et al., 2008; Yuan et al., 2004), lacustrine (e.g. An et al., 2011), and marine records (e.g. Caley et al., 2011; Clemens et al., 1991; Clemens and Prell, 2003), a particularly complete record of the paleo-monsoon in Asia is available, as summarized by the SCOR/IMAGES Working Group (P. Wang et al., 2005). Here, variability in all regional monsoon systems is addressed.

CPD
10, 2163–2291, 2014

Title Page
Abstract Introduction
Conclusions References
Tables Figures
◀ ▶
Back Close
Full Screen / Esc
Printer-friendly Version
Interactive Discussion

6.2 Precession and inter-hemispheric contrasts

The precession forcing of the GM is most evident in proxy records of the Holocene, given the richness of geological data archives and particularly the high-resolution cave and deep-sea records. Stalagmites from East Asia exhibit a long-term trend which is broadly similar to changes in summer insolation, with a general warm/wet period in NH monsoon regions from approximately 9.0–5.0 ka BP, during the so-called Holocene Climatic Optimum (HCO)(Fig. 13a). Speleothem records from Qunf cave, southern Oman (Fleitmann et al., 2003; Fig. 13b), Timta cave, northern India (Sinha et al., 2005) and Tianmen cave, Tibet (Cai et al., 2012), suggest that the Indian monsoon has varied in concert with the East Asian monsoon during the Holocene (Cheng et al., 2012a). The basic structures of variability for the East Asian and Indian monsoons are essentially similar, characterized by a broadly coherent pattern with a rather gradual long-term change that follows NH summer insolation (e.g., Yuan et al. 2004; Y. Wang et al., 2008; Cheng et al., 2009b, 2012b; Cai et al., 2010a, 2012; Zhang et al., 2011). A similar pattern has also been observed in marine proxy records of the North African monsoon (Weldeab et al., 2007; deMenocal et al., 2000; Fig. 13e, f).

Recently, a number of speleothem records from tropical-subtropical South America have demonstrated that Holocene variations in the South American monsoon also visually track changes in SH summer insolation (Cruz et al., 2005, 2007; X. Wang et al., 2004, 2006, 2007a; van Breukelen et al., 2008; Cheng et al., 2013) and thus, exhibit approximately an interhemispheric anti-phasing relationship with the Asian monsoon (Fig. 13g–i).

The Australian (aka. Austral-Indonesian) monsoon system is sometimes considered a part of the Asian monsoon (Beaufort et al., 2010) due to its link with the modern Asian monsoon system (Trenberth et al., 2000; B. Wang et al., 2003). Long-term continuous geological records for the Australian summer monsoon however are scarse. Recently, multi-proxy analysis of a core retrieved in the Eastern Banda Sea has provided some insight into the Australian monsoon history for the past 150 ka (Fig. 14c; Beaufort et

CPD
10, 2163–2291, 2014

al., 2010). These coccolith and pollen assemblages show that the primary production in the Banda Sea and length of the dry season in northern Australia and southeastern Indonesia, which primarily influenced by the winter monsoon, vary on precessional frequencies and are generally correlated with Asian summer monsoon records (Fig. 14a).

The monsoon systems are a key component of warm season precipitation in North and South America (Vera et al., 2006), yet monsoon research in the Americas generally began much later than for the Asian and African monsoons. Although the climate impact of modern day ITCZ shifts in the Americas has been a topic of research for decades, paleo-monsoon studies began only in recent years. In this work, it has been shown through the analyses of lacustrine deposits in New Mexico that periods of enhanced summer monsoon precipitation in MIS 11 and 13 are related to precessional forcing (Fawcett et al., 2011), while the Holocene drying trend observed in sediment cores from a lake in Nevada suggested a weakening of the North American monsoon, in conjunction with a weakening of monsoons across the Northern Hemisphere (Benson et al., 2002). A period of increased monsoon precipitation during the Holocene thermal maximum followed by a trend toward drier conditions since ∼5 ka has also been inferred from marine sediments in the Cariaco Basin (Haug et al., 2001) and Gulf of Mexico (Poore et al., 2003).

Better studied is the late Quaternary history of the South American monsoon whose changes have been documented in ice cores (Thompson et al., 1998), pollen (Pessenda et al., 2004), lake sedimentary and hydrologic data (Rowe et al., 2003). A δ^{18}O time series of calcite from Lake Junin with a well-constrained chronology has provided a record of hydrologic variability that spans the last glacial-interglacial transition in the southern tropics (Seltzer et al., 2000). The general trend of δ^{18}O closely resembles that of January insolation at 10° S, suggesting a role for procession- induced insolation variability. Recently, a number of speleothem records from tropical and subtropical South America have demonstrated that late Quaternary variations in the South American monsoon also accompany changes in Southern Hemisphere summer insolation (Cruz et al., 2005, 2007; X. Wang et al., 2004, 2006, 2007; van Breukelen et al.,

CPD
10, 2163–2291, 2014

2008; Cheng et al., 2013) and thus, exhibiting a marked interhemispheric out of phase relationship with the Asian monsoon (Fig. 15).

Africa is presently the only continent that is divided by the equator into two nearly equal parts, resulting in distinct monsoon systems in each hemisphere. Rich geological archives of the North Africa monsoon has been recovered from the East African Rift lakes (e.g., Gasse et al., 2008), the Mediterranean Sea (e.g., Ziegler et al., 2010), the North Atlantic (e.g., Pokras and Mix, 1987; Weldeab et al., 2007), as well as caves (Bar-Matthews et al., 2003). As a result, the history of the North African monsoon is better resolved by proxy data than its southern counterpart. As mentioned above, sapropel layers formed in the Mediterranean as a response to the Nile River flood induced by a strengthened North African monsoon, and the cyclic occurrences of sapropel suggest a strong role for precessional forcing of the monsoon (e.g., Rossignol-Strick, 1983; Rossignol-Strick et al., 1998; Ziegler et al., 2010). A recent record based on relative iron content from the Mediterranean corroborates the suggested precessional control (Revel et al., 2010).

In the North Atlantic, an extended marine record shows that the North African monsoon is marked by strong signals of the $\sim$20 ka frequency of precession (Fig. 13f; DeMenocal, 1995, 2000). Strong $\sim$20 ka precessional signals were also found in the Ba / Ca ratio sequence of planktonic foraminifera from the Gulf of Guinea, indicative of West African monsoon hydrology of the last glacial-interglacial cycle (Fig. 13e; Weldeab et al., 2007). Speleothem δ^{18}O records from Israel and Lebanon have also been linked to the North African monsoon change, as they, to first order, track surface seawater δ^{18}O changes in the Eastern Mediterranean Sea (Bar-Matthews et al., 2003), and the latter is influenced strongly by river discharge from the North African monsoon region. These speleothem records show a predominant Holocene pattern similar to others observed in the North African monsoon region (Bar-Matthews et al., 2003; Verheyden et al., 2008). Recently, a correlation has been revealed between the Eastern Mediterranean record (color reflectance from ODP 968 core) and Asian monsoon

CPD
10, 2163–2291, 2014

records (Ziegler et al., 2010), which suggest similar changes in the Asian and North African monsoons (Fig. 14b).

As for the South African monsoon, a speleothem record from the Makapansgat Valley, South Africa displays a Holocene pattern generally similar to the South American monsoon records discussed above(Fig. 13i; Holmgren et al., 2003). A 45 000 year record from the Masoko maar (southern Tanzania) lake reveals that the variability of deposition is strongly influenced by the precessional cycle and its harmonics (Garcin et al., 2006). Notable is the 200 kyr record from a crater lake on the interior plateau of South Africa. The summer rainfall proxy shows ∼ 20 ka signals linked with the precessional band adjacent to the North African record (Fig. 16; Partridge et al., 1997; Gasse, 2000). Recently, geochemical records offshore SE Africa have been used to document a Holocene precipitation pattern out of phase with its North African counterparts (Ziegler et al., 2013). In combination with the North African monsoon records, these data support the strong influence of low-latitude interhemispheric contrasts in insolation on the monsoon circulations that are broadly characterized by an anti-phase relationships between the subtropical South and North African monsoons.

6.3 Eccentricity modulation

The recent availability of high-resolution long-term records spanning over one million years has enabled the identification of longer orbital periodicities in monsoon variatiability. As mentioned above (Sect. 3.3.2), the 400 ka long eccentricity is of particular importance for paleo-monsoon studies. Eccentricity influences the climate system mainly through its modulation of the amplitude of climate precession, however unlike for precession, eccentricity forcing exhibits no interhemispheric contrast. The long eccentricity cycle far exceeds the glacial cycle in duration and modulates the monsoon variations on a 10^5 years scale. By controlling the weathering rate and other processes, these low frequency monsoon cycles also lead to periodic changes in the oceanic carbon reservoir. Since the residence time of carbon in the ocean is much longer than 100 ka (Kump, 1991; Katz et al., 2005), the 400 ka period of the monsoon is most evident

CPD
10, 2163–2291, 2014

in the inorganic $\delta^{13}C$ and carbonate reservoirs, representing a key mode of monsoon variability at orbital time scales, as supported by recent modeling experiments (Russon et al., 2010; Ma et al., 2011).

In spite of the Earth currently experiencing its long eccentricity minimum, the 400 kyr rhythm has been largely overlooked in Quaternary paleoclimatology, because of its obscuring since 1.6 Ma (P. Wang et al., 2010, 2014) and the inadequate length of most available proxy records. Nevertheless, long eccentricity of 400 ka is the most stable orbital parameter throughout the geological history (Berger et al., 1992; Matthews and Froelich, 2002), and recognition of their influence has increased remarkably over the last decade. Now, these long eccentricity cycles have been extensively documented in $\delta^{13}C$ records of various time intervals of the Cenozoic, including the transition from Paleocene to Eocene (Cramer et al., 2003), the Early Oligocene (30.5–34.0 Ma) (Salamy and Zachos, 1999; Zachos et al., 2005), the Middle Oligocene (Wade and Pälike, 2004), the Late Oligocene to Early Miocene (20.5–25.5 Ma; Paul et al., 2000; Zachos et al., 2001; Pälike et al., 2006b), the Early to Middle Miocene (13–24 Ma) (Billups et al., 2002; Holbourn et al., 2007), and up to the Pliocene (Ziegler et al., 2010; Tian et al., 2011). These studies document a fundamental forced mode in the Cenozoic hydrological and oceanic carbon cycles. Among those, typical 400 kyr cycles were reported from the Oligocene of the tropical Pacific and likened to be the Earth' "heartbeat"(Pälike et al., 2006a) as a fundamental rhythm of the global climate. As discussed earlier (Sect. 3.3.2), this basic rhythm is also a fundamental periodicity in GM variability, and the 400 kyr long eccentricity cycles act as the most prominent Milankovitch cycles in the first continuous high-resolution benthic $\delta^{13}C$ record for the past 23 Myr (Tian et al., 2011).

Of course, orbital forcing of the GM is not limited to the Cenozoic. A mounting body of evidence indicates that precession and eccentricity cycles have been manifested in paleomonsoon archives throughout the Phanerozoic. For example, the magnetic susceptibility record has been used to indicate the precession and semi-precession cycles of monsoon precipitation in Devonian limestone (De Vleeschouwer et al., 2012);

geochemical and lithological analyses of clay lake deposits revel precession, obliquity and eccentricity cycles in Triassic monsoon precipitation (Vollmer et al., 2008); and Cretaceous limestone and marlstone couplets have been shown to indicate precessional rhythms of monsoon-related hydrological cycling (Floegel et al., 2005). Although a global vision of the Pre-Quaternary paleomonsoon is hampered in most cases by a scarcity of data, the orbital forcing in monsoon variations is widely documented.

6.4 Other controlling factors

Thus far, we have described the precessional cycles and hemispheric asymmetries that characterize orbital forcing of the GM, demonstrating the global nature of orbital periodicities and confirming the ubiquity of responses across the regional monsoons. However, the variations of regional monsoons are not dictated by solar insolation alone, but also depend strongly on geographical boundary conditions. The following is an introduction to three major controlling factors that act to modulate the influence of orbital forcing including inter-hemispheric, high-latitude, and oceanic factors.

The *inter-hemispheric factor* is most significant in equatorial regions where cross-equatorial exchanges are strong. A prime example of such a region is North Africa, where lacustrine deposit sequences south of the Equator nonetheless are coherent with insolation variations in the NH. It was discovered in Lake Tanganyika (3.5–9° S) 25 years ago, that monsoon-driven lake level fluctuations during the past 26 kyr were in phase with those north of the Equator at orbital timescales (Gasse et al., 1989). Temperature and precipitation proxy records spanning the last 60 kyr from the same lake have been found to be influenced primarily by changes in Indian Ocean SST and the winter Indian monsoon rather than by ITCZ migration (Fig. 17; Tierney et al., 2008).

The *High-latitude factor* is largely related to the influence of the boreal ice- sheet. It is perhaps expected that the existence of huge polar ice-sheets impacted low-latitude climate in the Late Quaternary. As seen from Figs. 16 and 14b, the North and South African monsoons varied in response to precessional forcing, but the 20 kyr periodicity is blurred after ca. 50 ka, perhaps due to the growth of the Arctic ice-sheet (Gasse,

CPD
10, 2163–2291, 2014

2000). The influence of glacial cycles is documented even clearer in the loess-paleosoil sequences of China, where pedogenic intensity and chemical weathering of paleo-soil are largely dependent on summer rainfall . The chemical weathering indexes (such as the Fed/Fet) display clear signals of periodicity related to all orbit parameters, but the record shows a board similarity to the marine $\delta^{18}O$ record, the proxy of global ice-volume changes, with generally strong/weak monsoons correspondent to interglacial/glacial periods (Guo et al., 2000, 1998). This pattern is consistent with the low-latitude vegetation changes that are closely related to the monsoons (Zheng and Lei, 1999).

An *Oceanic factor* influencing monsoon variability is perhaps also expected because monsoon is generated in most instances by a land-sea thermal contrast. Modeling studies show that the responses of the monsoons to insolation variability and oceanic feedbacks differ substantially by region, with an oceanic influence that is particularly strong for the Australian monsoon (Liu et al., 2003; Wyrwoll et al., 2007). Consequently, both sea level and solar intensity in the monsoon regions are important for the intensity and southward extent of the Australian monsoon (Marshall and Lynch, 2008). For example, monsoon precipitation inferred from stalagmites in southeast Indonesia ($\sim 10^{\circ}$ S) basically follows the precession forced SH insolation, but it unexpectedly increased from 11 000 to 7000 years ago, when the Indonesian continental shelf was flooded by global sea-level rise (Griffiths et al., 2009). As mentioned earlier, oceanic factor also impact the long eccentricity cycles of GM (see Sect. 3.2.2).

In reality, however, these three factors may collectively interact to broaden the spectrum of monsoon changes from an otherwise regular 20 ka rhythm. An example of records exhibiting this complex spectrum is the lake-level history of Lake Eyre, central Australia (Magee et al., 2004). A continuous record of the Australian summer monsoon for the past 150 ka was reconstructed by the lake-level history of Lake Eyre with a well-calibrated chronology (Magee et al., 2004). Lake level changes at the precession band have been shown to sometimes match southern summer insolation changes, as is consistent with the modeling results (Wyrwoll et al., 2012). However, lake levels were also

CPD
10, 2163–2291, 2014

significantly higher during interglacials than during glacials. These clear signals in the Australian summer monsoon are also attributable to the cross-equatorial influence of the Asian winter monsoon that reinforces the Australian summer monsoon and is also consistent with the impact of sea-level changes (Griffiths et al., 2009). Longer geological records, although discontinuous, also show monsoon-induced lake level maxima during interglacial periods throughout the past 300 ka (Bowler et al., 2001).

6.5 Summary

Some basic features shared by the major regional monsoon systems emerge from the above review including: (1) ~ 20 ka signals related to the orbital precession are common across almost all the monsoon geological records despite their different geographical locations; (2) monsoon changes at the ~ 20 ka precession-related band are generally out of phase between the hemispheres (within the accuracy of their chronology) but the precession forcing is modulated by 400 ka long eccentricity which shows no hemispheric contrast; and (3) the regional monsoons are influenced by factors other than precession forcing. Many geological records show the existence of both 100 and 40 ka signals that are essentially synchronous in the Southern and Northern Hemispheres, with stronger monsoons during the interglacials than for the glacial periods.

Our understanding of the orbital forcing of monsoon climate, however, is based on records that are heavily biased towards the Quaternary and to the orbital cycles at 10^4 years timescale due to the scarcity of monsoon proxy sequences longer than 1 Ma. The longest records of monsoon history are largely restricted to the Asian sector. These limitations of paleomonsoon reconstructions hampers a broader understanding the influence of orbital variations in different climates, such as for example in a world devoid of large ice-sheets or with high greenhouse gas concentrations. As a consequence, little is known about the low frequency processes that modulate 10^4 years cycles.

One efficient way to extend monsoon records deeper in time is to conduct high-resolution analyses of deep-sea sediments. By using techniques such as magnetic measurements and X-ray fluorescence core scanning, a broad spectrum of

CPD
10, 2163–2291, 2014

periodicities has been found in Neogene records of African and Asian monsoon, ranging from semi-precession to long eccentricity timescales (Larrasoaña et al., 2003; Tian et al., 2011). Most promising are records from deep-seas where sedimentation rate is high, such as around large river estuaries. Long-term South American monsoon proxies, for example, may be reconstructed by analyzing the marine deposits outside the Amazon River estuary.

7 Global Monsoon at tectonic time scale

7.1 Pre-Quaternary monsoon

The above discussions deal with modern and Quaternary monsoon variations spanning inter-annual to orbital timescales. Tectonic processes usually measure 10^6 years or longer, and monsoon history at this time scale traces back beyond the Quaternary. Pre-Quaternary paleoclimatology has advanced rapidly over recent decades, and paleo-monsoon research now addressed variability spanning nearly the entire Phanerozoic. For the early Paleozoic, for example, Late Ordovician monsoon climate has been inferred from geological evidence of ITCZ migrations (Armstrong et al., 2009). Aspects of the Silurian monsoon have been inferred from paleoceanographic reconstructions (Wilde et al., 1991), and the variability of Middle Devoian monsoon climate has been reconstructed using magnetic susceptibility records (De Vleeschouwer et al., 2012). For the late Mesozoic, the monsoon-driven reversal of surface tropical currents in the Cretaceous Tethys Seaway has been simulated in models (Bush, 1997), and middle Cretaceous limestone–marlstone couplets have been interpreted as arising from precession-forced variability in monsoon precipitation (Floegel et al., 2005).

Despite of the modest number of papers devoted to Pre-Quaternary monsoon, two time intervals have attracted greater attention in paleo-monsoon studies: the late Paleozoic to early Mesozoic, and the late Cenozoic. The formation of the super-continent Pangaea gave rise to the concept of a “megamonsoon”, a single monsoon system on

CPD
10, 2163–2291, 2014

Pangea persisting from the Permian to early Jurassic periods. It is likely that with the evolution of the land distribution into multiple continents, this unique GM system collapsed into regional subsystems. After reorganization of the land-sea distribution, the modern monsoon sub-systems were established in the late Cenozoic, as suggested by emerging evidence, discussed below. Accordingly, these two intervals will be the focus of the following review of paleo-monsoon at tectonic time scale.

7.2 Super-continent and mega-monsoon

The GM global monsoon system would be uniquely simple if the Earth had only a single continent. Webster (1981) hypothesized that if all the continents were gathered around the northern pole, it would be a continental cap north of 14° N with a nearly complete aridity inland, and with monsoonal precipitation in summer along the coastal region. In fact, there were geological times when all the continents on the Earth assembled into a single continent, the last of which was termed "Pangaea", a result of the so-called "Wilson cycle" which governs the redistribution of landmasses globally across tectonic timescales. This Mega-continent generated Mega-monsoon (Kutzbach and Gallimore, 1989; Parrish, 1993), the most intensive monsoon system in geological history. Since enhanced monsoon circulations can drive enhanced aridity in non-monsoon regions (Rodwell and Hoskins, 1996), it is expected that a "Mega-desert" region should accompany the "mega- monsoon".

From the late Permian to Early Jurassic (~ 250–180 Ma) all continents assembled into two major landmasses, Laurasia and Gondwanaland, converged near the equator into the super-continent Pangaea, culminating at the early Triassic. Modeling results show Pangaea resulted in a Mega-monsoon of global scale with a reversal of surface winds between summer and winter (Fig. 18c, d) and large-scale meridional migration of the ITCZ over Pangaea. A precipitation maximum was located near the Tethys coast with the continental interior being extremely arid Fig. 18a, b (Kutzbach and Gallimore, 1989). This mega-continental climate is characterized as begin extremely "continental",

CPD
10, 2163–2291, 2014

with wide annual range of temperature (50 °C) in its interior (Rodwell and Hoskins, 1996).

The idea of a mega-monsoon first appeared in 1973 when Pamela Robinson drew the hypothetical position of the ITCZ for the late Permian and early Triassic with a 40-degree range of seasonal migration and a single extremely intense monsoon system (Lamb, 1977). Although the cross-equator mega-continent provided tectonic settings for the development of the mega-monsoon, the circulation itself could penetrate into the continental interior only with the presence of a pronounced highland (Parrish, 1993). The Appalachians in America and Variscan range in Europe reached a mean altitude of 4500 and 2000–3000 m, respectively, during this period (Fluteau et al., 2001). Such altitudes are lower than in Tibet today, but the presence of these mountain ranges at equatorial latitudes then were nonetheless of great importance for the monsoon development (Fig. 19; Tabor and Montañez, 2002). The Triassic was distinguished by both an intense monsoon and also by extreme aridity, and the Pangaea was the time of maximal accumulation of evaporites and eolian deposits (Gordon, 1975). In the south-western United States, wind-deposited sands accumulated to a thickness of 2500 m during the 160 million years when Pangaea straddled the Equator. These strata are the thickest and most widespread aeolian dune deposits known from the entire global sedimentary record (Loope et al., 2001), and are accompanied by loess accumulation in semi-arid regions (Soreghan et al., 2008).

The Pangaea mega-monsoon is likely to have experienced significant variations in its intensity due to orbital forcing, as manifested in the orbital cycles in the Triassic playas and lakes. In the Mid-German Basin, Late Triassic dolomite/red mudstone beds depict strong periodicity of the playa system. These periodic changes are believed to have been associated with monsoon variability in the northern low latitudes of the supercontinent (Vollmer et al., 2008). In northeast US, the micro-lamination in the lacustrine deposits of the Newark super-group recorded the alternation of dry/humid conditions and related lake level fluctuations in the Pangaea from the Late Triassic to Early Jurassic (Olsen, 1986). Detailed studies using the 6700 m-long section have revealed a broad range of periodicities in monsoon climate over the past 33 Ma: varves with 0.2–03 mm-thin couplets of alternating light (dry winter) and dark (rainy summer) layers from which seasonal contrast of monsoon climate can be inferred (Fig. 20b); thicker sediment variations representing the 20 ka precession cycles (4 m on average), 100 ka (20–25 m) and 400 ka (90 m) eccentricity cycles (Fig. 20c, d, Olsen and Kent, 1996).

In the Late Jurassic, the "mega-monsoon" collapsed with the break-up of Pangaea; but the spatial distribution of precipitation remains largely monsoonal throughout the Late Jurassic, replaced by a predominatly zonally symmetric distribution in the Cretaceous (Weissert and Mohr, 1996).

7.3 Establishment of the modern monsoon systems

As defined in Sect. 2, the GM can be regarded as an integrated system of six regional monsoon sub-systems (Fig. 2). In the recent decades, substantial amounts of proxy data have been derived for the onset of the Asian monsoon-dominated climate (referred *hereafter* as to Asian monsoon climate) for both temporal (Guo et al., 2002, 2008) and spatial (Sun and Wang, 2005) perspectives, while the onsets of the other monsoonal sub-systems are more poorly known, mainly because of the lack of pertinent geological evidence with well-constrained chronology.

7.3.1 Establishment of the Asian monsoon system

Two prominent features characterize the modern Asian environment: the moist southern regions, which are primarily under the influence of the southwest (South Asian) and southeast (East Asian) summer monsoons, and the arid environments of central Asia, which exist basically beyond the monsoon influence (B. Wang, 2006). This pattern significantly differs from the other parts of the world (Fig. 21) where dry conditions generally prevail across subtropical latitudes.

By the end of the 20th century, it was widely believed that the Asian monsoon strengthened substantially ~ 8 Ma ago, leading to the formation of a monsoon- dom-

CPD
10, 2163–2291, 2014

inated climate in Asia. The evidence for this conclusion was mainly derived from the southern side of the Himalayas. A record of planktonic foraminifera from the Arabian Sea revealed strong wind-induced upwelling since the late Miocene at ~ 8 Ma and this has been interpreted as an indication of the onset or strengthening of the Indian Ocean (South Asian) monsoon (Kroon et al., 1991; France-Lanord and Derry, 1994; Singh and Gupta, 2004). The expansion of plants that use C4 photosynthesis at ~ 8 Ma in South Asia is also suggestive of a strengthening of South Asian monsoon (Quade et al., 1989). Because climate models link the intensification of the Asian monsoon with the tectonic uplift of Tibetan Plateau (Kutzbach et al., 1989, 1993; Ruddiman and Kutzbach, 1989; Ruddiman et al., 1989; Prell and Kutzbach, 1997), the 8 Ma view was also been supported by a number of tectonic studies (Harrison et al., 1992) showing some prominent tectonic changes at the southern margins of the Himalayan-Tibetan complex. However, geological records acquired from the northern side of the Tibetan Plateau over the last two decades have led to major improvements in our understanding of the precise timing of these changes.

Transition from the zonal to monsoonal climate pattern

An examination of the spatial distribution of geological indicators in China has revealed the transformation of the dry areas in the Cenozoic from a zonally symmetric distribution across China to a region restricted to northwestern China (P. Wang, 1990). This shift is confirmed by a more detailed mapping of geological data (Liu and Guo, 1997), which shows the transition from a roughly zonal symmetric pattern of aridity during most of the Paleogene, to the modern monsoonal pattern, probably during the Oligocene or Miocene.

In carefully examining the chronologies and climate significance of the Cenozoic paleo-botanical and geological evidence, Sun and Wang (2005) compiled two sets of paleo-environmental maps for the Paleocene, Eocene, Oligocene, Miocene and Pliocene, one series using only vegetation proxies, with a clearer physical

CPD
10, 2163–2291, 2014

interpretation, and another based on lithological data. Both lines of evidence define consistent environmental pattern changes in China, indicating clearly that the climate patterns in Asia during the Paleogene were predominantly zonal while during the Neogene they were highly similar to the modern era. More detailed mapping specifically addressing the time slices within the Oligocene and Miocene (Guo et al., 2008) corroborates these observations (Fig. 22). The data also indicated that the transition from the zonal pattern to the modern monsoonal pattern of climate.

The Paleogene climate pattern in Asia is actually most similar to the modern-day configuration of the African monsoon region (Fig. 21), with strong subtropical subsidence to the north of the monsoonal zone in the Sahara desert and a dry climate comparable to the modern Mediterranean regime in regions immediately to the north of the desert region (Guo, 2010). Especially, an interior sea, referred to as the Paratethys, was still in existence during the Paleogene in the far western part of China (Dercourt et al., 1993), and presumably this provided a significant amount of moisture to the eastern half of the continent, a suggestion that has recently been confirmed by numerical stimulations on the early Eocene climate (Zhang et al., 2012) showing a Mediterranean-like climate for Central Asia in the Eocene.

The climate patterns for the Neogene are radically different from those in the Paleogene, but highly similar in shape to those of the modern monsoon-dominated era. The Paleogene dry belt in southern China disappeared and was replaced by moister conditions. In contrast to the Paleogene, arid conditions are now primarily observed for northwest China while the middle reaches of the Yellow River, including the Loess Plateau, were dominated by semi-arid conditions. The patterns for the early, mid- and late-Miocene are essentially similar, suggesting that they have existed at least since the early Miocene. The Pliocene pattern is essentially similar to that of the Miocene with only minor differences (Guo et al., 2008; Sun and Wang, 2005).

CPD
10, 2163–2291, 2014

The Global Monsoon across Time Scales

P. X. Wang et al.

Asian monsoon dated by aeolian deposits in China

Aeolian deposits are useful proxies of wind variability (Rea, 1994). The previously reported ∼8 Ma aeolian deposits, consisting of the Quaternary loess-soil sequence of the last 2.6 Ma (Liu, 1985) and the aeolian Red Clay (An et al., 2001; Ding et al., 1998; Guo et al., 2004; Sun et al., 1997), are key indicators of the instigation of the Asian monsoon at 8 Ma. However, much longer aeolian sequences, back to 22 Ma, have been found and dated over the last decade (Guo et al., 2002; Guo et al., 2008; Hao and Guo, 2007). The aeolian origin of these deposits has been well documented by various lines of evidence (Guo et al., 2002, 2008, Hao and Guo 2004, 2007; Li et al., 2006; Liang et al., 2009; Liu et al., 2005, 2006; Oldfield and Bloemendal, 2011; Qiao et al., 2006). Discontinuous aeolian portions likely dating to 24–25 Ma (Sun et al., 2010; Qiang et al., 2011) have also been reported. These new sequences, combined with the previously reported Quaternary loess-soil sequences and the underlying Red Clay, offer a unique aeolian continental record of paleoclimate.

Because eolian deflation only occurs in areas with poor vegetation cover (Pye, 1995; Tsoar and Pye, 1987; Sima et al., 2009), the thick and widespread Miocene aeolian deposits of China firmly attest to the existence of sizeable deserts in the Asian inlands by the early Miocene as dust sources (Guo et al., 2002, 2008). The existence of these deserts is also supported by the Quartz morphology (Liu et al., 2006) and geochemistry signatures (Liang et al., 2009). The near-continuous record of aeolian sequences in northern China, from the early Miocene to the Holocene, implies that inland deserts have been constantly maintained at least for the past 22 Ma (Guo et al., 2008), and that a northerly winter circulation, which is a key indicator of the Asian monsoon system (Liu and Yin, 2002), was already established by the early Miocene.

The Neogene aeolian deposits contain more than 400 visually definable paleosols (Guo et al., 2002; Hao and Guo, 2004). They are mostly luvisol (FAO-Unesco 1974) formed under humid forest environments (Guo et al., 2008), requiring a substantial amount of rainfall (Fedoroff and Goldberg, 1982). These Miocene paleosols imply the

CPD
10, 2163–2291, 2014

existence of another circulation bringing moisture from the ocean. Clearly, the dust carrying winds and moisture carrying winds must be both independent and seasonal. If so, these are strongly suggestive of a monsoonal circulation regime.

Pedological, sedimentological and geochemical approaches also demonstrate that the paleosols in the Miocene aeolian deposits are accretionary soils, resulting from the interactions between the summer and winter monsoon. In summer, monsoonal rainfall associated with high temperatures favors pedogenesis, but eolian dust continues to be added to the soil surface in winter and early spring, although at lower intensities (Guo et al 2008). These soils significantly differ from the paleosols in loess of non-monsoon regions where soil largely represents a sedimentary hiatus (Cremaschi et al., 1990; Fedoroff and Goldberg, 1982). Consequently, the accretionary properties of paleosols in the early Miocene loess can be regarded as strong evidence of a seasonally alternating circulations, and hence a monsoonal climate.

The aeolian deposits in China and paleo-environmental mappings thus provide consistent evidence with regards to the establishment of the Asian monsoon climate. These depict a new understanding of Cenozoic climate changes in Asia that contrast with the 8 Ma view. A number of other geological records corroborate aspects of this new understanding near the Oligocene-Miocene boundary. For example, a slight decrease in the content of xerophytes at ~23 Ma in a core from the Qaidam basin (J. Wang et al., 1999) is believed to be due to the influence of the summer monsoon. The earliest high $\delta^{13}C$ peaks appeared ~20 Ma ago in a carbon isotope record of terrestrial black carbon have also been interpreted as an indication of early monsoon initiation (Jia et al., 2003). A prominent change in the mammalian and floristic regions in China have also been found to have occurred in the early Miocene (Jia et al., 2003; Qiu and Li, 2005; Song et al., 1983) and sudden increases in aeolian dust accumulation rates have been inferred at ~25 Ma (Rea, 1994). A comprehensive geochemical analysis also shows a major increase in the delivery of Asian dust material since ~20 Ma in central Pacific (Ziegler et al., 2007), which has been interpreted as indicating the development of East Asian monsoon and formation of Asian loess. More recently, a

CPD
10, 2163–2291, 2014

study of Arabian Sea proxies showed no significant changes in wind-driving upwelling at 8 Ma, and thus does not support the initiation of an enhanced summer monsoon in the late Miocene (Huang et al., 2007). Weathering records in marine sediments also traced the existence of the Asian monsoon back to the early Miocene followed by a gradual weakening since ∼ 10 Ma (Clift et al., 2010).

7.3.2 Comparison of the regional monsoonal systems

Eolian deposits in China are useful proxies for the East Asian monsoon. An open question exists as to whether the establishments of the East Asian monsoon and South Asian (Indian) monsoons were synchronous. The changes in the climate pattern of China in the Oligocene and Miocene (Fig. 22) provide significant new insights with regards to this issue. They showed that the initially arid southwest and southeast China regions in the Paleogene were both transformed into much more humid climates in the early Miocene, a shift which supports a notion of synchronous onset/strengthening of the two Asian summer monsoon systems.

The Neogene monsoonal climate pattern in Asia differs radically from the other monsoon regions. The geographical reach of the other regional monsoon systems, except the Australian one, tends to be restricted by the southern and northern fronts of ITCZ, as is particularly true for the African monsoon. In contrast, the front of the East Asian monsoon can penetrate deep into Asia, and in summer extend to regions where northern hemispheric westerlies prevail in a mid-latitude zone well beyond the ITCZ (Fig. 22). This suggests that the East Asian summer monsoon circulation is able to break through the subtropical high-pressure belt, which usually acts as a barrier to moisture. This feature helps to explain the desert distribution pattern (Fig. 11) whereas in other continents deserts are located at the sub-tropical latitudes, while in the Asian interior they exist at much higher latitudes. The South American monsoon and Australian monsoons exhibit similar features, but with a lesser extent.

However, the Paleogene climate pattern in Asia is quite similar to today's African climates. The zonally oriented aridity belt is similar to that in the modern Sahara desert

CPD
10, 2163–2291, 2014

while the regions south of the Sahara are mainly under the influence of the African monsoon. The low latitude modern African monsoon is similar to southern-most China in the Paleogene where a tropical monsoon was present but did not extend far into the continent. In the region north of the aridity belt, a Mediterranean-like climate likely exists (Guo, 2010; Zhang et al., 2012), as is currently is the case for the North African continent.

To date, little is known about the origin of the African monsoon mainly because of a lack of relevant long-term geological records. The longest records in the African monsoon region have been derived from eolian dust and sapropel deposits in the ocean cores, but the monsoon climate likely predates the earliest of these records. The oldest monsoon-induced dust was dated to 11 Ma (De Menocal, 1995), and Mediterranean sapropel extends back only to the middle Miocene when the Mediterranean took on much of its present configuration (Kidd et al., 1978; Cramp and O'Sallivan, 1999). Although the oldest sapropel reported so far has dated to 13.8 Ma (Mourik et al., 2010), deposits showing humidity variations with a clear precessional periodicity have been traced back to 15Ma and beyond (Hüsing et al., 2010).

Climate models suggest that that the African monsoon and its associated dry regions may have existed in the Oligocene (Fluteau et al., 1999). However, the age of the Sahara has been traced back only to the late Miocene at ~7 Ma (Schuster et al., 2006). Confirmation of the model simulations is therefore hamped by the brevity of the geological record.

Similar model-data differences also exist for the Australian region. Climate model suggested that a weaker-than-present Australian monsoon was present during the Miocene (Herold et al., 2011a). However, the modern day aridity of Australia has been traced back only as far as the Pliocene (Fujioka and Chappell, 2010), before which time geological records are lacking. It should be mentioned that relatively arid conditions do not necessarily lead to the formation of deserts, which occur when some aridity threshold is exceeded, which itself can be modulated by other factors. For example, increases in the northern high-latitude ice sheets during the mid-Pliocene may have led

CPD
10, 2163–2291, 2014

to enhanced aridity in the Asian interior and been instrumental in the desertification of the region, independent of the monsoon that existed on the continent's southern fringe (Guo et al., 2004).

In summary, our understanding of origin of the Asian monsoon system has benefited greatly from a wealth of bio-geochemical evidence sampling both the spatial (P. Wang, 1990; Liu and Guo, 1997; Sun and Wang, 2005; Guo et al., 2008) and temporal (Guo et al., 2002, 2008) structure of the region's climate. Climate models (e.g., Herold et al., 2011) have also added important insight. In contrast, the proxy record and associated modeling analysis of the origin of other present-day monsoon systems remains scarce. Progress will require additional collaborative efforts aimed at documenting and simulating the historical evolution of these regional monsoon climates. However, our discussions in this section reinforce several lines of insights about the Cenozoic long-term changes of GM.

1. The geographical reach of the various regional monsoons are quite different, ranging between the extremes of far-reaching the East Asian monsoon and the relatively limited reach of the African monsoon. The first dominates a wide region at the mid-latitudes, well beyond the ITCZ, while the second primarily affects the low-latitudes within the seasonal oscillation ranges of the ITCZ. The other monsoon sub-systems could be approximately regarded as the intermediates of these two end members, though the south Asian monsoon has considerably zonal influence across the tropics. These distinctions are also clear for the orbital-scale aspects of the regional monsoons, as also discussed in Sect. 6.

2. The above features imply contrasting links between the monsoons and the broader atmospheric circulation, and proxy data support the possibility of differing times of initiation for the different regional monsoons. These contrasts are integral considerations in addressing the GM history and related forcing mechanisms. It was hypothesized that the African monsoon and aridity might be traced back to

CPD
10, 2163–2291, 2014

very earlier history of the Earth, depending on the timing when the African continent drifted to subtropical latitudes (Guo et al., 2008).

8 Global Monsoon in a warming world

8.1 The importance and complexity of monsoon projection

Foremost amongst the impacts of a changing climate are changes in rainfall, drought, and associated climate extremes in highly populated and agriculturally productive regions. Anticipated trends in the monsoon domains are complex, varying as a function of season and region (Lee and Wang, 2014), and in instances, varying in a potentially nonlinear fashion with respect to global mean temperature (e.g. Cook et al., 2010). The challenge in projecting future impacts also relates in part to the compensating nature of future changes, particularly over land, and thus the net future change is often the residual of larger competing influences including increases in both evaporation and precipitation.

The GM concept is likely to be useful in this context, given the consistency of monsoon responses to past external forcing (Y. Wang et al., 2005), and the relevance of fundamental constraints across monsoon domains, such as land-ocean portioning of moisture (Christensen et al., 2007; Fasullo, 2012; B. Wang et al., 2012), and interhemispheric contrasts (Lee and Wang, 2014).

Considerable insight into future monsoon shifts in a warming world can also be gained from consideration of past climate. A particularly useful analogue for the future monsoon is the Paleocene-Eocene Thermal Maximum event about 56 Ma ago, when 1500–4500 gigatons of carbon was released within < 20 ka, resulting in rapid global warming of 5–8 °C (Bowen et al., 2006; McInerney and Wing, 2011). This global warming was accompanied by drastic changes in hydrological cycling, with enhanced monsoon rain and increased seasonality in precipitation (Foreman et al., 2012). Although our understanding of the mechanisms behind these changes is insufficient to defini-

CPD
10, 2163–2291, 2014

tively project future changes, similar past greenhouse events may provide a glimpse of the future (Zachos et al., 2008).

8.2 Projected changes in the global monsoon using GCMs

A complementary approach for projecting future monsoon changes is with coupled ocean-atmosphere models and newly available Earth System Models (ESMs), which also include interactive chemistry, an active carbon cycle, and biogeochemistry. In recent years, the array of global models produced by individual modeling centers has been aggregated into multi-model archives (e.g. Meehl et al., 2007a; Taylor et al., 2012) in order to facilitate their inter-comparison and combined consideration of historical simulations and future projections.

One approach for evaluating future monsoon simulations is to select only those projections from models that best depict monsoons in the current climate. From the 20 coupled models that participated in the phase five of Coupled Model Intercomparison Project (CMIP5), the historical run for 1850–2005 and the Representative Concentration Pathway (RCP) 4.5 run for 2006–2100 have been used to assess current fidelity and future conditions (Lee and Wang, 2014). Metrics for evaluating model simulations were designed to document model performance for 1980–2005 and, based on these metrics, the four best models' multi-model ensemble (B4MME) was selected for its evaluation of future conditions, projecting the following changes in the twenty-first century. (1) Changes in monsoon precipitation exhibit huge differences between the NH and SH. The NH monsoon precipitation is expected to increase significantly due to a contrast in warming between the NH and SH, significant enhancement of the Hadley circulation during boreal summer, and atmospheric moistening, which together overcome an increase in tropospheric stability arising from greenhouse gases. There is a slight weakening of the Walker circulation in the B4MME but it is not statistically significant, given the inter-model spread. (2) The annual range of GM precipitation and the percentage of local summer rainfall will increase over most of the GM region, both over land and over ocean. (3) There will be a prominent east-west asymmetry in future changes with moistening of the eastern hemisphere monsoons and drying of the western hemisphere monsoon. (4) The NH monsoon onset will be advanced and its withdrawal will be delayed. (5) The land monsoon domain over Asia is projected to expand westward. There are important differences between an assessment of an earlier generation of models and these CMIP5 results. While some differences likely relate to contrasts in the forcings used in future conditions for each experiment, other differences are likely to be related to advances in model physics and particularly in the inclusion of cloud-aerosol interactions in CMIP5.

8.3 Heat waves, droughts, and floods in the global monsoon environment

Chief amongst the robustly simulated changes arising from anthropogenic forcing is a warming and moistening of the troposphere on a planetary scale (e.g. Meehl et al., 2007b). Warming of the globe brings with it a highly probable warming of the tropics. There is therefore a strong expectation that the frequency of heat waves will increase in the GM region (Kumar et al., 2011). Other effects, such as an increase in aridity over land in the pre-monsoon environment (Seth et al., 2011; Fasullo, 2012; Dirmeyer et al., 2013), are likely to delay monsoon onset in some regions, thereby exacerbating the warming of the base state and intensifying heat waves, which tend to occur prior to monsoon onset.

Increases in total atmospheric water vapor are tied strongly to warming and proportionate changes in extreme monsoon rainfall events are both anticipated (e.g. Trenberth, 2011; Kumar et al., 2011) and observed (Goswami et al., 2006b; Chang et al., 2012), though regional structure in such changes is also likely (e.g. Chang et al., 2012). Relevant to coastal flooding and impacts in the monsoon zones, increases in sea level arising from warming oceans and melting of snow and ice sheets are also robustly projected (Vermeer and Rahmstorf, 2009). Potentially augmented by increases in storm intensity (Unnikrishnan et al., 2011; Murakami et al., 2012), sea level rise is therefore very likely to lead to considerable societal and environmental impacts, particularly

CPD
10, 2163–2291, 2014

given the exceptional population densities and susceptibilities in coastal monsoon environments.

Changes in the tropical circulation arising from warming are also likely. From an energetic standpoint, the net radiative imbalance at the surface increases less quickly than atmospheric water vapor, which is governed instead by the Clausius - Clapeyron relationship ($\sim 2\,\%\,K^{-1}$ vs. $7\,\%\,K^{-1}$, respectively). As a result, total evaporation, and by extension rainfall, increases more slowly than does water vapor amount, and the residence time of atmospheric moisture therefore increases (e.g. Held and Soden, 2006; Seager et al., 2010) suggesting a decrease in the intensity of the divergent atmospheric circulation (Tanaka et al., 2005; Vecchi and Soden, 2007). Increases in tropical tropospheric stability act to suppress the divergent circulation and rainfall (Chou et al., 2001; Neelin et al., 2003). Yet downscaling these changes in the global hydrologic cycle to regional monsoon environments is non-trivial and projections show substantial variability across individual monsoon environments, some of which arises from internal variability (Deser et al., 2012). Another key source of variability across models is their contrasting structural representation of key processes. Understanding and constraining projections of future monsoon variability to account for these differences remains an active research topic.

8.4 The global monsoon as a climate feedback

While most studies on monsoon projection have focused on the impact of changes in the global environment on the monsoon, it can equally be asked what role the monsoons have in influencing global climate. One consequence of global warming on precipitation is the “rich-gets-richer” and “poor-gets-poorer” pattern identified in multi-model projections of climate change (Neelin et al., 2006). Over the last 30 years of global warming, a similar pattern has been observed (Fig. 23a). While the precipitation response to global warming is complex (Held and Soden, 2006) and not fully understood, increased atmospheric moisture and a relatively steady circulation are consistent with the observed trend and local summer monsoon precipitation bears a close

CPD
10, 2163–2291, 2014

resemblance to the trend (Fig. 23b). This arises from an increase in summer monsoon rainfall across the majority of the regional monsoon regions, except the South America. In contrast, most arid and semiarid desert or trade wind regimes, located to the west and poleward of each monsoon region, exhibit drying. Understanding the individual contributions of internal variability and forced change to this trend remains an active research topic.

Defined as the equilibrium response in global mean surface temperature to a doubling of carbon dioxide concentrations, climate sensitivity is a canonical measure of a changing climate. A persistent and important uncertainty surrounding the climate response to greenhouse gases is our inability to constrain climate sensitivity beyond the range of approximately 1.5 to 4.5 K. Large contributions to this uncertainty arise from inconsistencies in the modeling of the shortwave cloud feedback across models, particularly in the subtropics. Fasullo and Trenberth (2012) explore observational constraints on models and find the intensity of seasonal variations in subtropical subsidence and the related relative humidity (RH) of the free troposphere in models relate strongly to their simulated climate sensitivity. These so-called “dry zones”, whose origin and maintenance is explicitly linked to the global monsoon, have been proposed to be of fundamental importance in determining the shortwave cloud feedback under climate change, as they expand in a warming environment and erode the cloud field. Despite this importance, most models are systematically biased in representing them, with dry zones that are too moist arising from an overturning circulation that is too weak. The suggestion therefore is that improving the representation of the global monsoon and the effects of its overturning circulation is essential to narrowing the uncertainty of the global effects of forced climate change.

9 Concluding remarks

In this paper, recent progress in modern and paleo-monsoon studies is reviewed in an attempt to answer the question as to whether the regional monsoons constitute a global

CPD
10, 2163–2291, 2014

system. We pool together available observational data to explore where there is coherent variability of regional monsoons at various time scales. The following conclusions can be drawn:

1. There is a certain coherence in monsoon variability across regions. Although independent variability exists, the regional monsoons exhibit mutual coherence across various timescales, ranging from interannual, interdecadal, centennial and millennial, up to orbital and tectonic timescales. The available data, both from the modern observations and geological archives, support the utility of the GM concept.

2. Within the GM system, each subsystem has its own features depending on its geographic and topographic conditions, and recognition of the GM system does not negate the value of regional monsoon studies. On the contrary, the GM concept helps to enhance our understanding and to improve future projection of the regional monsoons, while discriminating between the global and regional components of their variability.

3. Two groups of proxies are used for assessing monsoon variations beyond instrumental records: proxies based on wind and on rain. In view of the better preservation of the precipitation signal in geological records, and the increasing role of hydrological cycle in modern climatology, the rain-based proxies offer a more promising opportunity for diagnosing monsoon variability across many timescales.

4. Historically, paleoclimatology originated from the Quaternary ice ages, and up to now, paleoclimatology in general remains ice-sheet centered, in contrast with modern climatology, which focuses mainly on low-latitude processes. Growing evidence shows that the GM exists at least throughout the 600-Ma Phanerozoic Eon. A systematical study of the GM history will shed light on the role of low-latitude processes in the climate evolution and variability.

5. With a rapidly growing number of publications dealing with paleo-monsoon, caution is required to avoid the misuse of monsoon proxies. Given the remarkable

CPD
10, 2163–2291, 2014

Title Page
Abstract | Introduction
Conclusions | References
Tables | Figures
◀| |▶
◀ ▶
Back | Close
Full Screen / Esc
Printer-friendly Version
Interactive Discussion

contrasts that exist in terms of the "best use" of monsoon proxies and the lack of mature proxies for the GM, it is crucial to strengthen exchanges and collaborations between the modern- and paleo-communities to better develop and calibrate monsoon proxies on the basis of modern observations.

In conclusion, the GM is a complex system of interacting processes that governs climate variability across multiple timescales. The goal of this paper is restricted to demonstrate the applicability of the GM concept for understanding variability across timescales. It does not attempt to disentangle complex physical interactions within the climate system. An in-depth discussion on driving mechanisms and outstanding issues in the GM studies will therefore be the subject of a follow-on companion paper "The Global Monsoon across Time Scales: Mechanisms and Outstanding Issues".

Acknowledgements. This work was supported by the PAGES project and written on the basis of two PAGES symposia on global changes. We thank all participants of the symposia whose contributions form the basis of the present paper. Jun Tian and Xiaolin Ma are acknowledged for their assistance. P. X. Wang is thankful to the support *by the NNSFC Grant* 91128000. B. Wang acknowledges support from the National Research Foundation (NRF) of Korea through a Global Research Laboratory (GRL) grant of the MEST, #2011-0021927.

References

Adams, J. and Faure, H.: Global land environments since the last interglacial, Oak Ridge National Laboratory, TN, USA, 1997.

Adkins, J., Demenocal, P., and Eshel, G.: The "African humid period" and the record of marine upwelling from excess 230Th in Ocean Drilling Program Hole 658C, Paleoceanography, 21, PA4203, doi:10.1029/2005PA001200, 2006.

Agnihotri, R., Dutta, K., Bhushan, R., and Somayajulu, B. L. K.: Evidence for solar forcing on the Indian monsoon during the last millennium, Earth Planet. Sci. Lett., 198, 521–527, 2002.

Alisov, B. P.: Die Klimat der Erde, Deutscher Verlag, Berlin, 1954.

Alley, R., Meese, D., Shuman, C., Gow, A., Taylor, K., Grootes, P., White, J., Ram, M., Waddington, E., and Mayewski, P.: Abrupt increase in Greenland snow accumulation at the end of the Younger Dryas event, Nature LONDON, 362, 527–527, 1993.

An, Z., Kutzbach, J. E., Prell, W. L., and Porter, S. C.: Evolution of Asian monsoons and phased uplift of the Himalaya–Tibetan plateau since Late Miocene times, Nature, 411, 62–66, 2001.

An, Z., Clemens, S. C., Shen, J., Qiang, X., Jin, Z., Sun, Y., Prell, W. L., Luo, J., Wang, S., and Xu, H.: Glacial-interglacial Indian summer monsoon dynamics, Science, 333, 719–723, 2011.

Armstrong, H. A., Baldini, J., Challands, T. J., Gröcke, D. R., and Owen, A. W.: Response of the Inter-tropical Convergence Zone to Southern Hemisphere cooling during Upper Ordovician glaciation, Palaeogeography, Palaeoclimatology, Palaeoecology, 284, 227–236, 2009.

Asmerom, Y., Polyak, V. J., and Burns, S. J.: Variable winter moisture in the southwestern United States linked to rapid glacial climate shifts, Nat. Geosci., 3, 114–117, 2010.

Ayliffe, L., Gagan, M., Zhao, J.-x., Drysdale,R., Hellstrom, J., Hantoro, W., Griffiths,M.L., Scott-Gagan, H., St Pierre, E., Cowley, J. A., and Suwargadi, B.: Rapid interhemispheric climate links via the Australasian monsoon during the last deglaciation, Nat. Commun., 4, 2908, doi:10.1038/ncomms3908, 2013.

Bar-Matthews, M., Ayalon, A., Gilmour, M., Matthews, A., and Hawkesworth, C. J.: Sea–land oxygen isotopic relationships from planktonic foraminifera and speleothems in the Eastern Mediterranean region and their implication for paleorainfall during interglacial intervals, Geochim. Cosmochim. Acta, 67, 3181–3199, 2003.

Bard, E., Ménot, G., Rostek, F., Licari, L., Böning, P., Edwards, R.L., Cheng, H., Wang, Y. J., and Heaton, T. J.: Radiocarbon calibration/comparison records based on marine sediments from the Pakistan and Iberian Margins, Radicarbon, 55, 1–21, 2013.

Bassinot, F. C., Beaufort, L., Vincent, E., Labeyrie, L. D., Rostek, F., Müller, P. J., Quidelleur, X., and Lancelot, Y.: Coarse fraction fluctuations in pelagic carbonate sediments from the tropical Indian Ocean: A 1500 kyr record of carbonate dissolution, Paleoceanography, 9, 579–600, 1994.

Beaufort, L., Lancelot, Y., Camberlin, P., Cayre, O., Vincent, E., Bassinot, F., and Labeyrie, L.: Insolation cycles as a major control of equatorial Indian Ocean primary productivity, Science, 278, 1451–1454, 1997.

CPD
10, 2163–2291, 2014

The Global Monsoon across Time Scales

P. X. Wang et al.

Beaufort, L., van der Kaars, S., Bassinot, F. C., and Moron, V.: Past dynamics of the Australian monsoon: precession, phase and links to the global monsoon concept, Clim. Past, 6, 695–706, doi:10.5194/cp-6-695-2010, 2010.

Becker, A., Finger, P., Meyer-Christoffer, A., Rudolf, B., Schamm, K., Schneider, U., and Ziese, M.: A description of the global land-surface precipitation data products of the Global Precipitation Climatology Centre with sample applications including centennial (trend) analysis from 1901-present, Earth Syst. Sci. Data, 5, 71–99, doi:10.5194/essd-5-71-2013, 2013.

Bender, M., Sowers, T., and Labeyrie, L.: The Dole effect and its variations during the last 130,000 years as measured in the Vostok ice core, Global Biogeochem. Cy., 8, 363–376, 1994.

Benson, L., Kashgarian, M., Rye, R., Lund, S., Paillet, F., Smoot, J., Kester, C., Mensing, S., Meko, D., and Lindström, S.: Holocene multidecadal and multicentennial droughts affecting Northern California and Nevada, Quaternary Sci. Rev., 21, 659–682, 2002.

Berger, A.: Long-term variations of caloric insolation resulting from the Earth's orbital elements, Quaternary Res., 9, 139–167, 1978.

Berger, A. and Loutre, M.-F.: Insolation values for the climate of the last 10 million years, Quaternary Sci. Rev., 10, 297–317, 1991.

Berger, A. and Loutre, M.-F.: Intertropical latitudes and precessional and half-precessional cycles, Science, 278, 1476–1478, 1997.

Berger, A., Loutre, M. F., and Laskar, J.: Stability of the astronomical frequencies over the Earth's history for paleoclimate studies, Science, 255, 560–566, 1992.

Berger, A., Loutre, M. F., and Mélice, J. L.: Equatorial insolation: from precession harmonics to eccentricity frequencies, Clim. Past, 2, 131–136, doi:10.5194/cp-2-131-2006, 2006.

Berkelhammer, M., Sinha, A., Stott, L., Cheng, H., Pausata, F., and Yoshimura, K.: An abrupt shift in the Indian Monsoon 4000 years ago, Geophys. Monograph Ser., 198, 75–87, doi:10.1029/2012GM001207, 2012.

Bianchi, G. G. and McCave, I. N.: Holocene periodicity in North Atlantic climate and deep-ocean flow south of Iceland, Nature, 397, 515–517, 1999.

Billups, K., Channell, K. J. E. T., and Zachos, J.: Late Oligocene to early Miocene geochronology and paleoceanography from the subantarctic South Atlantic, Paleoceanography, 17, 1004, doi:10.1029/2000PA000568, 2002.

CPD
10, 2163–2291, 2014

Bird, B. W., Abbott, M. B., Vuille, M., Rodbell, D. T., Stansell, N. D., and Rosenmeier, M. F.: A 2,300-year-long annually resolved record of the South Ameri- can summer monsoon from the Peruvian Andes, Proc. Natl. Acad. Sci., 108, 8583–8588, 2011.
Bjerklie, D. M., Lawrence Dingman, S., Vorosmarty, C. J., Bolster, C. H., and Congalton, R. G.: Evaluating the potential for measuring river discharge from space, J. Hydrol., 278, 17–38, 2003.
Blunier, T. and Brook, E. J.: Timing of millennial-scale climate change in Antarctica and Greenland during the last glacial period, Science, 291, 109–112, 2001.
Bluthgen, J.: Allgemeine Klimageographie. Second edition, de Gruyter, Berlin, 1966.
Boening, C., Willis, J. K., Landerer, F. W., Nerem, S., and Fasullo, J.: The 2011 La Niña: So strong, the oceans fell, Geophys. Res. Lett., 39, L19602, doi:10.1029/2012GL053055, 2011.
Bond, G., Broecker, W., Johnsen, S., McManus, J., Labeyrie, L., Jouzel, J., and Bonani, G.: Correlations between climate records from North Atlantic sediments and Greenland ice, Nature, 365, 143–147, 1993.
Bond, G., Showers, W., Cheseby, M., Lotti, R., Almasi, P., Priore, P., Cullen, H., Hajdas, I., and Bonani, G.: A pervasive millennial-scale cycle in North Atlantic Holocene and glacial climates, Science, 278, 1257–1266, 1997.
Bond, G. C. and Lotti, R.: Iceberg discharges into the North Atlantic on millennial time scales during the last glaciation, Science, 267, 1005–1010, 1995.
Bond, G., Kromer, B., Beer, J., Muscheler, R., Evans, M.N., Showers, W., Hoffmann, S., Lotti-Bond, R., Hajdas, I., and Bonani, G.: Persistent solar influence on North Atlantic climate during the Holocene, Science, 294, 2130–2136, 2001.
Bowen, G. J., Bralower, T. J., Delaney, M. L., Dickens, G. R., Kelly, D. C., Koch, P. L., Kump, L. R., Meng, J., Sloan, L. C., and Thomas, E.: Eocene hyperthermal event offers insight into greenhouse warming, Eos, Trans. Am. Geophys. Union, 87, 165–169, 2006.
Bowler, J. M., Wyrwoll, K.-H., and Lu, Y.: Variations of the northwest Australian summer monsoon over the last 300,000 years: the paleohydrological record of the Gregory (Mulan) Lakes System, Quaternary Int., 83, 63–80, 2001.
Broecker, W. S., Peteet, D. M., and Rind, D.: Does the ocean-atmosphere system have more than one stable mode of operation?, Nature, 315, 21–26, 1985.
Broecker, W. S. and Denton, G. H.: The role of ocean-atmosphere reorganizations in glacial cycles, Geochim. Cosmochim. Acta, 53, 2465–2501, 1989.

CPD
10, 2163–2291, 2014
The Global Monsoon across Time Scales
P. X. Wang et al.

Broecker, W. S.: Paleocean circulation during the last deglaciation: a bipolar seesaw?, Paleoceanography, 13, 119–121, 1998.
Broecker, W. S.: Does the trigger for abrupt climate change reside in the ocean or in the atmosphere?, Science, 300, 1519–1522, 2003.
Brovkin, V. and Claussen, M.: Comment on “Climate-Driven Ecosystem Succession in the Sahara: The Past 6000 Years”, Science, 322, 1326–1326, 2008.
Burns, S. J., Fleitmann, D., Matter, A., Kramers, J., and Al-Subbary, A. A.: Indian Ocean climate and an absolute chronology over Dansgaard/Oeschger events 9 to 13, Science, 301, 1365–1367, 2003.
Bush, A. B.: Numerical simulation of the Cretaceous Tethys circumglobal current, Science, 275, 807–810, 1997.
Cai, Y., Cheng, H., An, Z., Edwards, R. L., Wang, X., Tan, L., and Wang, J.: Large variations of oxygen isotopes in precipitation over south-central Tibet during Marine Isotope Stage 5, Geology, 38, 243–246, 2010a.
Cai, Y., Tan, L., Cheng, H., An, Z., Edwards, R. L., Kelly, M. J., Kong, X., and Wang, X.: The variation of summer monsoon precipitation in central China since the last deglaciation, Earth Planet. Sci. Lett., 291, 21–31, 2010b.
Cai, Y., Zhang, H., Cheng, H., An, Z., Lawrence Edwards, R., Wang, X., Tan, L., Liang, F., Wang, J., and Kelly, M.: The Holocene Indian monsoon variability over the southern Tibetan Plateau and its teleconnections, Earth Planet. Sci. Lett., 335, 135–144, 2012.
Caley, T., Malaizé, B., Zaragosi, S., Rossignol, L., Bourget, J., Eynaud, F., Martinez, P., Giraudeau, J., Charlier, K., and Ellouz-Zimmermann, N.: New Arabian Sea records help decipher orbital timing of Indo-Asian monsoon, Earth Planet. Sci. Lett., 308, 433–444, 2011.
Chang, C. P., Lei, Y., Sui, C. H., Lin, X., and Ren, F.: Tropical cyclone and extreme rainfall trends in East Asian summer monsoon since mid 20th century, Geophys. Res. Lett., 39, L18702, doi:10.1029/2012GL052945, 2012.
Chao, W. C. and Chen, B.: The origin of monsoons, J. Atmos. Sci., 58, 3497–3507, 2001.
Chappellaz, J., Barnola, J., Raynaud, D., Korotkevich, Y. S., and Lorius, C.: Ice-core record of atmospheric methane over the past 160,000 years, Nature, 345, 127–131, 1990.
Cheng, H., Edwards, R. L., Wang, Y., Kong, X., Ming, Y., Kelly, M. J., Wang, X., Gallup, C. D., and Liu, W.: A penultimate glacial monsoon record from Hulu Cave and two-phase glacial terminations, Geology, 34, 217–220, 2006.

CPD
10, 2163–2291, 2014
The Global Monsoon across Time Scales
P. X. Wang et al.

Cheng, H., Edwards, R. L., Broecker, W. S., Denton, G. H., Kong, X., Wang, Y., Zhang, R., and Wang, X.: Ice age terminations, Science, 326, 248–252, 2009a.

Cheng, H., Fleitmann, D., Edwards, R. L., Wang, X., Cruz, F. W., Auler, A. S., Mangini, A., Wang, Y., Kong, X., and Burns, S. J.: Timing and structure of the 8.2 kyr BP event inferred from δ^{18}O records of stalagmites from China, Oman, and Brazil, Geology, 37, 1007–1010, 2009b.

Cheng, H., Sinha, A., Wang, X., Cruz, F. W., and Edwards, R. L.: The Global Paleomonsoon as seen through speleothem records from Asia and the Americas, Clim. Dynam., 39, 1045–1062, 2012a.

Cheng, H., Zhang, P., Spötl, C., Edwards, R., Cai, Y., Zhang, D., Sang, W., Tan, M., and An, Z.: The climatic cyclicity in semiarid arid central Asia over the past 500,000 years, Geophys. Res. Lett., 39, L01705, doi:10.1029/2011GL050202, 2012b.

Cheng, H., Sinha, A., Cruz, F. W., Wang, X., Edwards, R. L., d'Horta, F. M., Ribas, C. C., Vuille, M., Stott, L. D., and Auler, A. S.: Climate change patterns in Amazonia and biodiversity, Nat. Commun., 4, 1411, doi:10.1038/ncomms2415, 2013.

Cheng, H. and Edwards, R.L.: Asian Monsoon Footprints in Chinese Cultural History, in: Des climats et des hommes, Découverte, 291–306, 2012.

Chou, C., Neelin, J., and Su, H.: Ocean atmosphere land feedbacks in an idealized monsoon, Q. J. Roy. Meteorol. Soc., 127, 1869–1891, 2001.

Christensen, J. H., Hewitson, B., Busuioc, A., Chen, A., Gao, X., Held, R., Jones, R., Kolli, R. K., Kwon, W., and Laprise, R.: Regional climate projections, Climate Change, 2007: The Physical Science Basis. Contribution of Working group I to the Fourth Assessment Report of the Intergovernmental Panel on Climate Change, University Press, Cambridge, Chapter 11, 847–940, 2007.

Claussen, M., Kubatzki, C., Brovkin, V., Ganopolski, A., Hoelzmann, P., and Pachur, H. J.: Simulation of an abrupt change in Saharan vegetation in the Mid Holocene, Geophys. Res. Lett., 26, 2037–2040, 1999.

Clemens, S.: Extending the historical record by proxy, in: The Asian Monsoon, edited by: Wang, B., Springer, 615–630, 2006

Clemens, S., Prell, W., Murray, D., Shimmield, G., and Weedon, G.: Forcing mechanisms of the Indian Ocean monsoon, Nature, 353, 720–725, 1991.

Clemens, S. C., Murray, D. W., and Prell, W. L.: Nonstationary phase of the Plio-Pleistocene Asian monsoon, Science, 274, 943–948, 1996.

CPD
10, 2163–2291, 2014

Clemens, S. C. and Prell, W. L.: A 350,000 year summer-monsoon multi-proxy stack from the Owen Ridge, Northern Arabian Sea, Mar. Geol., 201, 35–51, 2003.
Clemens, S. C. and Prell, W. L.: The timing of orbital-scale Indian monsoon changes, Quaternary Sci. Rev., 26, 275–278, 2007.
Clemens, S. C., Prell, W. L., and Sun, Y.: Orbital scale timing and mechanisms driving Late Pleistocene Indo Asian summer monsoons: Reinterpreting cave speleothem δ^{18}O, Paleoceanography, 25, PA4207, doi:10.1029/2010PA001926, 2010.
Clift, P. D., Tada, R., and Zheng, H. (Eds.): *Monsoon evolution and tectonic-climate linkage in Asia*: Introduction, Geological Society of London, Special Publication, 342, 185–218, 2010.
Clift, P. D., Wan, S., and Blusztajn, J.: Reconstructing Chemical Weathering, Physical Erosion and Monsoon Intensity since 25 Ma in the northern South China Sea: A review of competing proxies, Earth-Sci. Rev., 130, 86–102, 2014.
Cobb, K. M., Charles, C. D., Cheng, H., and Edwards, R. L.: El Niño/Southern Oscillation and tropical Pacific climate during the last millennium, Nature, 424, 271–276, 2003.
Compo, G. P., Whitaker, J. S., Sardeshmukh, P. D., Matsui, N., Allan, R., Yin, X., Gleason, B., Vose, R., Rutledge, G., and Bessemoulin, P.: The twentieth century reanalysis project, Q. J. Roy. Meteorol. Soc., 137, 1–28, 2011.
Cook, E. R., Anchukaitis, K. J., Buckley, B. M., D'Arrigo, R. D., Jacoby, G. C., and Wright, W. E.: Asian monsoon failure and megadrought during the last millennium, Science, 328, 486–489, 2010.
Cramer, B. S., Wright, J. D., Kent, D. V., and Aubry, M. P.: Orbital climate forcing of δ13C excursions in the late Paleocene–early Eocene (chrons C24n–C25n), Paleoceanography, 18, 1097, doi:10.1029/2003PA000909, 2003.
Cramp, A. and O'Sullivan, G.: Neogene sapropels in the Mediterranean: a review, Mar. Geol., 153, 11–28, 1999.
Cremaschi, M., Fedoroff, N., Guerreschi, A., Huxtable, J., Colombi, N., Castelletti, L., and Maspero, A.: Sedimentary and pedological processes in the Upper Pleistocene loess of northern Italy. The Bagaggera sequence, Quaternary Int., 5, 23–38, 1990.
Cruz, F. W., Burns, S. J., Karmann, I., Sharp, W. D., Vuille, M., Cardoso, A. O., Ferrari, J. A., Dias, P. L. S., and Viana, O.: Insolation-driven changes in atmospheric circulation over the past 116,000 years in subtropical Brazil, Nature, 434, 63–66, 2005.

Cruz Jr., F. W., Burns, S. J., Jercinovic, M., Karmann, I., Sharp, W. D., and Vuille, M.: Evidence of rainfall variations in Southern Brazil from trace element ratios (Mg/Ca and Sr/Ca) in a Late Pleistocene stalagmite, Geochim. Cosmochim., 71, 2250–2263, 2007.

Dansgaard, W., Johnsen, S., Clausen, H., Dahl-Jensen, D., Gundestrup, N., Hammer, C., Hvidberg, C., Steffensen, J., Sveinbjörnsdottir, A., and Jouzel, J.: Evidence for general instability of past climate from a 250-kyr ice-core record, Nature, 364, 218–220, 1993.

De Vleeschouwer, D., Da Silva, A. C., Boulvain, F., Crucifix, M., and Claeys, P.: Precessional and half-precessional climate forcing of Mid-Devonian monsoon-like dynamics, Clim. Past, 8, 337–351, doi:10.5194/cp-8-337-2012, 2012.

Dee, D., Uppala, S., Simmons, A., Berrisford, P., Poli, P., Kobayashi, S., Andrae, U., Balmaseda, M., Balsamo, G., and Bauer, P.: The ERA Interim reanalysis: Configuration and performance of the data assimilation system, Q. J. Roy. Meteorol. Soc., 137, 553–597, doi:10.1002/qj.828, 2011.

deMenocal, P. B. and Rind, D.: Sensitivity of Asian and African climate to variations in seasonal insolation, glacial ice cover, sea surface temperature, and Asian orography, J. Geophys. Res.-Atmos. (1984–2012), 98, 7265–7287, 1993.

deMenocal, P. B.: Plio-pleistocene African climate, Science, 270, 53–59, 1995.

deMenocal, P., Ortiz, J., Guilderson, T., and Sarnthein, M.: Coherent High- and Low-Latitude Climate Variability During the Holocene Warm Period, Science, 288, 2198–2202, 2000.

Denton, G. H. and Karlén, W.: Holocene climatic variations – their pattern and possible cause, Quaternary Res., 3, 155–205, doi:10.1016/0033-5894(73)90040-9, 1973.

Deplazes, G., Lückge, A., Peterson, L. C., Timmermann, A., Hamann, Y., Hughen, K. A., Röhl, U., Laj, C., Cane, M. A., and Sigman, D. M.: Links between tropical rainfall and North Atlantic climate during the last glacial period, Nat. Geosci., 6, 213–217, doi:10.1038/NGEO1712, 2013.

Dercourt, J., Ricou, L.-E., and Vrielynck, B.: Atlas Tethys palaeoenvironmental maps, Gauthier-Villars, 1993.

Deser, C., Phillips, A., Bourdette, V., and Teng, H.: Uncertainty in climate change projections: the role of internal variability, Clim. Dynam., 38, 527–546, 2012.

Ding, Z., Sun, J., Liu, T., Zhu, R., Yang, S., and Guo, B.: Wind-blown origin of the Pliocene red clay formation in the central Loess Plateau, China, Earth Planet. Sci. Lett., 161, 135–143, 1998.

CPD
10, 2163–2291, 2014

Ding, Z., Derbyshire, E., Yang, S., Sun, J., and Liu, T.: Stepwise expansion of desert environment across northern China in the past 3.5 Ma and implications for monsoon evolution, Earth Planet. Sci. Lett., 237, 45–55, 2005.
Dirmeyer, P. A., Jin, Y., Singh, B., and Yan, X.: Trends in Land-Atmosphere Interactions from CMIP5 Simulations, J. Hydrometeorol., 14, 829–849, doi:10.1175/JHM-D-12-0107.1, 2013.
Dykoski, C. A., Edwards, R. L., Cheng, H., Yuan, D., Cai, Y., Zhang, M., Lin, Y., Qing, J., An, Z., and Revenaugh, J.: A high-resolution, absolute-dated Holocene and deglacial Asian monsoon record from Dongge Cave, China, Earth Planet. Sci. Lett., 233, 71–86, 2005.
Emeis, K.-C. and Shipboard Scientific Party: Paleoceanography and sapropel introduction, in: Proc. ODP, Init. Repts., edited by: Emeis, K.-C., Robertson, A. H. F., Richter, C., et al., 160: College Station, TX (Ocean Drilling Program), 21–28, 1996.
FAO-UNESCO: Soil Map of The World, Volume 1UNESCO, Paris, 1974.
Fasullo, J.: A mechanism for land–ocean contrasts in global monsoon trends in a warming climate, Clim. Dynam., 39, 1137–1147, doi.org/10.1007/s00382-011-1270-3, 2012.
Fasullo, J. T. and Trenberth, K. E.: A less cloudy future: The role of subtropical subsidence in climate sensitivity, Science, 338, 792–794, doi:10.1126/science.1227465, 2012.
Fawcett, P. J., Werne, J. P., Anderson, R. S., Heikoop, J. M., Brown, E. T., Berke, M. A., Smith, S. J., Goff, F., Donohoo-Hurley, L., and Cisneros-Dozal, L. M.: Extended megadroughts in the southwestern United States during Pleistocene interglacials, Nature, 470, 518–521, 2011.
Fedoroff, N. and Goldberg, P.: Comparative micromorphology of two late Pleistocene paleosols (in the Paris Basin), Catena, 9, 227–251, 1982.
Feng, X., Cui, H., and Conkey, L. E.: Reply to the Letter to the Editor by Zhou on "Tree-Ring δD as an Indicator of Asian Monsoon Intensity", Quaternary Res., 58, 212–213, 2002.
Feng, X., Cui, H., Tang, K., and Conkey, L. E.: Tree-ring δD as an indicator of Asian monsoon intensity, Quaternary Res., 51, 262–266, 1999.
Fleitmann, D., Burns, S. J., Mudelsee, M., Neff, U., Kramers, J., Mangini, A., and Matter, A.: Holocene forcing of the Indian monsoon recorded in a stalagmite from southern Oman, Science, 300, 1737–1739, 2003.
Fleitmann, D., Burns, S. J., Mangini, A., Mudelsee, M., Kramers, J., Villa, I., Neff, U., Al-Subbary, A. A., Buettner, A., and Hippler, D.: Holocene ITCZ and Indian monsoon dynamics recorded in stalagmites from Oman and Yemen (Socotra), Quaternary Sci. Rev., 26, 170–188, 2007.

Floegel, S., Hay, W. W., DeConto, R. M., and Balukhovsky, A. N.: Formation of sedimentary bedding couplets in the Western Interior Seaway of North America – implications from climate system modeling, Palaeogeogr. Palaeocli. Palaeoecol., 218, 125–143, 2005.

Fluteau, F., Ramstein, G., and Besse, J.: Simulating the evolution of the Asian and African monsoons during the past 30 Myr using an atmospheric general circulation model, J. Geophys. Res.-Atmos. (1984–2012), 104, 11995–12018, 1999.

Fluteau, F., Besse, J., Broutin, J., and Ramstein, G.: The Late Permian climate. What can be inferred from climate modelling concerning Pangea scenarios and Hercynian range altitude?, Palaeogeogr. Palaeocli. Palaeoecol., 167, 39–71, 2001.

Foreman, B. Z., Heller, P. L., and Clementz, M. T.: Fluvial response to abrupt global warming at the Palaeocene/Eocene boundary, Nature, 491, 92–95, doi:10.1038/nature11513, 2012.

France-Lanord, C. and Derry, L. A.: δ^{13}C of organic carbon in the Bengal Fan: Source evolution and transport of C3 and C4 plant carbon to marine sediments, Geochim. Cosmochim. Acta, 58, 4809–4814, 1994.

Frierson, D. M. W., Hwang, Y.-T., Fučkar, N. S., Seager, R., Kang, S. M., Donohoe, A., Maroon, E. A., Liu, X. J., and Battisti, D. S.: Contribution of ocean overturning circulation to tropical rainfall peak in the Northern Hemisphere, Nat. Geosci., 6, 940–944, 2013.

Fujioka, T. and Chappell, J.: History of Australian aridity: chronology in the evolution of arid landscapes, Geol. Soc., London, Special Publications, 346, 121–139, 2010.

Gadgil, S.: Recent advances in monsoon research with particular reference to the Indian monsoon, Aust. Meteorol. Mag., 36, 193–204, 1988.

Garcin, Y., Williamson, D., Taieb, M., Vincens, A., Mathé, P.-E., and Majule, A.: Centennial to millennial changes in maar-lake deposition during the last 45,000 years in tropical Southern Africa (Lake Masoko, Tanzania), Palaeogeogr. Palaeocli. Palaeoecol., 239, 334–354, 2006.

Garcin, Y., Vincens, A., Williamson, D., Buchet, G., and Guiot, J.: Abrupt resumption of the African Monsoon at the Younger Dryas – Holocene climatic transition, Quaternary Sci. Rev., 26, 690–704, 2007.

Gasse, F., Lédée, V., Massault, M., and Fontes, J.-C.: Water-level fluctuations of Lake Tanganyika in phase with oceanic changes during the last glaciation and deglaciation, Nature, 342, 57–59, 1989.

Gasse, F.: Hydrological changes in the African tropics since the Last Glacial Maximum, Quaternary Sci. Rev., 19, 189–211, 2000.

Gasse, F., Chalié, F., Vincens, A., Williams, M. A., and Williamson, D.: Climatic patterns in equatorial and southern Africa from 30,000 to 10,000 years ago reconstructed from terrestrial and near-shore proxy data, Quaternary Sci. Rev., 27, 2316–2340, 2008.
Ge, Q. S., Zheng, J. Y., Fang, X. Q., Zhang, X. Q., and Zhang, P. W.: Winter half-year temperature reconstruction for the middle and lower reaches of the Yellow River and Yangtze River, China, during the past 2000 years, Holocene, 13, 933–940, 2003.
Gill, A. E.: Some simple solutions for heat induced tropical circulation, Q. J. Roy. Meteorol. Soc., 106, 447–462, 1980.
Giosan, L., Clift, P. D., Macklin, M. G., Fuller, D. Q., Constantinescu, S., Durcan, J. A., Stevens, T., Duller, G. A., Tabrez, A. R., and Gangal, K.: Fluvial landscapes of the Harappan civilization, Proc. Natl. Acad. Sci., 109, E1688–E1694, 2012.
Gordon, W. A.: Distribution by latitude of Phanerozoic evaporite deposits, The J. Geol., 83, 671–684, 1975.
Goswami, B. N., Madhusoodanan, M., Neema, C., and Sengupta, D.: A physical mechanism for North Atlantic SST influence on the Indian summer monsoon, Geophys. Res. Lett., 33, L02706, doi:10.1029/2005GL024803, 2006.
Goswami, B. N., Venugopal, V., Sengupta, D., Madhusoodanan, M., and Xavier, P. K.: Increasing trend of extreme rain events over India in a warming environment, Science, 314, 1442–1445, 2006b.
Griffiths, M., Drysdale, R., Gagan, M., Zhao, J.-x., Ayliffe, L., Hellstrom, J., Hantoro, W., Frisia, S., Feng, Y.-x., and Cartwright, I.: Increasing Australian–Indonesian monsoon rainfall linked to early Holocene sea-level rise, Nat. Geosci., 2, 636–639, 2009.
Grootos, P., Stulvor, I., and Whltoi, J.: Comparison of oxygen isotope records from the GISP2 and GRIP Greenland ice cores, Nature, 366, 552–554, 1993.
Guo, Q Y.: The summer monsoon intensity index in east Asia and its variation, Acta Geogr. Sin., 3, 207–217, 1983 (in Chinese).
Guo, Z., Liu, T., Guiot, J., Wu, N., Lü, H., Han, J., Liu, J., and Gu, Z.: High frequency pulses of East Asian monsoon climate in the last two glaciations: link with the North Atlantic, Clim. Dynam., 12, 701–709, 1996.
Guo, Z., Liu, T., Fedoroff, N., Wei, L., Ding, Z., Wu, N., Lu, H., Jiang, W., and An, Z.: Climate extremes in loess of China coupled with the strength of deep-water formation in the North Atlantic, Global Planet. Change, 18, 113–128, 1998.

CPD
10, 2163–2291, 2014
The Global Monsoon across Time Scales
P. X. Wang et al.

Guo, Z., Biscaye, P., Wei, L., Chen, X., Peng, S., and Liu, T.: Summer monsoon variations over the last 1.2 Ma from the weathering of loess soil sequences in China, Geophys. Res. Lett., 27, 1751–1754, 2000.

Guo, Z., Ruddiman, W. F., Hao, Q., Wu, H., Qiao, Y., Zhu, R. X., Peng, S., Wei, J., Yuan, B., and Liu, T.: Onset of Asian desertification by 22 Myr ago inferred from loess deposits in China, Nature, 416, 159–163, 2002.

Guo, Z., Peng, S., Hao, Q., Biscaye, P. E., An, Z., and Liu, T.: Late Miocene–Pliocene development of Asian aridification as recorded in the Red-Earth Formation in northern China, Global Planet. Change, 41, 135–145, 2004.

Guo, Z. T., Sun, B., Zhang, Z. S., Peng, S. Z., Xiao, G. Q., Ge, J. Y., Hao, Q. Z., Qiao, Y. S., Liang, M. Y., Liu, J. F., Yin, Q. Z., and Wei, J. J.: A major reorganization of Asian climate by the early Miocene, Clim. Past, 4, 153–174, doi:10.5194/cp-4-153-2008, 2008.

Guo, Z., Zhou, X., and Wu, H.: Glacial-interglacial water cycle, global monsoon and atmospheric methane changes, Clim. Dynam., 39, 1073–1092, doi:10.1007/s00382-011-1041-1, 2012.

Guo, Z.: 22-8 Ma eolian deposits and the monsoon history, in: A synthetic study on the environmental evolution in western China, Science Press, Beijing, 1–19, 2010.

Gupta, A. K., Anderson, D. M., and Overpeck, J. T.: Abrupt changes in the Asian southwest monsoon during the Holocene and their links to the North Atlantic Ocean, Nature, 421, 354–357, 2003.

Hadley, G.: Concerning the Cause of the General Trade-Winds: By Geo. Hadley, Esq; FRS, Philos. Trans., 39, 58–62, 1735.

Halley, E.: An Historical Account of the Trade Winds, and Monsoons, Observable in the Seas between and Near the Tropicks, with an Attempt to Assign the Phisical Cause of the Said Winds, By E. Halley, Philos. Trans., 16, 153–168, 1686.

Hann, J.: Handbuch der Klimatologie, Vol. i and iii, Part II, 1908.

Hao, Q. and Guo, Z.: Magnetostratigraphy of a late Miocene Pliocene loess soil sequence in the western Loess Plateau in China, Geophys. Res. Lett., 31, L09209, doi:10.1029/2003GL019392, 2004.

Hao, Q. and Guo, Z.: Magnetostratigraphy of an early middle Miocene loess soil sequence in the western Loess Plateau of China, Geophys. Res. Lett., 34, L18305, doi:10.1029/2007GL031162, 2007.

Harrison, T. M., Copeland, P., Kidd, W., and Yin, A.: Raising tibet, Science, 255, 1663–1670, 1992.
Haug, G. H., Hughen, K. A., Sigman, D. M., Peterson, L. C., and Röhl, U.: Southward migration of the Intertropical Convergence Zone through the Holocene, Science, 293, 1304–1308, 2001.
Heinrich, H.: Origin and consequences of cyclic ice rafting in the northeast Atlantic Ocean during the past 130,000 years, Quaternary Res., 29, 142–152, 1988.
Held, I. M. and Soden, B. J.: Robust responses of the hydrological cycle to global warming, J. Climate, 19, 5686–5699, doi:10.1175/JCLI3990.1, 2006.
Henderson, G. M.: Climate. Caving in to new chronologies, Science, 313, 620–622, 2006.
Hendy, I. L. and Kennett, J. P.: Dansgaard Oeschger Cycles and the California Current System: Planktonic foraminiferal response to rapid climate change in Santa Barbara Basin, Ocean Drilling Program Hole 893A, Paleoceanography, 15, 30–42, 2000.
Herold, N., Huber, M., Greenwood, D., Müller, R., and Seton, M.: Early to middle Miocene monsoon climate in Australia, Geology, 39, 3–6, 2011.
Higgins, R. W., Douglas, A., Hahmann, A., Berbery, E., Gutzler, D., Shuttleworth, J., Stensrud, D., Amador, J., Carbone, R., and Cortez, M.: Progress in Pan American CLIVAR research: the North American monsoon system, Atmósfera, 16, 29–62, 2003.
Higginson, M., Maxwell, J. R., and Altabet, M. A.: Nitrogen isotope and chlorin paleoproductivity records from the Northern South China Sea: remote vs. local forcing of millennial- and orbital-scale variability, Mar. Geol., 201, 223–250, 2003.
Hodell, D. A., Brenner, M., Curtis, J. H., Medina-González, R., Ildefonso-Chan Can, E., Albornaz-Pat, A., and Guilderson, T. P.: Climate change on the Yucatan Peninsula during the little ice age, Quaternary Res., 63, 109–121, 2005.
Holbourn, A., Kuhnt, W., Schulz, M., and Erlenkeuser, H.: Impacts of orbital forcing and atmospheric carbon dioxide on Miocene ice-sheet expansion, Nature, 438, 483–487, 2005.
Holbourn, A., Kuhnt, W., Schulz, M., Flores, J. A., and Andersen, N.: Orbitally-paced climate evolution during the middle Miocene “Monterey” carbon-isotope excursion, Earth Planet. Sci. Lett., 261, 534–550, 2007.
Holmgren, K., Lee-Thorp, J. A., Cooper, G. R., Lundblad, K., Partridge, T. C., Scott, L., Sithaldeen, R., Siep Talma, A., and Tyson, P. D.: Persistent millennial-scale climatic variability over the past 25,000 years in Southern Africa, Quaternary Sci. Rev., 22, 2311–2326, 2003.

Holzhauser, H., Magny, M., and Zumbuühl, H. J.: Glacier and lake-level variations in west-central Europe over the last 3500 years, The Holocene, 15, 789–801, 2005.
Hoskins, B.: On the existence and strength of the summer subtropical anticyclones: Bernhard Haurwitz memorial lecture, B. Am. Meteorol. Soc., 77, 1287–1292, 1996.
Huang, Y., Clemens, S. C., Liu, W., Wang, Y., and Prell, W. L.: Large-scale hydrological change drove the late Miocene C4 plant expansion in the Himalayan foreland and Arabian Peninsula, Geology, 35, 531–534, 2007.
Huffman, G. J., Adler, R. F., Bolvin, D. T., and Gu, G.: Improving the global precipitation record: GPCP version 2.1, Geophys. Res. Lett., 36, L17808, doi:10.1029/2009GL040000, 2009.
Hüsing, S., Cascella, A., Hilgen, F., Krijgsman, W., Kuiper, K., Turco, E., and Wilson, D.: Astrochronology of the Mediterranean Langhian between 15.29 and 14.17 Ma, Earth Planet. Sci. Lett., 290, 254–269, 2010.
Jia, G., Peng, P. A., Zhao, Q., and Jian, Z.: Changes in terrestrial ecosystem since 30 Ma in East Asia: Stable isotope evidence from black carbon in the South China Sea, Geology, 31, 1093–1096, 2003.
Jian, Z., Huang, B., Kuhnt, W., and Lin, H.-L.: Late Quaternary upwelling intensity and East Asian monsoon forcing in the South China Sea, Quaternary Res., 55, 363–370, 2001.
Jiang, W. and Liu, T.: Timing and spatial distribution of mid Holocene drying over northern China: Response to a southeastward retreat of the East Asian Monsoon, J. Geophys. Res.-Atmos. (1984–2012), 112, D24111, doi:10.1029/2007JD009050, 2007.
Jolly, D., Prentice, I. C., Bonnefille, R., Ballouche, A., Bengo, M., Brenac, P., Buchet, G., Burney, D., Cazet, J. P., and Cheddadi, R.: Biome reconstruction from pollen and plant macrofossil data for Africa and the Arabian peninsula at 0 and 6000 years, J. Biogeogr., 25, 1007–1027, 1998.
Jouzel, J., Masson-Delmotte, V., Cattani, O., Dreyfus, G., Falourd, S., Hoffmann, G., Minster, B., Nouet, J., Barnola, J.-M., and Chappellaz, J.: Orbital and millennial Antarctic climate variability over the past 800,000 years, Science, 317, 793–796, 2007.
Kalnay, E., Kanamitsu, M., Kistler, R., Collins, W., Deaven, D., Gandin, L., Iredell, M., Saha, S., White, G., and Woollen, J.: The NCEP/NCAR 40-year reanalysis project, B. Am. Meteorol. Soc., 77, 437–471, 1996.
Kanner, L. C., Burns, S. J., Cheng, H., and Edwards, R. L.: High-latitude forcing of the South American summer monsoon during the last glacial, Science, 335, 570–573, 2012.

Kao, Y.: Some problems on monsoons over East Asia, Collect. Papers, Inst. Geophys. Meteorol, Acad. Sinica, 5, 1961.
Katz, M. E., Wright, J. D., Miller, K. G., Cramer, B. S., Fennel, K., and Falkowski, P. G.: Biological overprint of the geological carbon cycle, Mar Geol., 217, 323–338, 2005.
Kelly, M. J., Edwards, R. L., Cheng, H., Yuan, D., Cai, Y., Zhang, M., Lin, Y., and An, Z.: High resolution characterization of the Asian Monsoon between 146,000 and 99,000 years BP from Dongge Cave, China and global correlation of events surrounding Termination II, Palaeogeogr. Palaeocli. Palaeoecol., 236, 20–38, 2006.
Khromov, S.: Die geographische verbreitung der monsune, Petermanns Geogr. Mitt., 101, 234–237, 1957.
Kidd, R. B., Cita, M. B., and Ryan, W. B.: Stratigraphy of eastern Mediterranean sapropel sequences recovered during DSDP Leg 42A and their paleoenvironmental significance, Initial Reports of the Deep Sea Drilling Project, 42, 421–443, 1978.
Kistler, R., Collins, W., Saha, S., White, G., Woollen, J., Kalnay, E., Chelliah, M., Ebisuzaki, W., Kanamitsu, M., and Kousky, V.: The NCEP-NCAR 50-year reanalysis: Monthly means CD-ROM and documentation, B. Am. Meteorol. Soc., 82, 247–267, 2001.
Kröpelin, S., Verschuren, D., Lézine, A.-M., Eggermont, H., Cocquyt, C., Francus, P., Cazet, J.-P., Fagot, M., Rumes, B., and Russell, J.: Climate-driven ecosystem succession in the Sahara: the past 6000 years, Science, 320, 765–768, 2008.
Kroon, D. and Ganssen, G.: Northern Indian Ocean upwelling cells and the stable isotope composition of living planktonic foraminifers, Deep Sea Res. Part A., 36, 1219–1236, 1989.
Kroon, D.: Onset of monsoonal related upwelling in the western Arabian Sea as revealed by planktonic foraminifers, Proc. ODP, Sci. Results, 117, 257–263, 1991.
Kumar, K. K., Rajagopalan, B., and Cane, M. A.: On the weakening relationship between the Indian monsoon and ENSO, Science, 284, 2156–2159, 1999.
Kumar, K. K., Kamala, K., Rajagopalan, B., Hoerling, M. P., Eischeid, J. K., Patwardhan, S., Srinivasan, G., Goswami, B., and Nemani, R.: The once and future pulse of Indian monsoonal climate, Clim. Dynam., 36, 2159–2170, 2011.
Kump, L. R.: Interpreting carbon-isotope excursions: Strangelove ocean, Geology, 19, 299–302, 1991
Kutzbach, J. E. and Street-Perrott, F. A.: Milankovitch forcing of fluctuations in the level of tropical lakes from 18 to 0 kyr BP, Nature, 317, 130–134, doi:10.1038/317130a0, 1985.

Kutzbach, J. E.: Estimates of past climate at Paleolake Chad, North Africa, based on a hydrological and energy-balanced model, Quaternary Res., 14, 210–223, 1980.
Kutzbach, J. E.: Monsoon climate of the early Holocene: climate experiment with the earth's orbital parameters for 9000 years ago, Science, 214, 59–61, 1981.
Kutzbach, J. and Gallimore, R.: Pangaean climates: megamonsoons of the megacontinent, J. Geophys. Res.-Atmos. (1984–2012), 94, 3341–3357, 1989.
Kutzbach, J. and Otto-Bliesner, B.: The sensitivity of the African-Asian monsoonal climate to orbital parameter changes for 9000 years BP in a low-resolution general circulation model, J. Atmos. Sci., 39, 1177–1188, 1982.
Kutzbach, J. E., Prell, W. L., and Ruddiman, W.: Sensitivity of Eurasian climate to surface uplift of the Tibetan Plateau, J. Geol., 101, 177–190, 1993.
Kutzbach, J., Bonan, G., Foley, J., and Harrison, S.: Vegetation and soil feedbacks on the response of the African monsoon to orbital forcing in the early to middle Holocene, Nature, 384, 623–626, doi:10.1038/384623a0, 1996.
Kutzbach, J., Chen, G., Cheng, H., Edwards, R., and Liu, Z.: Potential role of winter rainfall in explaining increased moisture in the Mediterranean and Middle East during periods of maximum orbitally-forced insolation seasonality, Clim. Dynam., 42, 1079–1095, 2014.
Kutzbach, J., Guetter, P., Ruddiman, W., and Prell, W.: Sensitivity of climate to late Cenozoic uplift in southern Asia and the American west: Numerical experiments, J. Geophys. Res.-Atmos. (1984–2012), 94, 18393–18407, 1989.
Kutzbach, J., Liu, X., Liu, Z., and Chen, G.: Simulation of the evolutionary response of global summer monsoons to orbital forcing over the past 280,000 years, Clim. Dynam., 30, 567–579, 2008.
Lachniet, M. S., Asmerom, Y., Bernal, J. P., Polyak, V. J., and Vazquez-Selem, L.: Orbital pacing and ocean circulation-induced collapses of the Mesoamerican monsoon over the past 22,000 y, Proc. Natl. Acad. Sci., 110, 9255–9260, 2013.
Lamb, H.: Climate: present, past and future, Vol. 2, Climatic history and the future, Methuen & Company, 1977.
Landais, A., Dreyfus, G., Capron, E., Masson-Delmotte, V., Sanchez-Goni, M., Desprat, S., Hoffmann, G., Jouzel, J., Leuenberger, M., and Johnsen, S.: What drives the millennial and orbital variations of δ^{18}O?, Quaternary Sci. Rev., 29, 235–246, 2010.
Larrasoaña, J., Roberts, A., Rohling, E., Winklhofer, M., and Wehausen, R.: Three million years of monsoon variability over the northern Sahara, Clim. Dynam., 21, 689–698, 2003.

Lee, J.-Y. and Wang, B.: Future change of global monsoon in the CMIP5, Clim. Dynam., 42, 101–119, doi:10.1007/s00382-012-1564-0, 2014.
Lewis, S. C., Gagan, M. K., Ayliffe, L. K., Zhao, J.-x., Hantoro, W. S., Treble, P. C., Hellstrom, J. C., LeGrande, A. N., Kelley, M., and Schmidt, G. A.: High-resolution stalagmite reconstructions of Australian–Indonesian monsoon rainfall variability during Heinrich stadial 3 and Greenland interstadial 4, Earth Planet. Sci. Lett., 303, 133–142, 2011.
Li, F., Wu, N., and Rousseau, D.-D.: Preliminary study of mollusk fossils in the Qinan Miocene loess-soil sequence in western Chinese Loess Plateau, Sci. China Ser. D, 49, 724–730, 2006.
Liang, M., Guo, Z., Kahmann, A. J., and Oldfield, F.: Geochemical characteristics of the Miocene eolian deposits in China: their provenance and climate implications, Geochem. Geophys. Geosyst., 10, Q04004, doi:10.1029/2008GC002331, 2009.
Lisiecki, L. E. and Raymo, M. E.: A Pliocene Pleistocene stack of 57 globally distributed benthic δ18O records, Paleoceanography, 20, PA1003, doi:10.1029/2004PA001071, 2005.
Liu, J. F., Guo, Z., Qiao, Y., Hao, Q., and Yuan, B.: Eolian origin of the Miocene loess-soil sequence at Qin'an, China: Evidence of quartz morphology and quartz grain-size, Chinese Sci. Bull., 51, 117–120, 2006.
Liu, J. F., Guo, Z.-T., Hao, Q. Z., Peng, S. Z., Qiao, Y.-S., Sun, B., and Ge, J.-Y.: Magnetostratigraphy of the Miziwan Miocene eolian deposits in Qin'an county (Gansu Province), Quaternary Sci, 25, 503–508, 2005.
Liu, J., Wang, B., Ding, Q., Kuang, X., Soon, W., and Zorita, E.: Centennial Variations of the Global Monsoon Precipitation in the Last Millennium: Results from ECHO-G Model, J. Climate, 22, 2356–2371, doi:10.1175/2008JCLI2353.1, 2009.
Li, J. and Zeng, Q.: A new monsoon index and the geographical distribution of the global monsoons, Adv. Atmos. Sci., 20, 299–302, 2003.
Liu, T.: Loess and the Environment, Beijing: China Ocean Press, 31, 65, 1985.
Liu, T. and Guo, Z.: Geological environment in China and global change, in: Selected Works of Liu Tungsheng, edited by: An, Z., 192–202, Beijing: Science Press, 1997.
Liu, X. and Yin, Z.-Y.: Sensitivity of East Asian monsoon climate to the uplift of the Tibetan Plateau, Palaeogeogr. Palaeocli. Palaeoecol., 183, 223–245, 2002.
Liu, Y., Henderson, G., Hu, C., Mason, A., Charnley, N., Johnson, K., and Xie, S.: Links between the East Asian monsoon and North Atlantic climate during the 8,200 year event, Nat. Geosci., 6, 117–120, 2013.

Liu, Z., Harrison, S., Kutzbach, J., and Otto-Bliesner, B.: Global monsoons in the mid-Holocene and oceanic feedback, Clim. Dynam., 22, 157–182, 2004.

Liu, Z., Otto-Bliesner, B., Kutzbach, J., Li, L., and Shields, C.: Coupled climate simulation of the evolution of global monsoons in the Holocene, J. Climate, 16, 2472–2490, doi:10.1175/1520-0442(2003)016<2472:CCSOTE>2.0.CO;2, 2003.

Liu, Z., Wang, Y., Gallimore, R., Gasse, F., Johnson, T., DeMenocal, P., Adkins, J., Notaro, M., Prentice, I., and Kutzbach, J.: Simulating the transient evolution and abrupt change of Northern Africa atmosphere-ocean-terrestrial ecosystem in the Holocene, Quaternary Sci. Rev., 26, 1818–1837, doi:10.1016/j.quascirev.2007.03.002, 2007.

Liu, Z., Wang, Y., Gallimore, R., Notaro, M., and Prentice, I. C.: On the cause of abrupt vegetation collapse in North Africa during the Holocene: Climate variability vs. vegetation feedback, Geophys. Res. Lett., 33, L22709, doi:10.1029/2006GL028062, 2006.

Loope, D. B., Rowe, C. M., and Joeckel, R. M.: Annual monsoon rains recorded by Jurassic dunes, Nature, 412, 64–66, 2001.

Loulergue, L., Schilt, A., Spahni, R., Masson-Delmotte, V., Blunier, T., Lemieux, B., Barnola, J.-M., Raynaud, D., Stocker, T. F., and Chappellaz, J.: Orbital and millennial-scale features of atmospheric CH_4 over the past 800,000 years, Nature, 453, 383–386, 2008.

Lourens, L., Hilgen, F., Shackleton, N. J., Laskar, J., and Wilson, D.: The Neogene period, in: A Geologic Time Scale 2004, Cambridge, 409–440, 2004.

Luz, B. and Barkan, E.: The isotopic composition of atmospheric oxygen, Global Biogeochem. Cy., 25, GB3001, doi:10.1029/2010GB003883, 2011.

Ma, W., Tian, J., Li, Q., and Wang, P.: Simulation of long eccentricity (400 kyr) cycle in ocean carbon reservoir during Miocene Climate Optimum: Weathering and nutrient response to orbital change, Geophys. Res. Lett., 38, L10701, doi:10.1029/2011GL047680, 2011.

Magee, J. W., Miller, G. H., Spooner, N. A., and Questiaux, D.: Continuous 150 ky monsoon record from Lake Eyre, Australia: insolation-forcing implications and unexpected Holocene failure, Geology, 32, 885–888, 2004.

Mantua, N.J., Hare, S.R.: The Pacific Decadal Oscillation, J. Oceanogr., 58, 35–44, 2002.

Marshall, A. and Lynch, A.: The sensitivity of the Australian summer monsoon to climate forcing during the late Quaternary, J. Geophys. Res.-Atmos. (1984–2012), 113, D11107, doi:10.1029/2007JD008981, 2008.

Matthews, R. K. and Froelich, C.: Maximum flooding surfaces and sequence boundaries: comparisons between observations and orbital forcing in the Cretaceous and Jurassic (65–190 Ma), GeoArabia, Middle East Petrol. Geosci., 7, 503–538, 2002.

McBride, J. L.: The Australian summer monsoon, in: Monsoon Meteorology, edited by: Chang, C.-P. and Krishnamutri, T. N., Oxford University Press, Oxford, UK, 203–232, 1987.

McGee, D., deMenocal, P., Winckler, G., Stuut, J., and Bradtmiller, L.: The magnitude, timing and abruptness of changes in North African dust deposition over the last 20,000 yr, Earth Planet. Sci. Lett., 371, 163–176, 2013.

McInerney, F. A. and Wing, S. L.: The Paleocene-Eocene Thermal Maximum: a perturbation of carbon cycle, climate, and biosphere with implications for the future, Annu. Rev. Earth Planet. Sci., 39, 489–516, 2011.

McIntyre, A., Ruddiman, W. F., Karlin, K., and Mix, A. C.: Surface water response of the equatorial Atlantic Ocean to orbital forcing, Paleoceanography, 4, 19–55, 1989.

McIntyre, A. and Molfino, B.: Forcing of Atlantic equatorial and subpolar millennial cycles by precession, Science, 274, 1867–1870, 1996.

Meehl, G. A., Covey, C., Taylor, K. E., Delworth, T., Stouffer, R. J., Latif, M., McAvaney, B., and Mitchell, J. F.: The WCRP CMIP3 multimodel dataset: A new era in climate change research, B. Am. Meteorol. Soc., 88, 1383–1394, 2007a.

Meehl, G. A., Stocker, T. F., Collins, W. D., Friedlingstein, P., Gaye, A. T., Gregory, J. M., Kitoh, A., Knutti, R., Murphy, J. M., and Noda, A.: Global climate projections, Clim. Change, 2007, 3–4, 2007b.

Meigs, P.: World distribution of arid and semi-arid homoclimates, Rev. Res. Arid Zone Hydrol., 1, 203–209, 1953.

Merrifield, M. A., Thompson, P. R., and Lander, M.: Multidecadal sea level anomalies and trends in the western tropical Pacific, Geophys. Res. Lett., 39, L13602, doi:10.1029/2012GL052032, 2012.

Molfino, B. and McIntyre, A.: Precessional forcing of nutricline dynamics in the Equatorial Atlantic, Science(Washington), 249, 766–769, 1990.

Morrill, C., Overpeck, J. T., and Cole, J. E.: A synthesis of abrupt changes in the Asian summer monsoon since the last deglaciation, The Holocene, 13, 465–476, 2003.

Mosblech, N. A., Bush, M. B., Gosling, W. D., Hodell, D., Thomas, L., van Calsteren, P., Correa-Metrio, A., Valencia, B. G., Curtis, J., and van Woesik, R.: North Atlantic forcing of Amazonian precipitation during the last ice age, Nat. Geosci., 5, 817–820, 2012.

CPD
10, 2163–2291, 2014

Mourik, A., Bijkerk, J., Cascella, A., Hüsing, S., Hilgen, F., Lourens, L., and Turco, E.: Astronomical tuning of the La Vedova High Cliff Section (Ancona, Italy) – Implications of the middle Miocene climate transition for Mediterranean sapropel formation, Earth Planet. Sci. Lett., 297, 249–261, 2010.
Mulitza, S., Prange, M., Stuut, J. B., Zabel, M., von Dobeneck, T., Itambi, A. C., Nizou, J., Schulz, M., and Wefer, G.: Sahel megadroughts triggered by glacial slowdowns of Atlantic meridional overturning, Paleoceanography, 23, PA4206, doi:10.1029/2008PA001637, 2008.
Murakami, H., Sugi, M., and Kitoh, A.: Future changes in tropical cyclone activity in the North Indian Ocean projected by high-resolution MRI-AGCMs, Clim. Dynam., 40, 1949–1968, 2012.
Neelin, J., Chou, C., and Su, H.: Tropical drought regions in global warming and El Niño teleconnections, Geophys. Res. Lett., 30, 2275, doi:10.1029/2003GL018625, 2003.
Neelin, J. D., Münnich, M., Su, H., Meyerson, J. E., and Holloway, C. E.: Tropical drying trends in global warming models and observations. Proc. Natl. Acad. Sci., 103, 6110–6115, 2006.
Newton, A., Thunell, R., and Stott, L.: Climate and hydrographic variability in the Indo Pacific Warm Pool during the last millennium, Geophys. Res. Lett., 33, L19710, doi:10.1029/2006GL027234, 2006.
Nicholson, S. E. and Kim, J.: The relationship of the El Nino-Southern oscillation to African rainfall, Int. J. Climatol., 17, 117–135, 1997.
Novello, V. F., Cruz, F. W., Karmann, I., Burns, S. J., Stríkis, N. M., Vuille, M., Cheng, H., Lawrence Edwards, R., Santos, R. V., and Frigo, E.: Multidecadal climate variability in Brazil's Nordeste during the last 3000 years based on speleothem isotope records, Geophys. Res. Lett., 39, L23706, doi:10.1029/2012GL053936, 2012.
O'Brien, S. R., Mayewski, P. A., Meeker, L. D., Meese, D. A., Twickler, M.S ., and Whitlow, S. I:. Complexity of Holocene climate as reconstructed from a Greenland ice core, Science, 270, 1962–1964, 1995.
Oldfield, F. and Bloemendal, J.: Rock-magnetic properties confirm the eolian origin of Miocene sequences from the west of the Chinese Loess Plateau, Sediment. Geol., 234, 70–75, 2011.
Olsen, P. E.: A 40-million-year lake record of early Mesozoic orbital climatic forcing, Science, 234, 842–848, 1986.
Olsen, P. E. and Kent, D. V.: Milankovitch climate forcing in the tropics of Pangaea during the Late Triassic, Palaeogeogr. Palaeocl. Palaeoecol., 122, 1–26, 1996.

CPD
10, 2163–2291, 2014
The Global Monsoon across Time Scales
P. X. Wang et al.

Onogi, K., Tsutsui, J., Koide, H., Sakamoto, M., Kobayashi, S., Hatsushika, H., Matsumoto, T., Yamazaki, N., Kamahori, H., and Takahashi, K.: The JRA-25 reanalysis, J. Meteorol. Soc. Jpn, 85, 369–432, 2007.
Oppo, D. W., Schmidt, G. A., and LeGrande, A. N.: Seawater isotope constraints on tropical hydrology during the Holocene, Geophys. Res. Lett., 34, L13701, doi:10.1029/2007GL030017, 2007.
Ortloff, C. R. and Kolata, A. L.: Climate and collapse: agro-ecological perspectives on the decline of the Tiwanaku state, J. Archaeol. Sci., 20, 195–221, 1993.
Pälike, H., Frazier, J., and Zachos, J. C.: Extended orbitally forced palaeoclimatic records from the equatorial Atlantic Ceara Rise, Quaternary Sci. Rev., 25, 3138–3149, 2006a.
Pälike, H., Norris, R. D., Herrle, J. O., Wilson, P. A., Coxall, H. K., Lear, C. H., Shackleton, N. J., Tripati, A. K., and Wade, B. S.: The heartbeat of the Oligocene climate system, Science, 314, 1894–1898, 2006b.
Parker, D., Folland, C., Scaife, A., Knight, J., Colman, A., Baines, P., and Dong, B.: Decadal to multidecadal variability and the climate change background, J. Geophys. Res.-Atmos. (1984–2012), 112, D18115, 2007.
Parrish, J. T.: Climate of the supercontinent Pangea, The J. Geol., 101, 215–233, 1993.
Partridge, T., Demenocal, P., Lorentz, S., Paiker, M., and Vogel, J.: Orbital forcing of climate over South Africa: a 200,000-year rainfall record from the Pretoria Saltpan, Quaternary Sci. Rev., 16, 1125–1133, 1997.
Paul, H. A., Zachos, J. C., Flower, B. P., and Tripati, A.:. Orbitally induced climate and geochemical variability across the Oligocene/Miocene boundary. Paleoceanography, 15, 471–485, 2000.
Pessenda, L. C. R., Ribeiro, A. d. S., Gouveia, S. E. M., Aravena, R., Boulet, R., and Bendassolli, J. A.: Vegetation dynamics during the late Pleistocene in the Barreirinhas region, Maranhão State, northeastern Brazil, based on carbon isotopes in soil organic matter, Quaternary Res., 62, 183–193, 2004.
Peterson, L. C., Haug, G. H., Hughen, K. A., and Röhl, U.: Rapid changes in the hydrologic cycle of the tropical Atlantic during the last glacial, Science, 290, 1947–1951, 2000.
Petit, J. R., Jouzel, J. Raynaud, D., Barkov, N.I., Barnola, J.-M., Basile, I., Bender, M., Chappellaz, J., Davisk,M., Delaygue, D., Delmotte,M., Kotlyakov, V. M., Legrand, M., Lipenkov, V. Y., Lorius, C., Pe'pin, L., Ritz, C., Saltzmank, E., and Stievenard, M.: Climate and atmospheric

history of the past 420,000 years from the Vostok ice core, Antarctica. Nature, 399, 429–436, 1999.
Philander, S., Gu, D., Lambert, G., Li, T., Halpern, D., Lau, N., and Pacanowski, R.: Why the ITCZ is mostly north of the equator, J. Climate, 9, 2958–2972, 1996.
Pokras, E. M. and Mix, A. C.: Earth's precession cycle and Quaternary climatic change in tropical Africa, Nature, 326, 486–487, 1987.
Poore, R., Dowsett, H., Verardo, S., and Quinn, T. M.: Millennial to century scale variability in Gulf of Mexico Holocene climate records, Paleoceanography, 18, 1048, doi:10.1029/2002PA000868, 2003.
Porter, S. C. and An Z.: Correlation between climate events in the North Atlantic and China during the last glaciation, Nature, 375, 305–308, doi:10.1038/375305a0, 1995.
Power, S., Casey, T., Folland, C., Colman, A., and Mehta, V.: Inter-decadal modulation of the impact of ENSO on Australia, Clim. Dynam., 15, 319–324, 1999.
Prell, W. L.: Monsoonal climate of the Arabian Sea during the Late Quaternary: a response to changing solar radiation, in: Milankovitch and Climate, edited by: Berger, A. L., Imbrie, J., Hays, J., Kukla, G., and Saltzman, B., D. Riedel, Hingham, 349–366, 1984.
Prell, W. L. and Kutzbach, J. E.: The impact of Tibet-Himalayan elevation on the sensitivity of the monsoon climate system to changes in solar radiation, in: Tectonic Uplift and Climate Change, Springer, 171–201, 1997.
Pye, K.: The nature, origin and accumulation of loess, Quaternary Sci. Rev., 14, 653–667, 1995.
Qiang, X. K., An, Z. S., Song, Y. G., Chang, H., Sun, Y. B., Liu, W. G., Ao, H., Dong, J. B., Fu, C. F., Wu, F., Lu, F. Y., Cai, Y. L., Zhao, W. J., Cao, J. J., Xu, X. W., and Ai, L.: New eolian red clay sequence on the western Chinese Loess Plateau linked to onset of Asian desertification about 25 Ma ago, Sci. China Earth Sci., 54, 136–144, 2011.
Qiao, Y., Guo, Z., Hao, Q., Yin, Q., Yuan, B., and Liu, T.: Grain-size features of a Miocene loess-soil sequence at Qinan: Implications on its origin, Sci. China Ser. D, 49, 731–738, 2006.
Qiu, Z. and Li, C.: Evolution of Chinese mammalian faunal regions and elevation of the Qinghai-Xizang (Tibet) Plateau, Sci. China Ser. D, 48, 1246–1258, 2005.
Quade, J., Cerling, T. E., and Bowman, J. R.: Development of Asian monsoon revealed by marked ecological shift during the late 67st Miocene in northern Pakistan, Nature, 342, 163–166, 1989.

Discussion Paper | Discussion Paper | Discussion Paper | Discussion Paper |

Rühlemann, C., Mulitza, S., Müller, P. J., Wefer, G., and Zahn, R.: Warming of the tropical Atlantic Ocean and slowdown of thermohaline circulation during the last deglaciation, Nature, 402, 511–514, 1999.

Rahmstorf, S.: Timing of abrupt climate change: A precise clock, Geophys. Res. Lett., 30, 1510, doi:10.1029/2003GL017115, 2003.

Ramage, C. S.: Monsoon meteorology, Int. Geophys. Ser., 15, Academic Press, California, 296, 1971.

Rea, D. K.: The paleoclimatic record provided by eolian deposition in the deep sea: The geologic history of wind, Rev. Geophys., 32, 159–195, 1994.

Renssen, H., Goosse, H., and Muscheler, R.: Coupled climate model simulation of Holocene cooling events: oceanic feedback amplifies solar forcing, Clim. Past, 2, 79–90, doi:10.5194/cp-2-79-2006, 2006.

Reuter, J., Stott, L., Khider, D., Sinha, A., Cheng, H., and Edwards, R. L.: A new perspective on the hydroclimate variability in northern South America during the Little Ice Age, Geophys. Res. Lett., 36, L21706, doi:10.1029/2009GL041051, 2009.

Revel, M., Ducassou, E., Grousset, F., Bernasconi, S., Migeon, S., Revillon, S., Mascle, J., Murat, A., Zaragosi, S., and Bosch, D.: 100,000 years of African monsoon variability recorded in sediments of the Nile margin, Quaternary Sci. Rev., 29, 1342–1362, 2010.

Rienecker, M. M., Suarez, M. J., Gelaro, R., Todling, R., Bacmeister, J., Liu, E., Bosilovich, M. G., Schubert, S. D., Takacs, L., and Kim, G.-K.: MERRA: NASA"s Modern-Era Retrospective Analysis for Research and Applications, J. Climate, 24, 3624–3648, doi:10.1175/JCLI-D-11-00015.1, 2011.

Ritchie, J., Eyles, C., and Haynes, C. V.: Sediment and pollen evidence for an early to mid-Holocene humid period in the eastern Sahara, Nature, 314, 352–355, 1985.

Rodwell, M. J. and Hoskins, B. J.: Monsoons and the dynamics of deserts, Q. J. Roy. Meteorol. Soc., 122, 1385–1404, 1996.

Rodysill, J. R., Russell, J. M., Crausbay, S. D., Bijaksana, S., Vuille, M., Edwards, R. L., and Cheng, H.: A severe drought during the last millennium in East Java, Indonesia, Quaternary Sci. Rev., 80, 102–111, 2013.

Rohling, E. J. and Bigg, G. R.: Paleosalinity and δ^{18}O: a critical assessment, J. Geophys. Res.-Oceans (1978–2012), 103, 1307–1318, 1998.

Rossignol-Strick, M.: African monsoons, an immediate climate response to orbital insolation, Nature, 304, 46–49, 1983.

Discussion Paper | Discussion Paper | Discussion Paper | Discussion Paper |

CPD
10, 2163–2291, 2014

The Global Monsoon across Time Scales

P. X. Wang et al.

Rossignol-Strick, M., Nesteroef, W., Olive, P., and Vergnaud-Grazzini, C.: After the deluge: Mediterranean stagnation and sapropel formation, Nature, 295, 105–110, 1982..
Rossignol-Strick, M., Paterne, M., Bassinot, F., Emeis, K.-C., and De Lange, G.: An unusual mid-Pleistocene monsoon period over Africa and Asia, Nature, 392, 269–272, 1998.
Rowe, H. D., Guilderson, T. P., Dunbar, R. B., Southon, J. R., Seltzer, G. O., Mucciarone, D. A., Fritz, S. C., and Baker, P. A.: Late Quaternary lake-level changes constrained by radiocarbon and stable isotope studies on sediment cores from Lake Titicaca, South America, Global Planet. Change, 38, 273–290, 2003.
Ruddiman, W. and Kutzbach, J.: Forcing of late Cenozoic Northern Hemisphere climate by plateau uplift in southern Asia and the American west, J. Geophys. Res.-Atmos. (1984–2012), 94, 18409–18427, 1989.
Ruddiman, W., Prell, W., and Raymo, M.: Late Cenozoic uplift in southern Asia and the American West: Rationale for general circulation modeling experiments, J. Geophys. Res.-Atmos. (1984–2012), 94, 18379–18391, 1989.
Ruddiman, W. F.: Earth's Climate: past and future, Macmillan, 2001.
Ruddiman, W. F. and Raymo, M. E.: A methane-based time scale for Vostok ice, Quaternary Sci. Rev., 22, 141–155, 2003.
Ruddiman, W. F.: What is the timing of orbital-scale monsoon changes?, Quaternary Sci. Rev., 25, 657–658, 2006.
Rühlemann, C., Mulitza, S., Muller, P. J., Wefer, G., and Zahn, R.: Warming of the tropical Atlantic Ocean and slowdown of thermohaline circulation during the last deglaciation, Nature, 402, 511–514, 1999.
Russell, J. M. and Johnson, T. C.: A high-resolution geochemical record from Lake Edward, Uganda Congo and the timing and causes of tropical African drought during the late Holocene, Quaternary Sci. Rev., 24, 1375–1389, 2005.
Russon, T., Paillard, D., and Elliot, M.: Potential origins of 400-500 kyr periodicities in the ocean carbon cycle: A box model approach, Global Biogeochem. Cy., 24, GB2013, doi:10.1029/2009GB003586, 2010.
Sachs, J. P., Sachse, D., Smittenberg, R. H., Zhang, Z., Battisti, D. S., and Golubic, S.: Southward movement of the Pacific intertropical convergence zone AD 1400–1850, Nat. Geosci., 2, 519–525, 2009.

CPD
10, 2163–2291, 2014
The Global Monsoon across Time Scales
P. X. Wang et al.

Salamy, K. A. and Zachos, J. C.: Latest Eocene-Early Oligocene Climate Change and Southern Ocean Fertility: Inferences from Sediment Accumulation and Stable Isotope Data, Palaeogeogr. Palaeocli. Palaeoecol., 145, 61–77, 1999
Sarnthein, M., Tetzlaff, G., Koopmann, B., Wolter, K., and Pflaumann, U.: Glacial and interglacial wind regimes over the eastern subtropical Atlantic and North-West Africa, Nature, 293, 193–196, 1981.
Schuster, M., Duringer, P., Ghienne, J.-F., Vignaud, P., Mackaye, H. T., Likius, A., and Brunet, M.: The age of the Sahara desert, Science, 311, 821–821, 2006.
Seager, R., Naik, N., and Vecchi, G. A.: Thermodynamic and Dynamic Mechanisms for Large-Scale Changes in the Hydrological Cycle in Response to Global Warming*, J. Climate, 23, 4651–4668, doi:10.1175/2010JCLI3655.1, 2010.
Seltzer, G., Rodbell, D., and Burns, S.: Isotopic evidence for late Quaternary climatic change in tropical South America, Geology, 28, 35–38, 2000.
Seth, A., Rauscher, S. A., Rojas, M., Giannini, A., and Camargo, S. J.: Enhanced spring convective barrier for monsoons in a warmer world?, Clim. Change, 104, 403–414, doi:10.1007/s10584-010-9973-8, 2011.
Severinghaus, J. P., Beaudette, R., Headly, M. A., Taylor, K., and Brook, E. J.: Oxygen-18 of O_2 records the impact of abrupt climate change on the terrestrial biosphere, Science, 324, 1431–1434, 2009.
Shackleton, N. J.: The 100,000-year ice-age cycle identified and found to lag temperature, carbon dioxide, and orbital eccentricity, Science, 289, 1897–1902, 2000.
Shapaev, V. M.: Monsoon characteristics of of the atmospheric circulation in Soviet Arctic (in Russian). Geographicheskoe Obshchestov, ssr, Izv. 92, 176–180, 1960.
Schick, M.: Die Geographiche Verbureitung des Monsunes, Nova Acta Leopoldina, 16, No. 12, 1953.
Short, D. A., Mengel, J. G., Crowley, T. J., Hyde, W. T., and North, G. R.: Filtering of Milankovitch cycles by Earth's geography, Quaternary Res., 35, 157–173, 1991.
Sima, A., Rousseau, D.-D., Kageyama, M., Ramstein, G., Schulz, M., Balkanski, Y., Antoine, P., Dulac, F., and Hatté, C.: Imprint of North-Atlantic abrupt climate changes on western European loess deposits as viewed in a dust emission model, Quaternary Sci. Rev., 28, 2851–2866, 2009.

Singh, R. K. and Gupta, A. K.: Late Oligocene–Miocene paleoceanographic evolution of the southeastern Indian Ocean: evidence from deep-sea benthic foraminifera (ODP Site 757), Mar. Micropaleontol., 51, 153–170, 2004.

Sinha, A., Cannariato, K. G., Stott, L. D., Li, H.-C., You, C.-F., Cheng, H., Edwards, R. L., and Singh, I. B.: Variability of southwest Indian summer monsoon precipitation during the Bølling-Ållerød, Geology, 33, 813–816, 2005.

Sinha, A., Berkelhammer, M., Stott, L., Mudelsee, M., Cheng, H., and Biswas, J.: The leading mode of Indian Summer Monsoon precipitation variability during the last millennium, Geophys. Res. Lett., 38, L15703, doi:10.1029/2011GL047713, 2011.

Sirocko, F., Sarnthein, M., Erlenkeuser, H., Lange, H., Arnold, M., and Duplessy, J. C.: Century-scale events in monsoonal climate over the past 24,000 years, Nature, 364, 322–324, doi:10.1038/364322a0, 1993.

Sletten, H. R., Railsback, L. B., Liang, F., Brook, G. A., Marais, E., Hardt, B. F., Cheng, H., and Edwards, R. L.: A petrographic and geochemical record of climate change over the last 4600years from a northern Namibia stalagmite, with evidence of abruptly wetter climate at the beginning of southern Africa's Iron Age, Palaeogeogr. Palaeocli. Palaeoecol., 376, 149–162, 2013.

Song, Z., Li, H., Zheng, Yi., and Liu, G.: Miocene floristic region of China, in: Palaeobiogeographic provinces of China, Beijing Science Press, Beijing, 1983.

Soreghan, G. S., Soreghan, M. J., and Hamilton, M. A.: Origin and significance of loess in late Paleozoic western Pangaea: A record of tropical cold?, Palaeogeogr. Palaeocli. Palaeoecol., 268, 234–259, 2008.

Stocker, T. F., Wright, D. G., and Broecker, W. S.: The influence of high latitude surface forcing on the global thermohaline circulation, Paleoceanography, 7, 529–541, 1992.

Stocker, T. F. and Johnsen, S. J.: A minimum thermodynamic model for the bipolar seesaw, Paleoceanography, 18, 1087, doi:10.1029/2003PA000920, 2003.

Stríkis, N. M., Cruz, F. W., Cheng, H., Karmann, I., Edwards, R. L., Vuille, M., Wang, X., de Paula, M. S., Novello, V. F., and Auler, A. S.: Abrupt variations in South American monsoon rainfall during the Holocene based on a speleothem record from central-eastern Brazil, Geology, 39, 1075–1078, 2011.

Sun, D., Liu, D., Chen, M., An, Z., and John, S.: Magnetostratigraphy and palaeoclimate of red clay sequences from Chinese Loess Plateau, Sci. China Ser. D, 40, 337–343, 1997.

Sun, D.: Monsoon and westerly circulation changes recorded in the late Cenozoic aeolian sequences of Northern China, Global Planet. Change, 41, 63–80, 2004.
Sun, J., Ye, J., Wu, W., Ni, X., Bi, S., Zhang, Z., Liu, W., and Meng, J.: Late Oligocene–Miocene mid-latitude aridification and wind patterns in the Asian interior, Geology, 38, 515–518, 2010.
Sun, X. and Wang, P.: How old is the Asian monsoon system? – Palaeobotanical records from China, Palaeogeogr. Palaeocli. Palaeoecol., 222, 181–222, 2005.
Sun, Y., Clemens, S. C., Morrill, C., Lin, X. ,Wang, X., and An, Z.: Influence of Atlantic meridional overturning circulation on the East Asian winter monsoon. Nat. Geosci., 5, 46–49, 2012.
Svensson, A., Andersen, K. K., Bigler, M., Clausen, H. B., Dahl-Jensen, D., Davies, S. M., Johnsen, S. J., Muscheler, R., Parrenin, F., Rasmussen, S. O., Röthlisberger, R., Seierstad, I., Steffensen, J. P., and Vinther, B. M.: A 60 000 year Greenland stratigraphic ice core chronology, Clim. Past, 4, 47–57, doi:10.5194/cp-4-47-2008, 2008.
Tabor, N. J. and Montañez, I. P.: Shifts in late Paleozoic atmospheric circulation over western equatorial Pangea: Insights from pedogenic mineral δ^{18}O compositions, Geology, 30, 1127–1130, 2002.
Talbot, M. and Delibrias, G.: Holocene variations in the level of Lake Bosumtwi, Ghana, Nature, 268, 722–724, 1977.
Tan, L., Cai, Y., An, Z., Edwards, R. L., Cheng, H., Shen, C.-C., and Zhang, H.: Centennial- to decadal-scale monsoon precipitation variability in the semi-humid region, northern China during the last 1860 years: Records from stalagmites in Huangye Cave, The Holocene, 21, 287–296, 2011.
Tanaka, H., Ishizaki, N., and Nohara, D.: Intercomparison of the intensities and trends of Hadley, Walker and monsoon circulations in the global warming projections, SOLA, 1, 77–80, 2005.
Tao, S. and Chen, L.: A review of recent research on the East Asian summer monsoon in China, in: Monsoon Meteorology, edited by: Chang, C.-P. and Krishnamurti, T. N., Oxford University Press, 60–92, 1987.
Taylor, K. E., Stouffer, R. J., and Meehl, G. A.: An Overview of CMIP5 and the Experiment Design, B. Am. Meteorol. Soc., 93, 485–498, doi:10.1175/BAMS-D-11-00094.1, 2012.
Thomas, E. R., Wolff, E. W., Mulvaney, R., Steffensen, J. P., Johnsen, S. J., Arrowsmith, C., White, J. W., Vaughn, B., and Popp, T.: The 8.2 ka event from Greenland ice cores, Quaternary Sci. Rev., 26, 70–81, 2007.

CPD
10, 2163–2291, 2014
The Global Monsoon across Time Scales
P. X. Wang et al.

Thompson, L. G., Mosley-Thompson, E., Dansgaard, W., and Grootes, P. M. : The Little Ice Age as recorded in the stratigraphy of the tropical Quelccaya Ice Cap, Science, 234, 361–364, 1986.

Thompson, L. G., Davis, M. E., Mosley-Thompson, E., Sowers, T., Henderson, K. A., Zagorodnov, V. S., Lin, P.-N., Mikhalenko, V. N., Campen, R. K., and Bolzan, J. F.: A 25,000-year tropical climate history from Bolivian ice cores, Science, 282, 1858–1864, 1998.

Tian, J., Shevenell, A., Wang, P., Zhao, Q., Li, Q., and Cheng, X.: Reorganization of Pacific deep waters linked to middle Miocene Antarctic cryosphere expansion: A perspective from the South China, Palaeogeogr. Palaeocli. Palaeoecol., 284, 375–382 , 2009.

Tian, J., Xie, X., Ma, W., Jin, H., and Wang, P.: X ray fluorescence core scanning records of chemical weathering and monsoon evolution over the past 5 Myr in the southern South China Sea, Paleoceanography, 26, PA4202, doi:10.1029/2007PA001552, 2011.

Tiedemann, R., Sarnthein, M., and Shackleton, N. J.: Astronomic timescale for thePliocene Atlantic δ^{18}O and dust flux records from Ocean Drilling Program Site 659, Paleoceanography, 9, 619–638, 1994.

Tierney, J. E., Russell, J. M., Huang, Y., Damsté, J. S. S., Hopmans, E. C., and Cohen, A. S.: Northern hemisphere controls on tropical southeast African climate during the past 60,000 years, Science, 322, 252–255, 2008.

Trenberth, K. E., Stepaniak, D. P., and Caron, J. M.: The global monsoon as seen through the divergent atmospheric circulation, J. Climate, 13, 3969–3993, doi:10.1175/1520-0442(2000)013<3969:TGMAST>2.0.CO;2, 2000.

Trenberth, K. E.: Changes in precipitation with climate change, Clim. Res., 47, 123–138, doi:10.3354/cr00953, 2011.

Tsoar, H. and Pye, K.: Dust transport and the question of desert loess formation, Sedimentology, 34, 139–153, 1987.

Unnikrishnan, A., Kumar, M., and Sindhu, B.: Tropical cyclones in the Bay of Bengal and extreme sea-level projections along the east coast of India in a future climate scenario, Current Sci., 101, 327–331, 2011.

Uppala, S. M., Kållberg, P., Simmons, A., Andrae, U., Bechtold, V., Fiorino, M., Gibson, J., Haseler, J., Hernandez, A., and Kelly, G.: The ERA40 re-analysis, Qu. J. Roy. Meteorol. Soc., 131, 2961–3012, 2005.

CPD
10, 2163–2291, 2014

Title Page
Abstract | Introduction
Conclusions | References
Tables | Figures
◀| |▶
◀ ▶
Back | Close
Full Screen / Esc
Printer-friendly Version
Interactive Discussion

Van Breukelen, M., Vonhof, H., Hellstrom, J., Wester, W., and Kroon, D.: Fossil dripwater in stalagmites reveals Holocene temperature and rainfall variation in Amazonia, Earth.Planet. Sci. Lett., 275, 54–60, 2008.
Vecchi, G. A. and Soden, B. J.: Global warming and the weakening of the tropical circulation, J. Climate, 20, 4316–4340, 2007.
Vera, C., Higgins, W., Amador, J., Ambrizzi, T., Garreaud, R., Gochis, D., Gutzler, D., Lettenmaier, D., Marengo, J., and Mechoso, C.: Toward a unified view of the American monsoon systems, J. Climate, 19, 4977–5000, 2006.
Verheyden, S., Nader, F. H., Cheng, H. J., Edwards, L. R., and Swennen, R.: Paleoclimate reconstruction in the Levant region from the geochemistry of a Holocene stalagmite from the Jeita cave, Lebanon, Quaternary Res., 70, 368–381, 2008.
Vermeer, M. and Rahmstorf, S.: Global sea level linked to global temperature, Proc. Natl. Acad. Sci., 106, 21527–21532, 2009.
Verschuren, D., Laird, K. R., and Cumming, B. F.: Rainfall and drought in equatorial east Africa during the past 1,100 years, Nature, 403, 410–414, 2000.
Vollmer, T., Werner, R., Weber, M., Tougiannidis, N., Röhling, H.-G., and Hambach, U.: Orbital control on Upper Triassic Playa cycles of the Steinmergel-Keuper (Norian): a new concept for ancient playa cycles, Palaeogeogr. Palaeocli. Palaeoecol., 267, 1–16, 2008.
Vuille, M., Burns, S. J., Taylor, B. L., Cruz, F. W., Bird, B. W., Abbott, M. B., Kanner, L. C., Cheng, H., and Novello, V. F.: A review of the South American monsoon history as recorded in stable isotopic proxies over the past two millennia, Clim. Past, 8, 1309–1321, doi:10.5194/cp-8-1309-2012, 2012.
Wade, B. S. and Pälike, H.: Oligocene climate dynamics. Paleoceanography, 19, PA4019, doi:10.1029/2004PA001042, 2004.
Waelbroeck, C., Labeyrie, L., Michel, E., Duplessy, J. C., McManus, J., Lambeck, K., Balbon, E., and Labracherie, M.: Sea-level and deep water temperature changes derived from benthic foraminifera isotopic records, Quaternary Sci. Rev., 21, 295–305, 2002.
Wagner, J. D. M., Cole, J. E., Beck, J. W., Patchett, P. J., Henderson, G. M., and Barnett, H. R.: Moisture variability in the southwestern United States linked to abrupt glacial climate change, Nat. Geosci., 3, 110–113, 2010.
Wang, B.: Climatic regimes of tropical convection and rainfall, J. Climate, 7, 1109–1118, 1994.
Wang, B. and LinHo: Rainy seasons of the Asian-Pacific monsoon, J. Climate, 15, 386–398, 2002.

CPD
10, 2163–2291, 2014

The Global Monsoon across Time Scales

P. X. Wang et al.

Wang, B. and Wang, Y.: Dynamics of the ITCZ-equatorial cold tongue complex and causes of the latitudinal climate asymmetry, J. Climate, 12, 1830–1847, 1999.
Wang, B., Clemens, S. C., and Liu, P.: Contrasting the Indian and East Asian monsoons: implications on geologic timescales, Mar. Geol., 201, 5–21, 2003.
Wang, B.: The Asian Monsoon, Springer, 2006.
Wang, B. and Ding, Q.: Changes in global monsoon precipitation over the past 56 years, Geophys. Res. Lett., 33, L06711, doi:10.1029/2005GL025347, 2006.
Wang, B. and Ding, Q.: Global monsoon: Dominant mode of annual variation in the tropics, Dynam. Atmos. Oceans, 44, 165–183, doi:10.1016/j.dynatmoce.2007.05.002, 2008.
Wang, B., Yang, J., and Zhou, T.: Interdecadal Changes in the Major Modes of Asian–Australian Monsoon Variability: Strengthening Relationship with ENSO since the Late 1970s, J. Climate, 21, 1771–1789, doi:10.1175/2007JCLI1981.1, 2008.
Wang, B., Liu, J., Kim, H.-J., Webster, P. J., and Yim, S.-Y.: Recent change of the global monsoon precipitation (1979–2008), Clim. Dynam., 39, 1123–1135, doi:10.1007/s00382-011-1266-z, 2012.
Wang, B., Liu, J., Kim, H.-J., Webster, P. J., Yim, S.-Y., and Xiang, B.: Northern Hemisphere summer monsoon intensified by mega-El Niño/southern oscillation and Atlantic multidecadal oscillation, Proc. Natl. Acad. Sci., 110, 5347–5352, 2013.
Wang, J., Wang, Y. J., Liu, Z. C., Li, J. Q., and Xi, P.: Cenozoic environmental evolution of the Qaidam Basin and its implications for the uplift of the Tibetan Plateau and the drying of central Asia, Palaeogeogr. Palaeocli. Palaeoecol., 152, 37–47, 1999.
Wang, L., Sarenthein, M., Erlenkeuser, H., Grimalt, J., Grootes, P., Heilig, S., Ivanova, E., Kienast, M., Pelejero, C., and Pflaumann, U.: East Asian monsoon Climate during the late Pleistocene: high- resolution sediment records from the South China Sea, Mar. Geol., 156, 245–284, 1999.
Wang, P.: Neogene stratigraphy and paleoenvironments of China, Palaeogeogr. Palaeocli. Palaeoecol., 77, 315–334, 1990.
Wang, P.: Global monsoon in a geological perspective, Chinese Sci. Bull., 54, 1–24, 2009.
Wang, P., Prell, W. L., and Blum, P. (Eds): Proceedings of Ocean Drilling Program, Initial. Reports, 184 [CD-ROM], Ocean Drilling Program, Texas A&M University, College Station TX 77845-9547, USA, 2000.

Wang, P., Tian, J., Cheng, X., Liu, C., and Xu, J.: Major Pleistocene stages in a carbon perspective: The South China Sea record and its global comparison, Paleoceanography, 19, PA4005, doi:10.1029/2003PA000991, 2004.

Wang, P., Clemens, S., Beaufort, L., Braconnot, P., Ganssen, G., Jian, Z., Kershaw, P., and Sarnthein, M.: Evolution and variability of the Asian monsoon system: state of the art and outstanding issues, Quaternary Sci. Rev., 24, 595–629, 2005.

Wang, P., Wang, B., and Kiefer, T.: Global monsoon in observations, simulations and geological records, PAGES News, 17, 82–83, 2009.

Wang, P., Wang, B., and Kiefer, T.: Linking monsoon systems across timescales, PAGES News, 19, 86–87, 2012a.

Wang, P., Tian, J., and Lourens, L. J.: Obscuring of long eccentricity cyclicity in Pleistocene oceanic carbon isotope records, Earth Planet. Sci. Lett., 290, 319–330, 2010.

Wang, P., Wang, B., and Kiefer, T.: Global Monsoon across timescales, Clim. Dynam., 39, 1–2, 2012b.

Wang, P. and Li, Q.: Monsoons: Pre-Quaternary, in: Encyclopedia of Paleoclimatology and Ancient Environments, Springer, 583–589, 2009.

Wang, P., Li, Q., Tian, J., Jian, Z., Liu, C., Li, L., and Ma, W.: Long-term cycles in the carbon reservoir of the Quaternary ocean: a perspective from the South China Sea, National Science Review, 1, 119–143, Oxford University Press, 2014

Wang, X., Auler, A. S., Edwards, R. L., Cheng, H., Cristalli, P. S., Smart, P. L., Richards, D. A., and Shen, C.-C.: Wet periods in northeastern Brazil over the past 210 kyr linked to distant climate anomalies, Nature, 432, 740–743, 2004.

Wang, X., Auler, A. S., Edwards, R. L., Cheng, H., Ito, E., and Solheid, M.: Interhemispheric anti-phasing of rainfall during the last glacial period, Quaternary Sci. Rev., 25, 3391–3403, 2006.

Wang, X., Auler, A. S., Edwards, R., Cheng, H., Ito, E., Wang, Y., Kong, X., and Solheid, M.: Millennial scale precipitation changes in southern Brazil over the past 90,000 years, Geophys. Res. Lett., 34, L23701, doi:10.1029/2007GL031149, 2007a.

Wang, X., Edwards, R. L., Auler, A. S., Cheng, H., and Ito, E.: Millennial Scale Interhemispheric Asymmetry of Low Latitude Precipitation: Speleothem Evidence and Possible High Latitude Forcing. In: A.Schmittner et al., Ocean Circulation: Mechanisms and Impacts-Past and Future Changes of Meridional Overturning, Geophys. Monogr., 137, 279–294, 2007b.

Wang, Y., Cheng, H., Edwards, R. L., An, Z., Wu, J., Shen, C.-C., and Dorale, J. A.: A high-resolution absolute-dated late Pleistocene monsoon record from Hulu Cave, China, Science, 294, 2345–2348, 2001.
Wang, Y., Cheng, H., Edwards, R. L., He, Y., Kong, X., An, Z., Wu, J., Kelly, M. J., Dykoski, C. A., and Li, X.: The Holocene Asian monsoon: links to solar changes and North Atlantic climate, Science, 308, 854–857, 2005.
Wang, Y., Cheng, H., Edwards, R. L., Kong, X., Shao, X., Chen, S., Wu, J., Jiang, X., Wang, X., and An, Z.: Millennial-and orbital-scale changes in the East Asian monsoon over the past 224,000 years, Nature, 451, 1090–1093, 2008.
Wanner, H. and Bütikofer, J. :Holocene Bond Cycles – real or imaginary?, Geografie, 4, 338–349, 2008.
Wanner, H., Beer, J., Bütikofer, J., Crowley, T. J., Cubasch, U., Flückiger, J., Goosse, H., Grosjean, M., Joos, F., Kaplan, J. O., Küttel, M., Müller, S. A., Prentice, I. C., Solomina, O., Stocker, T. F., Tarasov, P., Wagner, M., and Widmann, M.: Mid- to late Holocene climate change: an overview, Quaternary Sci. Rev., 27, 1791–1828, 2008.
Wanner, H., Solomina, O., Grosjean, M., Ritz, S. P., and Jetel, M.: Structure and origin of Holocene cold events, Quaternary Sci. Rev., 30, 3109–3123, 2011.
Weber, S. L. and Tuenter, E.: The impact of varying ice sheets and greenhouse gases on the intensity and timing of boreal summer monsoons, Quaternary Sci. Rev., 30, 469–479, 2011.
Webster, P. J.: Response of the tropical atmosphere to local, steady forcing, Mon. Weather Rev., 100, 518–541, 1972.
Webster, P. J.: Monsoons, Scientific American, 245, 108–118, 1981.
Webster, P. J.: The variable and interactive monsoon, Monsoons, Wiley, New York, 269, 1987.
Webster, P. J., Magana, V. O., Palmer, T., Shukla, J., Tomas, R., Yanai, M. U., and Yasunari, T.: Monsoons: Processes, predictability, and the prospects for prediction, J. Geophys. Res.-Oceans (1978–2012), 103, 14451–14510, 1998.
Weissert, H. and Mohr, H.: Late Jurassic climate and its impact on carbon cycling, Palaeogeogr. Palaeocli. Palaeoecol., 122, 27–43, 1996.
Weldeab, S., Lea, D. W., Schneider, R. R., and Andersen, N.: 155,000 years of West African monsoon and ocean thermal evolution, Science, 316, 1303–1307, 2007.
Weldeab, S.: Bipolar modulation of millennial-scale West African monsoon variability during the last glacial (75,000–25,000 years ago), Quaternary Sci. Rev., 40, 21–29, 2012.

CPD
10, 2163–2291, 2014

Wilde, P., Berry, W., and Quinby-Hunt, M.: Silurian oceanic and atmospheric circulation and chemistry, Special Papers in Palaeontology, 44, 123–143, 1991.
Winkler, M. G. and Wang, P. K.: The late-Quaternary vegetation and climate of China, Global climates since the last glacial maximum, University of Minnesota Press, Minneapolis, 221–264, 1993.
Wu, W. and Liu, T.: Possible role of the "Holocene Event 3" on the collapse of Neolithic Cultures around the Central Plain of China, Quaternary Int., 117, 153–166, 2004.
Wyrwoll, K.-H., Liu, Z., Chen, G., Kutzbach, J. E., and Liu, X.: Sensitivity of the Australian summer monsoon to tilt and precession forcing, Quaternary Sci. Rev., 26, 3043–3057, 2007.
Wyrwoll, K.-H., Hopwood, J. M., and Chen, G.: Orbital time-scale circulation controls of the Australian summer monsoon: a possible role for mid-latitude Southern Hemisphere forcing?, Quaternary Sci. Rev., 35, 23–28, 2012.
Yan, Z. and Petit-Maire, N.: The last 140 ka in the Afro-Asian arid/semi-arid transitional zone, Palaeogeogr. Palaeocli. Palaeoecol., 110, 217–233, 1994.
Yanai, M. and Wu, G.-X.: Effects of the Tibetan Plateau, in: The Asian Monsoon", edited by: Wang, B., Springer, 513–549, 2006.
Yancheva, G., Nowaczyk, N. R., Mingram, J., Dulski, P., Schettler, G., Negendank, J. F., Liu, J., Sigman, D. M., Peterson, L. C., and Haug, G. H.: Influence of the intertropical convergence zone on the East Asian monsoon, Nature, 445, 74–77, 2007.
Yim, S.-Y., Wang, B., Liu, J., and Wu, Z.: A comparison of regional monsoon variability using monsoon indices, Clim. Dynam., 1–15, doi:10.1007/s00382-013-1956-9, in press, 2013.
Yuan, D., Cheng, H., Edwards, R. L., Dykoski, C. A., Kelly, M. J., Zhang, M., Qing, J., Lin, Y., Wang, Y., and Wu, J.: Timing, duration, and transitions of the last interglacial Asian monsoon, Science, 304, 575–578, 2004.
Zachos, J., Pagani, M., Sloan, L., Thomas, E., and Billups, K.: Trends, rhythms, and aberrations in global climate 65 Ma to present, Science, 292, 686–693, 2001.
Zachos, J. C. and Kump, L. R.: Carbon cycle feedbacks and the initiation of Antarctic glaciation in the earliest Oligocene, Global Planet. Change, 47, 51–66, 2005.
Zachos, J. C., Dickens, G. R., and Zeebe, R. E.: An early Cenozoic perspective on greenhouse warming and carbon-cycle dynamics, Nature, 451, 279–283, 2008.
Zhang, J., Chen, F., Holmes, J. A., Li, H., Guo, X., Wang, J., Li, S., Lü, Y., Zhao, Y., and Qiang, M.: Holocene monsoon climate documented by oxygen and carbon isotopes from lake sedi-

CPD
10, 2163–2291, 2014

ments and peat bogs in China: a review and synthesis, Quaternary Sci. Rev., 30, 1973–1987, 2011.
Zhang, P., Cheng, H., Edwards, R. L., Chen, F., Wang, Y., Yang, X., Liu, J., Tan, M., Wang, X., and Liu, J.: A test of climate, sun, and culture relationships from an 1810-year Chinese cave record, Science, 322, 940–942, 2008.
Zhang, R. and Delworth, T. L.: Impact of Atlantic multidecadal oscillations on India/Sahel rainfall and Atlantic hurricanes, Geophys. Res. Lett., 33, L17712, doi:10.1029/2006GL026267, 2006.
Zhang, Z., Flatøy, F., Wang, H., Bethke, I., Bentsen, M., and Guo, Z.: Early Eocene Asian climate dominated by desert and steppe with limited monsoons, J. Asian Earth Sci., 44, 24–35, 2012.
Zhao, P., Wang, B., and Zhou, X.: Boreal summer continental monsoon rainfall and hydroclimate anomalies associated with the Asian-Pacific Oscillation, Clim. Dynam., 39, 1197–1207, doi:10.1007/s00382-012-1348-6, 2012.
Zheng, Z. and Lei, Z.-Q.: A 400,000 year record of vegetational and climatic changes from a volcanic basin, Leizhou Peninsula, southern China, Palaeogeogr. Palaeocli. Palaeoecol., 145, 339–362, 1999.
Zhou, H.: Comment on "Tree-Ring δD as an Indicator of Asian Monsoon Intensity", Quaternary Res., 58, 210–211, 2002.
Zhou, J. and Lau, K.-M.: Does a monsoon climate exist over South America?, J. Climate, 11, 1020–1040, 1998.
Zhou, T., Yu, R., Li, H., and Wang, B.: Ocean forcing to changes in global monsoon precipitation over the recent half-century, J. Climate, 21, 3833–3852, doi:10.1029/2008GL034881, 2008a.
Zhou, T., Zhang, L., and Li, H.: Changes in global land monsoon area and total rainfall accumulation over the last half century, Geophys. Res. Lett., 35, L16707, doi:10.1029/2008GL034881, 2008b.
Ziegler, C., Murray, R., Hovan, S., and Rea, D.: Resolving eolian, volcanogenic, and authigenic components in pelagic sediment from the Pacific Ocean, Earth Planet. Sci. Lett., 254, 416–432, 2007.
Ziegler, M., Tuenter, E., and Lourens, L. J.: The precession phase of the boreal summer monsoon as viewed from the eastern Mediterranean (ODP Site 968), Quaternary Sci. Rev., 29, 1481–1490, 2010.

Ziegler, M., Simon, M. H., Hall, I. R., Barker, S., Stringer, C., and Zahn, R.: Development of Middle Stone Age innovation linked to rapid climate change, Nat. Communic., 4, 1905, doi:10.1038/ncomms2897, 2013.

CPD
10, 2163–2291, 2014

Table 1. A simplified overview of frequently used monsoon proxies.

Features and Processes	Proxies	Archives
	Wind-based proxies	
Wind transport	Eolian dust	Loess, ice-core
		Lacustrine and marine sediments
	Wind-borne pollen	
Wind-driven upwelling	Upwelling-indicative phyto- & zooplankton, e.g. *Globigerina bulloides* Benthic foraminifera indicative of high carbon flux Geochemical proxies indicative of high productivity, e.g. C_{org}, opal, Ba, Cd / Ca, etc.	Marine sediments
Wind-induced structure of surface ocean	Horizontal SST gradient Thermocline depth based on microfossils	
	Rain-based proxies	
River runoff	Sea surface salinity based on plankton & its δ^{18}O Laminated deposits due to water column stratification Sapropel deposits (Mediterranean)	Marine sediments
Precipitation rate	Lake level	Lacustrine deposits
	Lake salinity based on microfossils and isotopes Pollen-based vegetation, charcoal	
	Speleotheme δ^{18}O, trace elements, GDGT-based proxies	Cave speleotheme
	Tree ring growth and isotopes	Tree rings
	Atmospheric CH_4% and $\delta^{18}O_{atm}$	Ice-core air bubble
	^{10}Be, $\delta^{13}C_{org}$	Loess deposits
Weathering and pedogenesis	Clay minerals Chemical weathering indices Magnetic susceptibility Pegonenesis indices, e.g. FeD / FeT	Marine, lacustrine and loess deposits

CPD
10, 2163–2291, 2014
The Global Monsoon across Time Scales
P. X. Wang et al.

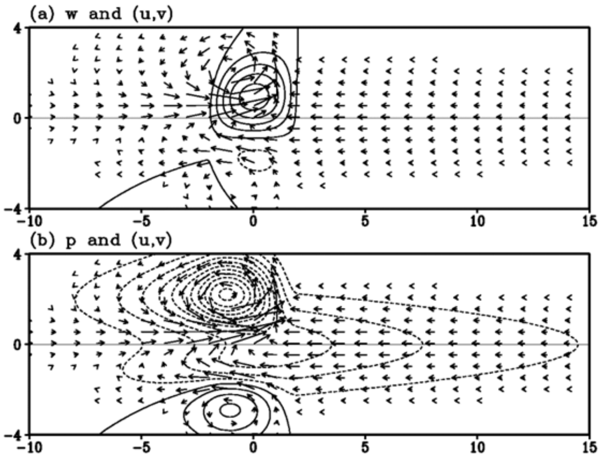

Fig. 1. Gill's solution for atmospheric response to a "monsoon-like heating" in an idealized equatorial plane of longitude and latitude (units: 1000 km) **(a)** Upward motion (*w*, solid contours) is collocated with imposed heating at 0 longitude just north of the equator. Low-level zonal (*u*) and meridional (*v*) winds respond to imposed heating, leading to convergence on the equator and cyclonic circulations north of it, in a pattern that resembles the monsoons. **(b)** The response to the heating of surface pressure (*p*, contours, dashed for negative values) is in approximate geostrophic balance with near surface winds.

CPD
10, 2163–2291, 2014

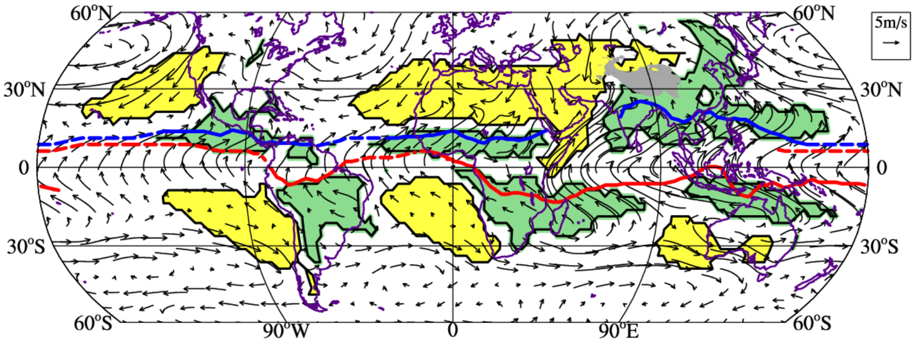

Fig. 2. The GM precipitation domain defined by local summer-minus-winter precipitation rate exceeds 2 mm day^{-1} and the local summer precipitation exceeds 55 % of the annual total (in green). Summer denotes May through September for the northern hemisphere and November through March for the southern hemisphere. The dry regions, where the local summer precipitation is less than 1 mm day^{-1} are shown (yellow). The arrows show August minus February 925hPa winds. The blue lines indicate ITCZ position for August, the red lines indicate ITCZ position for February (solid for monsoon trough and dashed for trade wind convergence). The 3000 m height contour surrounding Tibetan Plateau is shaded. The merged Global Precipitation Climatology Project/Climate Prediction Center Merged Analysis of Precipitation data and ERA interim data were used for 1979–2012.

CPD
10, 2163–2291, 2014

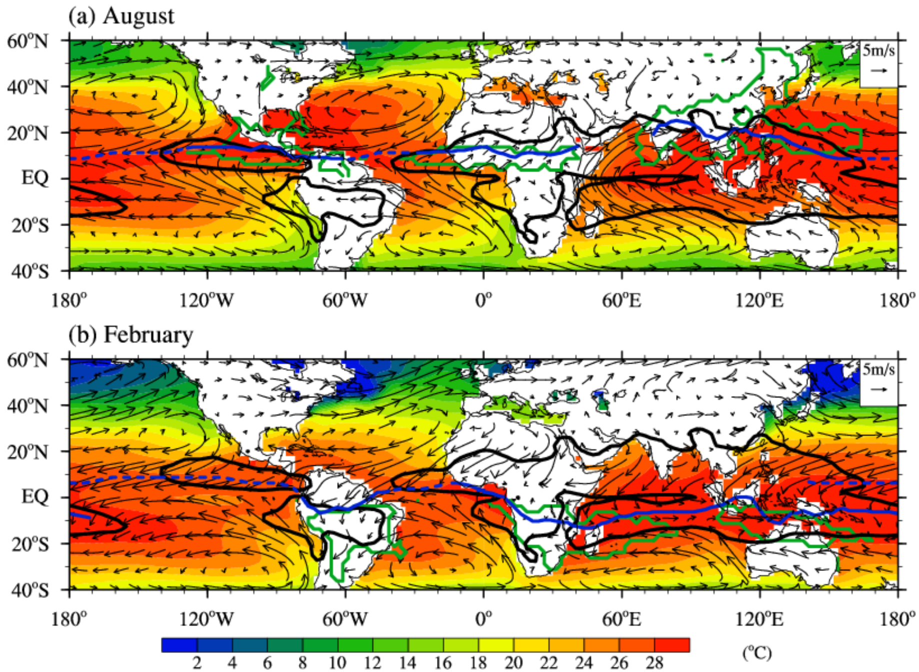

Fig. 3. Climatological mean SST (shading) and 925 hPa winds (vector) in **(a)** August and **(b)** February. The blue lines indicate the locations of ITCZ (solid for monsoon trough and dashed for trade wind convergence). The tropical monsoon wind domains are outlined by the black lines, which are delineated by the annual reversal of the zonal winds (westerlies in the local summer and easterlies during the local winter). The monsoon precipitation domain is outlined by the green curves.

CPD
10, 2163–2291, 2014

The Global Monsoon across Time Scales

P. X. Wang et al.

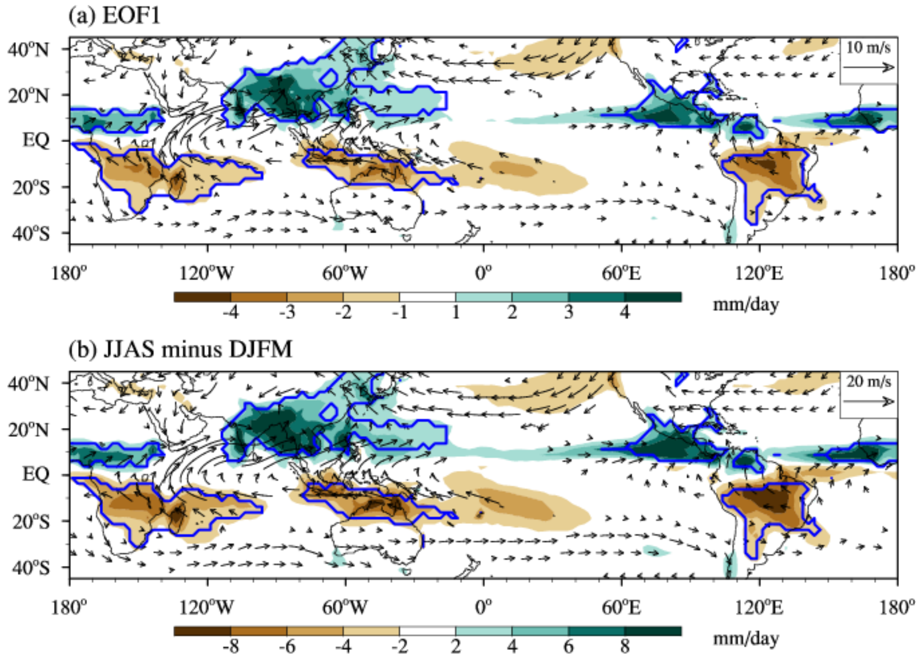

Fig. 4. **(a)** The spatial pattern of the leading multi-variable EOF of precipitation rate (shading, unit: mm day^{-1}) and winds (vectors in units of m s^{-1}) at 850 hPa that correspond to a normalized principal component, and **(b)** the precipitation rate (mm day^{-1}) and 850 hPa wind differences between June through September and December through March (JJAS minus DJFM). Winds with wind speed less than 1 and 2 m s^{-1} are omitted in **(a)** and **(b)**, respectively. The monsoon precipitation domain is outlined by the blue curves.

CPD
10, 2163–2291, 2014

The Global Monsoon across Time Scales

P. X. Wang et al.

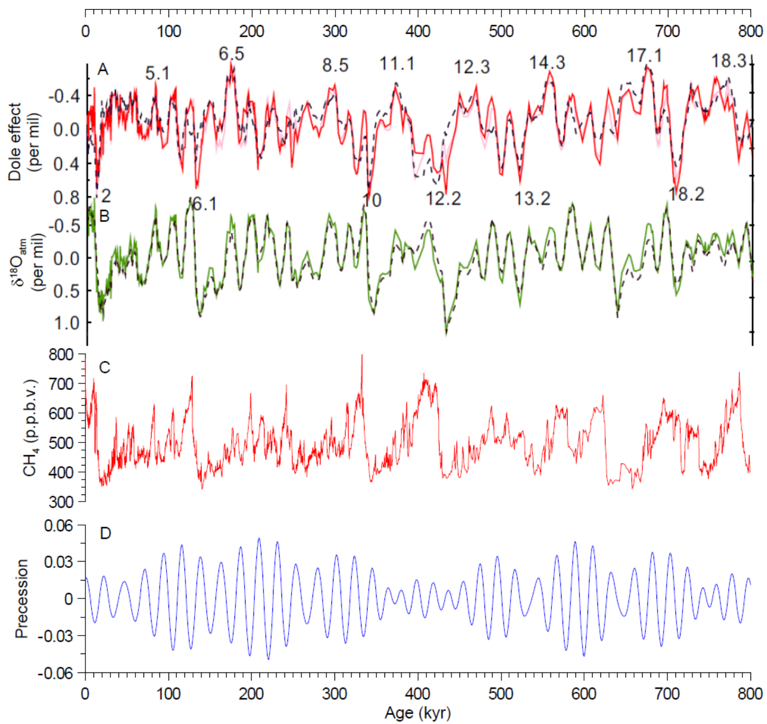

Fig. 5. Proxies related to the GM in Antarctic ice-cores. **(A)** Dole effect; **(B)** $\delta^{18}O_{atm}$, based on the composite Antarctic ice-cores (Landais et al., 2010 dotted lines in **A** and **B** represent principle components PC2 and PC1, respectively); **C** CH_4 concentration in EPICA/Dome C (Loulergue et al., 2008); **D** precession periodicity.

CPD
10, 2163–2291, 2014

The Global Monsoon across Time Scales

P. X. Wang et al.

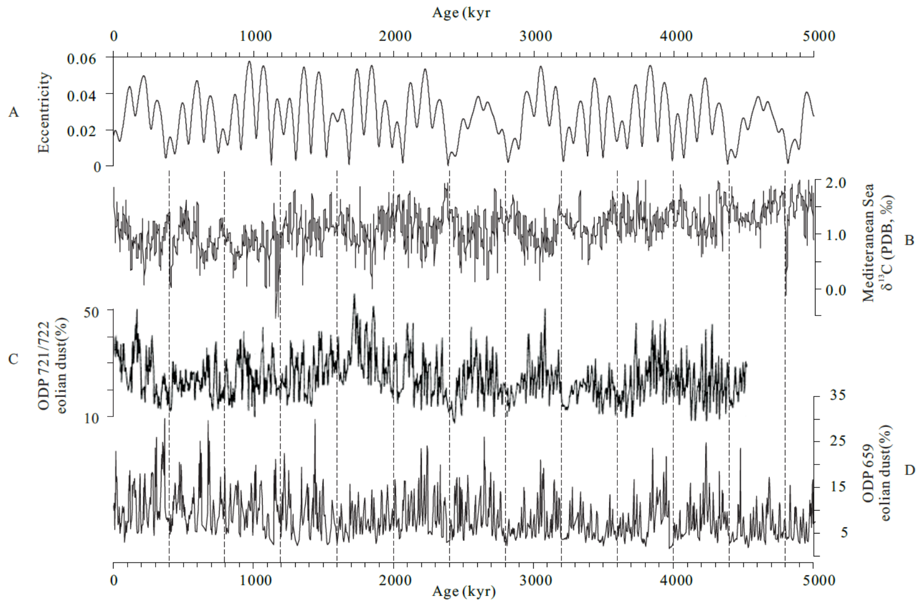

Fig. 6. Long-eccentricity cycles and the GM over the last 5 Ma. **(A)** Eccentricity cycles (100 and 400 ka); **(B)** Planktonic δ^{13}C from Rossello composite section, Sicily, and ODP 964, Mediterranean (after Lourens, 1994); C. Eolian dust% in ODP 721/722 (16°38′ N, 59°50′ E), Arabian Sea (DeMenocal, 1995); **(D)** Dust flux (g m^{-2} a^{-1}) at ODP 659(18°05′ N, 21°02′ W), eastern equatorial Atlantic off Africa (Tiedemann et al., 1994).

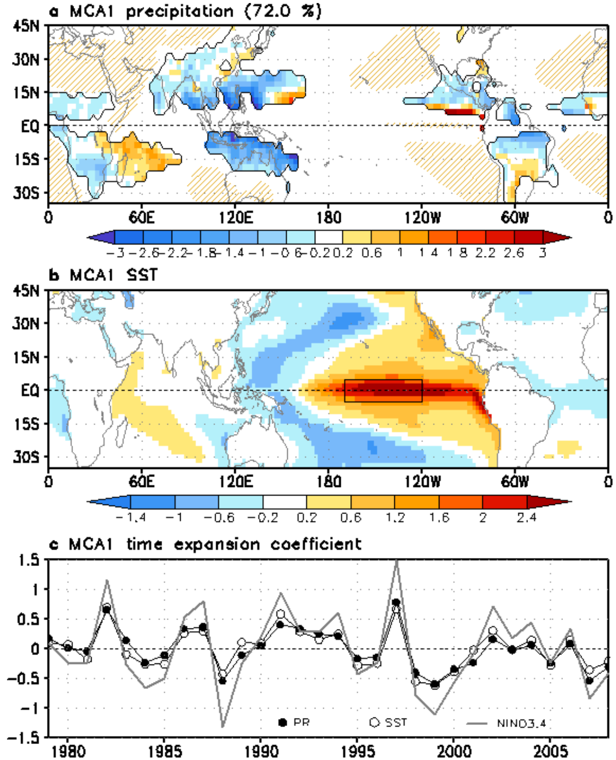

Fig. 7. The leading coupled mode of monsoon-year mean precipitation rate (mm day^{-1}) in GM domains and the corresponding global SST (K) derived by maximum covariance analysis, which explains about 72 % of the total covariance. Spatial patterns of monsoon precipitation **(a)** and SST **(b)** are shown together with their corresponding time expansion coefficients **(c)**. For comparison, the Niño 3.4 SST anomaly (an ENSO index averaged over the box inserted in panel **b**) averaged over the monsoon years are also shown in the panel **(c)**. The GM precipitation domain and hatched dry regions are defined in Fig. 2. The merged GPCP-CMAP data ERSST were used.

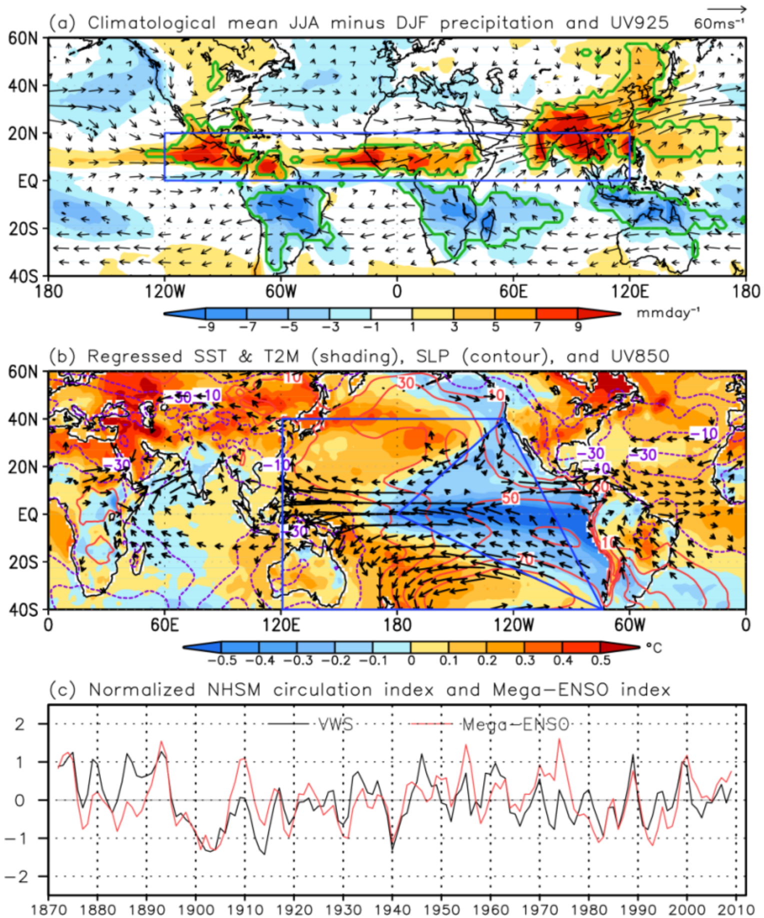

CPD
10, 2163–2291, 2014

The Global Monsoon across Time Scales

P. X. Wang et al.

Fig. 8. **(a)** NH monsoon precipitation domain and annual reversal of the vertical wind shear: JJA minus DJF mean rainfall Color shading) and vertical wind shear (850 minus 200 hPa winds, vectors). The monsoon precipitation domains are shown (green contours) while the blue boxed region indicates where the vertical wind shear index is defined. **(b)** Climate anomalies associated with the NHSM circulation index: regressed 2 m air temperature anomalies over land and SST anomalies over ocean (shading, °C), sea-level pressure anomalies (contours, Pa) and significant 850 hPa wind anomalies (vector) with respect to the NHSM circulation (VWS) index for the period of 1979–2010. The blue lines outline the eastern Pacific triangle and western Pacific K-shape regions where the Mega-ENSO index is defined. **(c)** Relationship between normalized NHSM circulation index (black) and Mega-ENSO index (red) for the period of 1871–2010. Shown are the NHSM index derived from 20th century reanalysis data and the Mega-ENSO index derived from the HadISST dataset. All data used are 3 year running means (adapted from B. Wang et al. 2013).

CPD
10, 2163–2291, 2014

The Global Monsoon across Time Scales

P. X. Wang et al.

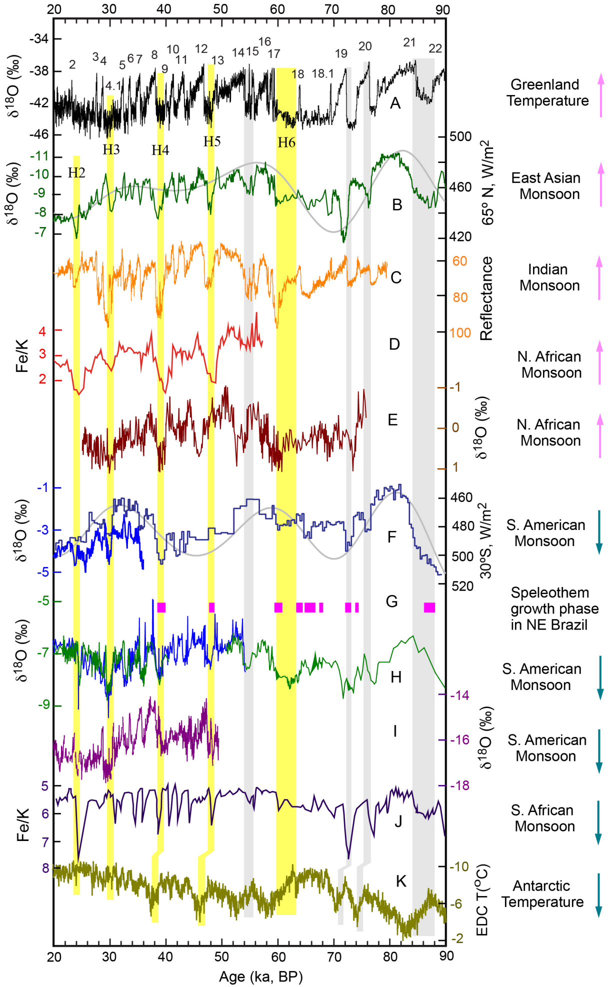

CPD
10, 2163–2291, 2014

The Global Monsoon across Time Scales

P. X. Wang et al.

Title Page
Abstract | Introduction
Conclusions | References
Tables | Figures
◀| |▶
◀ ▶
Back | Close
Full Screen / Esc
Printer-friendly Version
Interactive Discussion

Fig. 9. Comparison among millennial events in Asian, American and African monsoon regions. **(A)** Greenland ice core δ^{18}O record (NGRIP, Svensson et al., 2008). **(B)** East Asian monsoon record composited by using Hulu and Sanbao records (Cheng et al., 2009a). **(C)** Indian monsoon record inferred from Arabian Sea sediment total reflectance form core SO130-289KL (Deplazes et al., 2013). **(D)** Bulk Fe / K ratios from core GeoB9508–5 indicate arid (low) and humid (high) condition in the North African monsoon region (Mulitza et al., 2008). **(E)** The North African monsoon proxy record based on the age model tuning to the GISP2 chronology (Weldeab, 2012). **(F)** South American monsoon records from Botuvera cave (blue, X. Wang et al., 2006; dark blue, X. Wang et al., 2007a). **(G)** Northeastern Brazil speleothem growth (wet) periods (X. Wang et al., 2004). **(H)** South American monsoon record from northern Peru (Cheng et al., 2013). **(I)** South American monsoon record from Pacupahuain cave (Kanner et al. 2012). **(J)** Fe / K record (marine sediment core CD154-17-17K) from the South Aferican monsoon region (Ziegler et al., 2013) show anti-phased relationship with the North African counterpart **(D)**. **(K)** Antarctic ice core temperature record (EDC, Jouzel et al., 2007). The anti-phased relationship between Northern and Southern Hemisphere summer monsoons is evident for the millennial-scale oscillations. Monsoon millennial events have a clear teleconnection with the Greenland record (A) and their relation to the Antarctic record (K) is however still ambiguous. Numbers indicate Greenland Interstadials. Vertical yellow bars denote H events (H2–H6) and grey bars indicate correlations among northeastern Brazil wet periods, strong South American events and cold Greenland-weak Asian monsoon events. Summer insolation (grey curves) at 65° N (JJA, in **B**) and 30° S (DJF, in **F**) (Berger, 1978) were plotted for comparison. Arrows on the right side depict anti-phase changes of monsoons between two Hemispheres.

CPD
10, 2163–2291, 2014

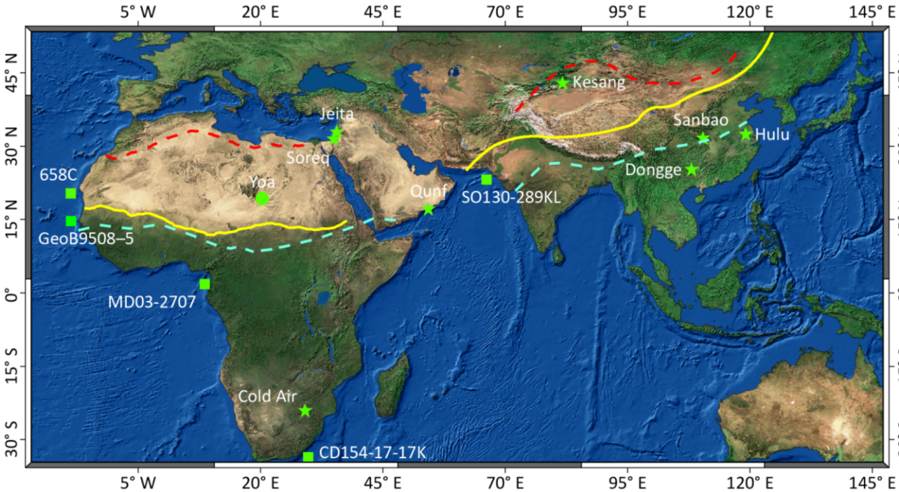

Fig. 10. Location of selected monsoon records over the Holocene. Stars indicate locations of speleothem $\delta^{18}O$ records (i.e. the Hulu, Dongge, Sanbao, Kesang, Qunf, Jeita Soreq and Cold Air records), squares show marine sediment records (i.e., the Hole 658C, GeoB9508-5, MD03-2707, SO130-289KL and CD154-17-17K records), and circle the lake Yoa sediment record. See the Holocene record in next section. The yellow line depicts approximately the modern summer monsoon fringe of Asian and North African monsoons. The red dashed line shows the estimated farmost North African (Adams, 1997) and Asian (Winkler and Wang, 1993; Jiang and Liu, 2007) summer monsoon fringe during the mid-early Holocene. The blue dashed line is the estimated Asian and North African monsoon fringe during the Last Glacial Maximum (Yan and Petit-Maire, 1994).

CPD
10, 2163–2291, 2014

The Global Monsoon across Time Scales

P. X. Wang et al.

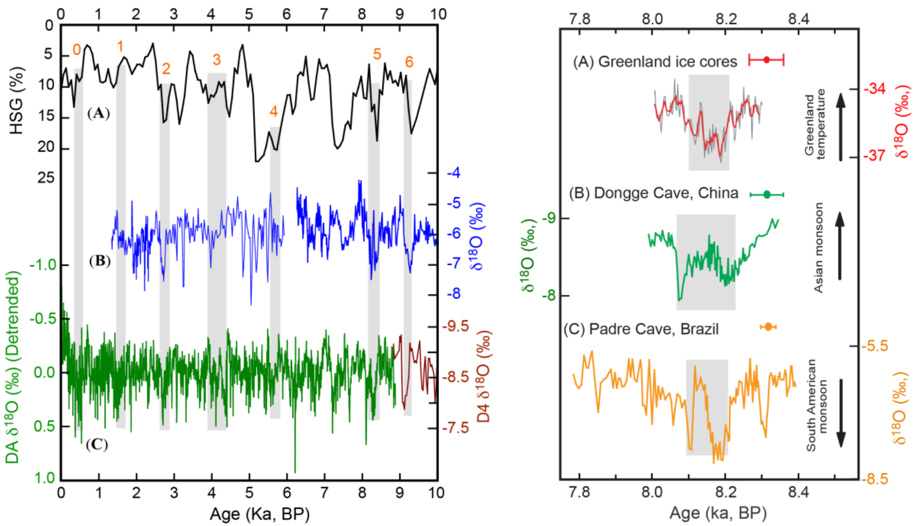

Fig. 11. Left: comparison of Bond events among the North Atlantic, Asian monsoon and South American monsoon records (adapted from Stríkis et al., 2011 and Cheng, 2012a). **(A)** Hematite stained quartz grain (HSG) record from the North Atlantic deep-sea core VM 29-191 (Bond et al., 1997). **(B)** South American monsoon record from Lapa Grande cave in central-eastern Brazil (Stríkis et al., 2011). **(C)** Asian monsoon δ^{18}O record from two stalagmites DA (green, detrended) and D4 (brown) from Dongge cave, southeastern China (Y. Wang et al., 2005; Dykoski et al., 2005). Grey bars indicate apparent Bond events 0–6 in monsoon regions. Right: Paleoclimate records over the 8.2 ka BP event (modified from Cheng et al., 2009b). **(A)** Stacked composite δ^{18}O data of Greenland ice cores (Dye3, GRIP, GISP2, and NGRIP; resolution of $\sim$2.5 years in gray and four-point average in red; Thomas et al., 2007). **(B)** DA, Dongge cave, China (Cheng et al., 2009a). **(C)** PAD07, Padre cave, Brazil (Cheng et al., 2009b). The δ^{18}O scales are reversed for the Dongge record (increasing down) to compare with the South American monsoon record. Arrows depict anti-phase changes between South American monsoon and Asian monsoon-Greenland temperature. Color-coded error bars indicate typical dating errors (2σ) for each record around the 8.2 ka BP event.

CPD
10, 2163–2291, 2014

The Global Monsoon across Time Scales

P. X. Wang et al.

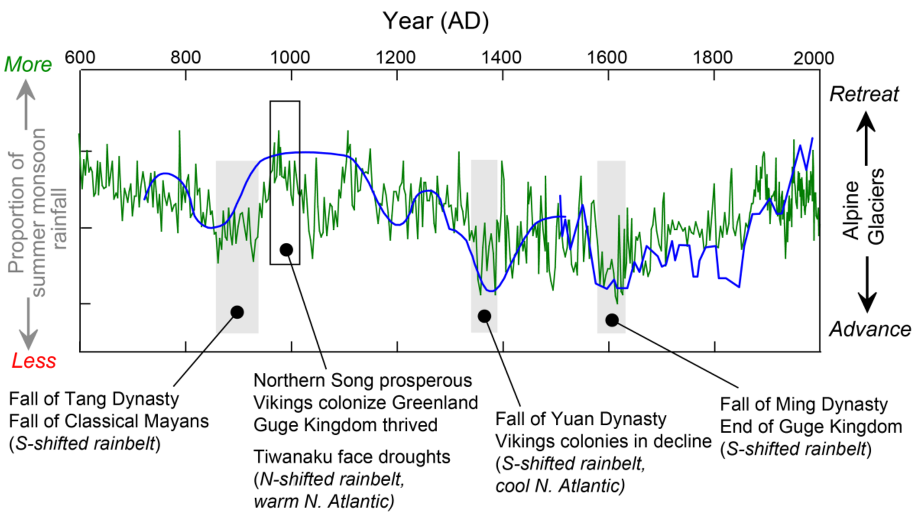

Fig. 12. Possible link between climate event and human culture (adapted from Cheng and Edwards, 2012). The Asian summer monsoon (green, Zhang et al., 2008) tracks the Alpine glacial advance and retreat (blue, Holzhauser et al., 2005), demonstrating that when temperatures were colder in Western Europe, conditions were drier in the monsoonal regions of China. The grey bars show some climate events that likely had influence on human cultural history over the past 2000 years.

CPD
10, 2163–2291, 2014

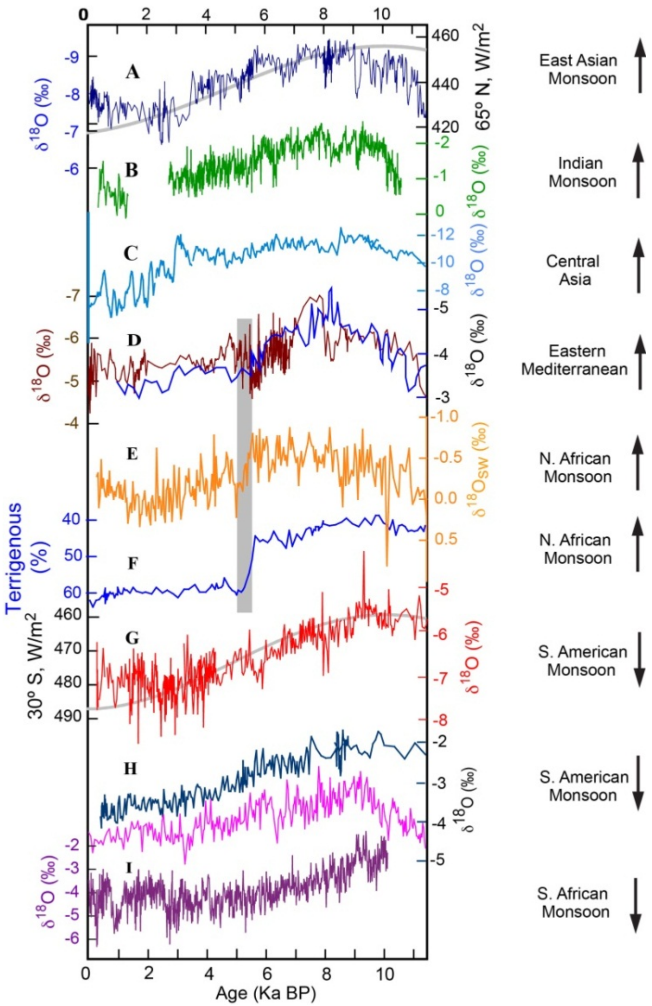

CPD
10, 2163–2291, 2014

The Global Monsoon across Time Scales

P. X. Wang et al.

Fig. 13. Holocene monsoon records from different monsoon regions. (**A**) The East Asian monsoon record from Dongge cave (Dykoski et al., 2005). (**B**) The Indian monsoon record from Qunf Cave (Fleitmann et al., 2003). (**C**) The Kesang record, eastern central Asia. Although it is outside of the modern Asian monsoon domain, it may be influenced by the summer monsoon incursions during the mid-Holocene (Cheng et al., 2012b; Kutzbach et al., 2014). (**D**) Eastern Mediterranean records from Soreq cave (brown, Bar-Matthews et al., 2003) and Jeita Cave Lebanon (blue, Verheyden et al., 2008). (**E**) The seawater δ^{18}O record from the marine sediment core (MD03-270) (Weldeab et al., 2007). (**F**) The terrigenous concentration (%) record from the northwest African margin sediment (core Hole 658C, deMenocal et al., 2000). (**G**) The South American monsoon record from Cueva del Tigre Perdido cave, northern Peru (van Breukelen et al., 2008). (**H**) South American monsoon records from Botuverá cave (pink, Cruz et al. 2005; blue, X. Wang et al., 2006). **(I)** The speleothem record from Cold Air cave, the Makapansgat Valley, South Africa (Holmgren et al., 2003). The records from Southern Hemisphere monsoon regions (**G-I**) are plotted inversely relative to their Northern Hemisphere counterparts **(A–F)**. Some of locations of above records are shown in Fig. 5-2. Summer insolation (grey curves) at 65° N (JJA, in **A**) and 30° S (DJF, in **G**) are also plotted inversely for comparison (Berger, 1978). It appears that the abrupt fall of the North African monsoon (the grey bar) correlates with low δ^{18}O values in Eastern Mediterranean records **(D)** and the latter is causally linked to weakening of the North African monsoon.

CPD
10, 2163–2291, 2014
The Global Monsoon across Time Scales
P. X. Wang et al.

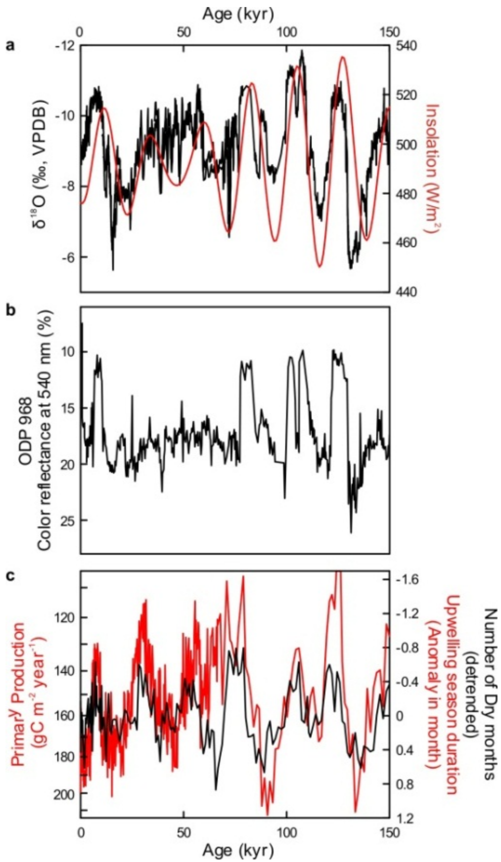

CPD
10, 2163–2291, 2014

The Global Monsoon across Time Scales

P. X. Wang et al.

Fig. 14. Comparative changes of Asian, North African and Australian monsoons over the past 150 ka. **(a)** Asian monsoon variability inferred from the stalagmite $\delta^{18}O$ record (black) from Hulu and Sanbao Caves (Y. Wang et al., 2008). Insolation at N 30° (Berger, 1978) is shown in red. **(b)** North African monsoon variability inferred from the color reflectance from the Eastern Mediterranean ODP 968 site (Ziegler et al., 2010). **(c)** Australian monsoon variability inferred from Banda Sea primary productivity and its estimated upwelling season anomaly in months (red) and number of dry months reconstructed using palynology data (Beaufort et al., 2010). The two curves have the same scale in month on the right axis. The colors of labels to the right refer to the color of the curves.

CPD
10, 2163–2291, 2014

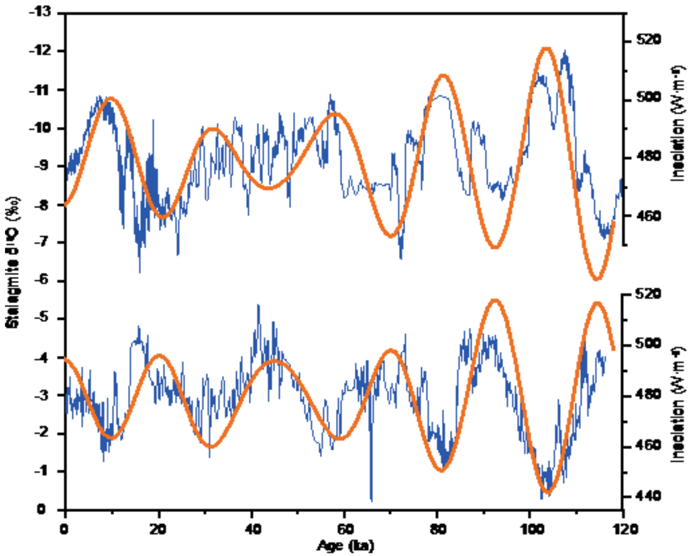

Fig. 15. Late Quaternary variations of the Asian (upper panel) and South American (lower) monsoons as indicated by stalagmite δ^{18}O records (blue) from southern China (Hulu and Dongge Caves) (Y. Wang et al., 2008) and Brazil (Caverna Botuverá)(Cruz et al., 2005). Thick orange lines represent summer daily insolation changes at 30° N (21 June, upper curve) and 30° S (21 December, lower curve) (Berger and Loutre, 1991).

CPD
10, 2163–2291, 2014

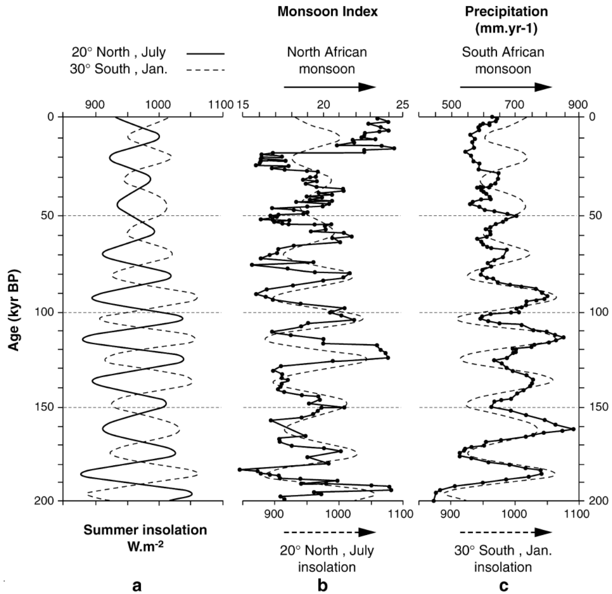

Fig. 16. Comparison of: **(c)** variations in South monsoon precipitation reconstructed from a 200 kyr sedimentary record from the Pretoria Saltpan, South Africa (Partridge et al., 1997), with: **(b)** a monsoonal precipitation index at 203N based on fossil faunal assemblage variations in deep-seasediment core RC24-07 (203N; McIntyre et al., 1989); and **(a)** changes in summer solar radiation in the northern and southern subtropics (Partridge et al., 1997).

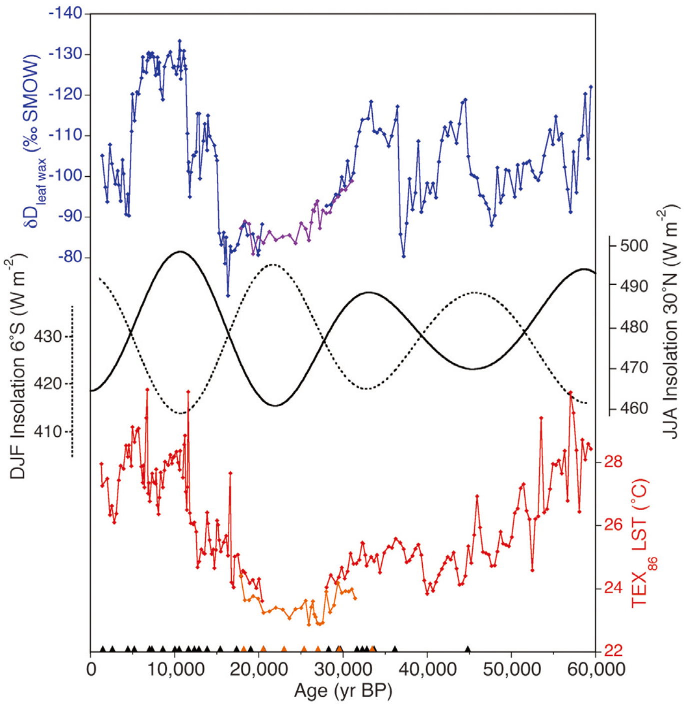

Fig. 17. Temperature and precipitation proxy records from Lake Tanganyika compared with insolation. Organic geochemical indices TEX_{86} (red) and $\delta D_{\text{leaf wax}}$ (blue) indicate temperature and monsoon precipitation, respectively. The curves follow June-July- August insolation for 30° N (solid line) of the Northern Hemisphere, anti-phasing the December-January-February insolation in the local area (6° S) (dotted line) (Tierney et al., 2008).

CPD
10, 2163–2291, 2014

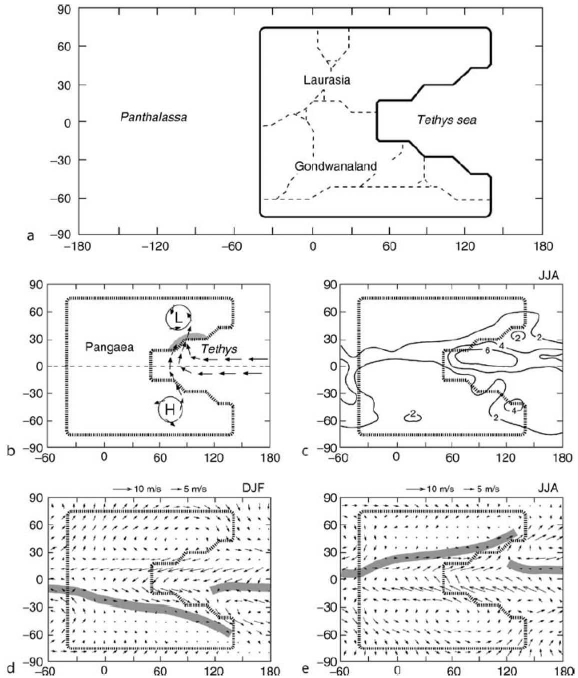

Fig. 18. Mega-monsoon of the Pangaea. **(a)** The idealized Pangaean continent. Fine dashed lines indicate the approximate outlines of modern landmasses. **(b)** Schematic diagram illustrating monsoonal circulation in northern summer. Arrows show surface winds, stippling indicates heavy seasonal rains. **(c)** Modeled precipitation rate (mm d^{-1}) on Pangaea for summer. **(d)**, **(e)** Modeled surface winds on Pangaea for winter **(d)** and summer **(e)**, note the seasonal reversal of the wind direction. The gray bar shows the poleward limit of summer monsoon over land and the Intertropical Convergence Zone over ocean (Wang and Li, 2009, modified from Kutzbach and Gallimore, 1989).

CPD
10, 2163–2291, 2014

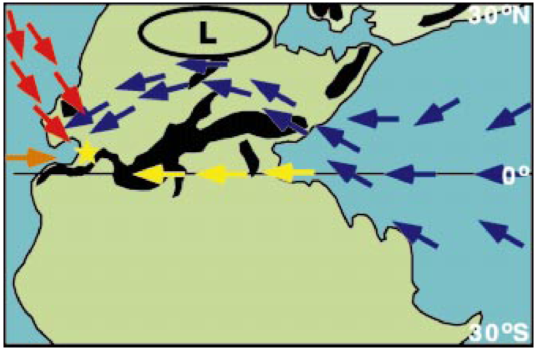

Fig. 19. Paleogeographic reconstruction of late Carboniferous–Early Permian Pangaea (30° N–30° S). Black – highlands (1000 m); blue arrows – monsoonal circulation; yellow arrows – zonal easterly flow in ITCZ; red arrows – northwesterly extension of westerlies (Tabor and Montañez, 2002).

CPD
10, 2163–2291, 2014

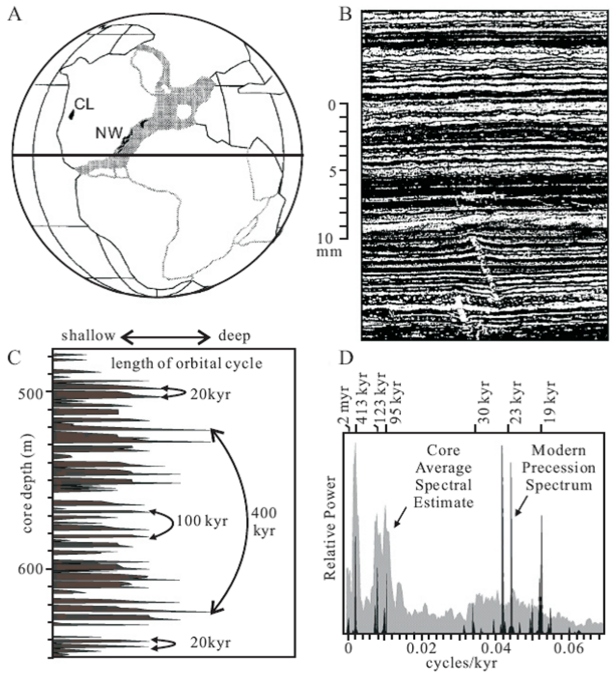

Fig. 20. Late Triassic monsoon records in North America. **(A)** Paleogeographic map showing the locations of the Colorado Plateau with the Chinle Formation (CL) indicative of margin of the tropical monsoon region, and a chain of rifted basins on the East with the Newark Supergroup (NW). **(B)** Photograph of microlaminated mudstone showing organic-rich/ carbonate-rich couplets as annual varves. **(C)** Lake-level fluctuations in a section of the Newark lake sediments, showing 20, 100, and 400 ka cycles. **(D)** Average spectral estimates of sediment cycles in the Newark Basin with the modern precession spectrum. (Wang and Li, 2009; Modified from Olsen and Kent, 1996 and Ruddiman, 2001).

CPD
10, 2163–2291, 2014

The Global Monsoon across Time Scales

P. X. Wang et al.

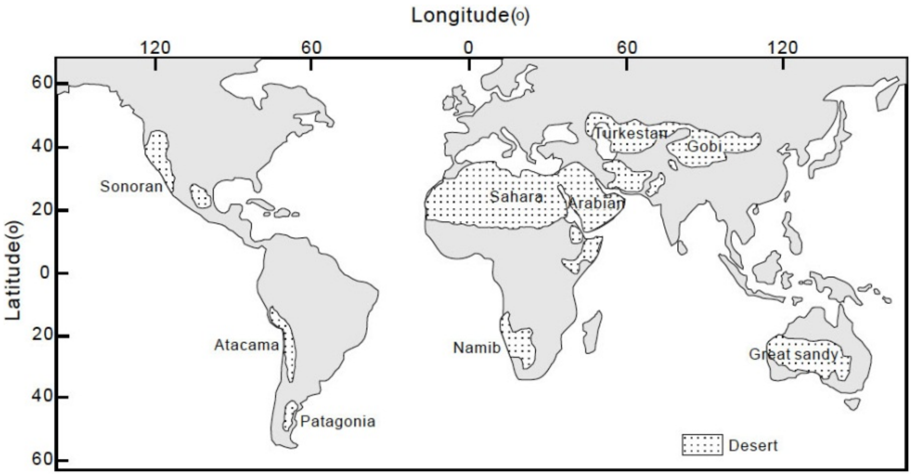

Fig. 21. Distribution of world major deserts (modified after Meigs, 1953).

CPD
10, 2163–2291, 2014

The Global Monsoon across Time Scales

P. X. Wang et al.

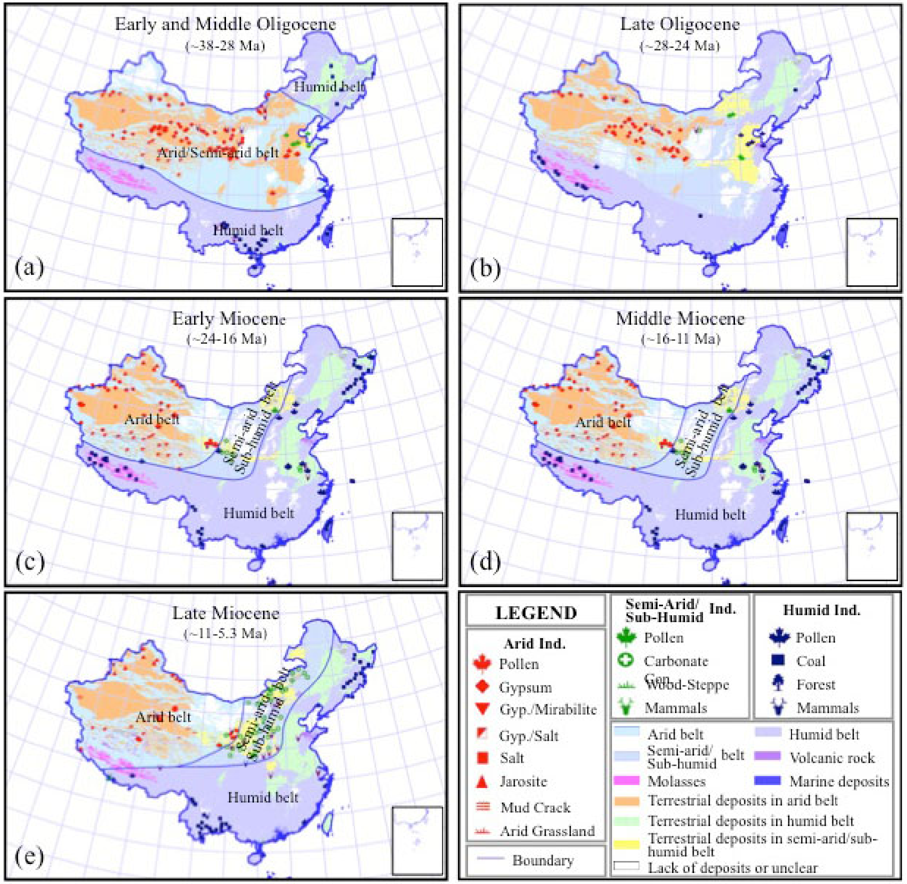

Fig. 22. Paleo-environmental patterns within the Oligocene and Miocene in China (modified after Guo et al., 2008). **(a)** Early and Middle Oligocene; **(b)** Late Oligocene; **(c)** Early Miocene; **(d)** Middle Miocene; **(e)** Late Miocene.occurred near the Oligocene- Miocene boundary.

CPD
10, 2163–2291, 2014
The Global Monsoon across Time Scales
P. X. Wang et al.

Title Page
Abstract
Introduction
Conclusions
References
Tables
Figures
◀◀
▶▶
◀
▶
Back
Close
Full Screen / Esc
Printer-friendly Version
Interactive Discussion

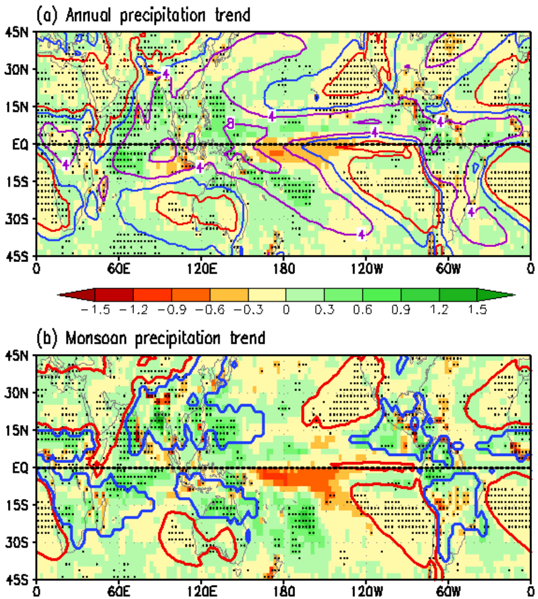

Fig. 23. Recent trends (1979-2008) in **(a)** global annual precipitation and **(b)** precipitation in summer monsoon season (i.e., MJJAS for NH and NDJFM for SH) in units of mm day^{-1} decade^{-1} The significance of the linear trends was tested using the trend-to-noise ratio. Areas passing 90 % confidence level were stippled. The GPCP data were used. In **(a)** the climotological annual mean precipitation rate was shown by contours (1 (red), 2 (blue), 4, and 8 (purple) mm day^{-1}). In **(b)** the monsoon and desert regions as defined in Fig. 2 were delineated by blue and red, respectively.

CPD

10, 2163–2291, 2014

The Global Monsoon across Time Scales

P. X. Wang et al.